Contents

Irreversible deposition/adsorption processes on solid surfaces

P. Schaaf, J.-C. Voegel and B. Senger

Article published by EDP Sciences and available at http://www.annphys.org or http://dx.doi.org/10.1051/anphys:199806001

Irreversible deposition/adsorption processes on solid surfaces

P. Schaaf[1,2], J.-C. Voegel[3] and B. Senger[3]

Abstract

In this article, we summarize the knowledge in the field of irreversible deposition processes of large molecules or colloidal particles on solid surfaces. An irreversible adsorption process is defined as a process in which, once adsorbed, a particle can neither diffuse along, nor desorb from the surface. We first introduce the basic tools used in these studies, one of the most important being the concept of available surface function. General results relative to these processes are then presented. We discuss, in particular, the connection between the reduced variance of the number density fluctuations of adsorbed particles and the available surface function. We then review the main models which were introduced in the literature to account for these phenomena. They can be divided in two classes: (i) the models which are based entirely on statistical and geometrical grounds. The best known and most widely studied of them is the *Random Sequential Adsorption* (RSA) model which is discussed in details. For the processes in which gravity plays an important role one uses the *Ballistic Deposition* (BD) *model*. We also present models which are aimed at accounting for the behavior lying between the ballistic deposition and the RSA. (ii) The second type of models corresponds to those which take explicitly the diffusion of the particles in the vicinity of the adsorption plane into account. The results relative to these models, called *diffusional models*, are discussed in details. Finally, the last part of the review is devoted to experimental results. We show, in particular, that the Langmuir model, which is the most widely used model in the literature to account for the protein adsorption kinetics, does not predict correctly the experimental observations. We present and discuss in a critical way experimental evidence which seems to indicate the validity of the RSA and ballistic models.

1. Institut Charles Sadron, Centre National de la Recherche Scientifique et Université Louis Pasteur, 6 rue Boussingault, 67083 Strasbourg Cedex, France
e-mail: schaaf@ics.u-strasbg.fr
2. École Européenne de Chimie, Polymères et Matériaux, Université Louis Pasteur, 25 rue Becquerel, 67087 Strasbourg Cedex 2, France
3. Institut National de la Santé et de la Recherche Médicale, Unité 424, Fédération de Recherche "Odontologie", Université Louis Pasteur, 11 rue Humann, 67085 Strasbourg Cedex, France

Ann. Phys. Fr. **23** • N° 6 • 1998

Résumé

Processus d'adsorption irréversible sur des surfaces solides

Cet article présente une synthèse des connaissances dans le domaine des processus d'adsorption irréversible de grosses molécules ou de particules colloïdales sur des surfaces solides. Par adsorption irréversible nous entendons les phénomènes d'adsorption au cours desquels, une fois adsorbée, une molécule ne peut plus ni diffuser en surface ni se désorber de la surface. Nous décrivons d'abord les outils utilisés dans l'étude de ces phénomènes, en particulier la notion de fonction de surface accessible. Nous présentons ensuite quelques résultats généraux relatifs à ces processus d'adsorption. Nous discutons plus particulièrement du lien entre la variance réduite du nombre de particules adsorbées et la fonction de surface accessible. Nous passons ensuite en revue les principaux modèles qui ont été introduits dans la littérature pour rendre compte des phénomènes d'adsorption. Ces modèles peuvent être classés en deux catégories : (i) les modèles qui relèvent uniquement de considérations statistiques et géométriques. Le plus connu et le plus étudié est celui de l'*Adsorption Séquentielle Aléatoire* (RSA) qui est discuté en détails. Pour les processus dans lesquels la gravité joue un rôle important on utilise le *modèle du dépôt balistique*. Enfin nous abordons des modèles qui doivent rendre compte de comportements intermédiaires entre le comportement balistique et le comportement RSA. (ii) Le second type de modèles correspond à ceux qui tiennent compte de la diffusion des particules au voisinage de la surface d'adsorption. Les résultats relatifs à ces modèles, appelés *modèles diffusionels*, sont discutés en détails. Enfin, la dernière partie de cet article de revue est consacrée aux résultats expérimentaux. Nous montrons, en particulier, que le modèle de Langmuir, qui est le plus utilisé dans la littérature pour rendre compte des cinétiques d'adsorption de protéines, ne permet pas une bonne correspondance entre expérience et prédictions théoriques. Nous présentons et discutons de façon critique les indices expérimentaux qui semblent indiquer la validité des modèles RSA et balistique.

1

Introduction

Adsorption and deposition phenomena play a fundamental role in many physical, chemical and biological processes: solid catalysts function often through adsorption processes; the first event that takes place when a solid surface is brought into contact with a biological fluid is the adsorption of proteins on the surface; coagulation of colloidal particles can be prevented by adsorbing polymers onto the particles. Due to their great diversity, adsorption phenomena do not all exhibit the same features and a first rough classification leads to two main types of processes: (i) reversible adsorption processes and (ii) irreversible ones. By irreversible we mean processes in which, once a particle has interacted with the surface it will no longer be able to diffuse along the surface or be desorbed from it. The first class of adsorption processes can be analyzed by means of the methods of statistical mechanics. Indeed, due to the possibility for the adsorbed particles to desorb from the surface or at least to diffuse along the surface, the system can explore all the possible configurations and thus be described within the framework of equilibrium statistical mechanics. This is typically the case for the adsorption of small molecules on surfaces and the name of Langmuir is closely related to this problem.

On the other hand, macromolecules in contact with surfaces can establish a great number of links with the surface, the interaction energy being thus usually much larger than the thermal energy kT. This leads to the fact that adsorbed macromolecules usually do not desorb from the surface and if so only very slowly. The same behavior is often observed for the adsorption or deposition of colloidal particles on solid surfaces. In addition to the fact that the adsorbed particles do not desorb from the surface, it is also often observed that they do not diffuse along the surface. Thus, they undergo "irreversible" deposition/adsorption processes. It is clear that the classical methods and postulates of statistical mechanics do no longer apply for such irreversible processes.

It is the aim of this article to review some results that have been obtained in the description and comprehension of these phenomena. Our presentation will not be exhaustive, recent reviews perfectly fulfill this objective [1, 2]. We will merely present a view based on the results of our group and which were obtained over the last ten years. Moreover, as for equilibrium statistical mechanics, many 1D

irreversible deposition processes can be solved exactly. The resolution of these 1D problems has allowed to get a better understanding of these processes and to test the validity of different approximations introduced for the treatments of deposition processes on surfaces for example. We will however not discuss these one-dimensional cases and focus our attention on the irreversible deposition on planar surfaces which has a closer connection to experimental results.

2

General concepts used in the study of irreversible deposition processes

As it has been pointed out in the introduction, equilibrium statistical mechanics does not apply to systems of particles deposited on surfaces through irreversible deposition processes. However, some concepts and tools that have been developed in equilibrium statistical mechanics still remain useful for the description of irreversible deposition processes and will be briefly introduced.

1. Available surface function

The available surface function $\Phi(\theta)$, which is a function of the surface coverage θ (ratio of area covered to total area), was first introduced by Widom [3, 4]. He defined this function in the following way: consider an assembly of spheres which can interact through a pair interaction potential $u(r_{ij})$ assumed to be additive, r_{ij} being the length of the vector joining the centers of the two interacting particles labeled i and j. Now let a "wandering particle" explore all the positions of the deposition plane. At each position determine the Boltzmann factor $\exp(-U(\mathbf{r})/kT)$, where $U(\mathbf{r})$ is the total interaction potential energy of the wandering particle located at the position $\mathbf{r}$ with all the deposited particles, k and T representing the Boltzmann constant and the absolute temperature, respectively. The available surface function $\Phi(\theta)$ for this particular surface, which is assumed to be a function of the coverage only, is then defined as the mean value of the Boltzmann factor taken over the deposition plane:

$$\Phi(\theta) = \langle \exp[-U(\mathbf{r})/kT] \rangle. \tag{2.1}$$

Widom applied this definition to equilibrium configurations as well as to the Random Sequential Adsorption (RSA) case which constitutes the minimum model for irreversible processes and will be defined precisely in Chapter 4. For the RSA, as well as for the equilibrium case of hard spheres, the available surface function $\Phi(\theta)$ is given by the ratio of the undashed area to the total area in Figure 1. For the equilibrium case $\Phi(\theta)$ is directly related to the thermodynamic activity z of the deposited particles by the relation [3]:

$$z = \rho\Phi(\theta) \tag{2.2}$$

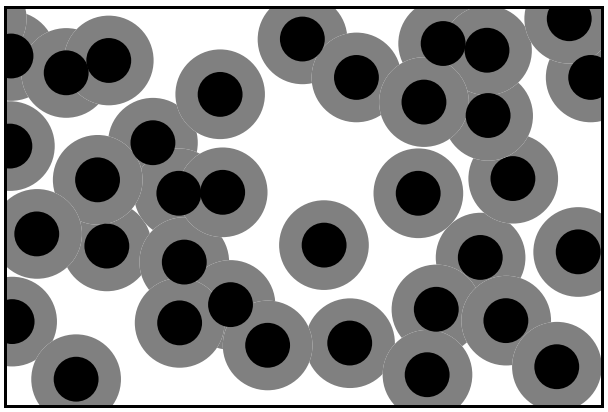

Figure 1. *Available surface function: a typical configuration of hard spheres adhering irreversibly on a surface. The black disks represent the particles themselves, whereas the dashed zones indicate the additional areas excluded by the particles for the center of a new particle. In contrast, any point located in a white region can be occupied by the center of a new particle. The ratio of the white area to the total area corresponds to the available surface function.*

where ρ is the number density of the adhering particles. For the RSA case as we will see, the available surface function is directly related to the adsorption probability of a particle on a surface.

We will define the available surface function in another and more general way which is better adapted to adsorption processes and which is equivalent to Widom's definition in the equilibrium and RSA cases. If the thickness of the deposition layer is well defined and if no desorption occurs from the surface, the available surface function is equal to the ratio of the adsorption flux onto the surface, at a given coverage θ, to the adsorption flux onto the empty surface ($\theta = 0$). It is assumed that the concentration of particles in the bulk, up to the interface, is fixed and equal in both cases. Moreover both fluxes have to be determined in steady-state conditions. The quantity $1 - \Phi(\theta)$ thus represents the probability that a particle, present in the vicinity of the adsorbing surface, will not adhere on it due to the presence of particles already deposited. This implies that, *if the probability of adherence of a particle in the vicinity of an empty surface is equal to 1*, $\Phi(\theta)$ corresponds to the probability of adhesion of a particle in the presence of already deposited particles, the surface coverage being θ. If no desorption occurs, each successful adsorption trial increases irreversibly the covered area by πR^2 which corresponds to an increase of the coverage by an amount equal to $\pi R^2/A$ where A is the area of the adsorbing surface and R the radius of the depositing disks or spheres. Using the property $\Phi(0) = 1$, one can write the kinetic equation of the process as:

$$d\theta = \frac{\pi R^2}{A}\Phi(\theta)dt' \tag{2.3a}$$

which expresses the increment of the coverage θ during the time interval dt'. Note that it is assumed here that exactly one adsorption trial occurs within dt'. The redefinition of the time by $t = (\pi R^2/A)t'$ leads to the simple differential equation:

$$\frac{d\theta}{dt} = \Phi(\theta). \tag{2.3b}$$

Conversely, the rescaled time necessary to reach the coverage θ is given by:

$$t = \int_0^\theta \frac{d\theta'}{\Phi(\theta')}\,. \tag{2.4}$$

2. Radial distribution function

The radial distribution function $g(r)$ is defined in the following way. Let us take any particle deposited on the surface as a center (or reference) particle and let ρ be the number density of deposited particles on the surface. Then, $2\pi\rho g(r)rdr$ represents the probability to find the center of another particle in the circular shell of radii r and $r + dr$ centered on the reference particle. In fact, it represents also the mean number of particles having their centers in the circular shell of area $2\pi rdr$. This mean number can be written as:

$$2\pi\rho g(r)rdr = p_1 + 2p_2 + 3p_3 + \ldots$$

where p_1 represents the probability to find one and only one particle in the circular shell, p_2 the probability to find exactly two particles in the circular shell, *etc.* When the area of the shell becomes vanishingly small, the ratios $p_n/p_1 \to 0$ for $n > 1$ and thus the mean number of particles in the circular shell becomes equal to the probability to find a particle in this shell.

The radial distribution function plays a central role in liquid state theory. If the particles were deposited in a totally random way (no interactions between the particles), $g(r)$ would be equal to 1 everywhere. A value of $g(r) > 1$ means that at the distance r from the reference particle, the probability to find the center of another particle is higher when compared to a fully random deposition process. It is obvious that for hard spheres, $g(r) = 0$ for any distance r smaller than the diameter of the spheres. The function $g(r)$ thus constitutes one way to characterize the structure of an assembly of deposited particles.

3. Density fluctuations of deposited particles

As for systems at equilibrium, the number density of deposited particles, and in particular the reduced variance of the distribution of the number of particles deposited on sub-systems of the adsorbing surface, is also a characteristic property of the system. The reduced variance can be obtained from experiments and from computer simulations in the following way. Consider a large system which can be subdivided in an ensemble of smaller sub-systems, the size of the latter being

still large compared to the size of the particles. The sub-systems have also to be independent one from each other. One can determine the number n_i of particles in each sub-system labeled by i. From the distribution of the number of particles in the sub-systems for a given coverage of the large system, one defines the reduced variance of the number as:

$$\frac{\sigma^2}{\langle n\rangle} = \frac{\dfrac{1}{\nu-1}\displaystyle\sum_{i=1}^{\nu}(n_i - \langle n\rangle)^2}{\dfrac{1}{\nu}\displaystyle\sum_{i=1}^{\nu} n_i} = \frac{\nu}{\nu-1}\frac{\displaystyle\sum_{i=1}^{\nu} n_i^2 - \nu\langle n\rangle^2}{\displaystyle\sum_{i=1}^{\nu} n_i} \tag{2.5}$$

where the sums are performed over the ν sub-systems constituting the whole system and where $\langle n\rangle$ represents the mean value of the n_i. When exactly one particle is deposited on the surface, we have obviously $\sum n_i = 1$, $\langle n\rangle = 1/\nu$ and $\sum n_i^2 = 1$, hence, $\sigma^2/\langle n\rangle = 1$. It follows that $\sigma^2/\langle n\rangle \to 1$ when $\theta \to 0$, whatever the mechanism involved in the deposition. In the special case where no interaction at all exists between the particles, $\sigma^2/\langle n\rangle = 1$ for any number of particles on the surface. This corresponds to a binomial distribution of the n_i among the ν sub-systems.

It can be proven in a general way that the reduced variance is related to the radial distribution function $g(r)$ by [5]:

$$\frac{\sigma^2}{\langle n\rangle} = 1 + \rho\int_0^{\infty}[g(r)-1]2\pi r dr. \tag{2.6}$$

This relation neglects all the effects which are due to the finite size of the sub-systems. If one takes such finite size effects into account, one can show that the reduced variance takes the following form [6, 7]:

$$\frac{\sigma^2}{\langle n\rangle} = \left(\frac{\sigma^2}{\langle n\rangle}\right)_0 + a^{-1/2}\left(\frac{\sigma^2}{\langle n\rangle}\right)_1 + a^{-1}\left(\frac{\sigma^2}{\langle n\rangle}\right)_2 \tag{2.7}$$

where $a = A/\nu$ represents the area of a sub-system. $(\sigma^2/\langle n\rangle)_0$ corresponds to the reduced variance of the number of particles for a large sub-system in which border effects can be neglected, whereas the two other terms originate from the border effects.

4. Jamming limit coverage

For a system at equilibrium in which the particles diffuse along the surface, the maximum coverage is reached when the particles organize themselves on the surface as a hexagonal crystal. Then, when each particle has six neighbors at contact, the fractional area covered amounts to $\pi/2\sqrt{3} \approx 0.91$. This, however, is not possible for irreversible deposition processes because once deposited, the particles can no longer move along the surface. This leads to a reduction of the maximum surface coverage which is observed for irreversible deposition processes if compared

to a crystallized assembly. For an infinitely large surface, this value, called the jamming limit coverage, usually denoted by θ_∞, is a well-defined number which characterizes partially the deposition process. For systems with finite area, the deposition process leads in general to a different value of the saturation coverage for each system. Indeed, the jamming limit is a stochastic quantity. Hence, the term "jamming limit" or "saturation coverage" is to be understood as the *mean value* of the highest coverage reached on a series of equal surfaces covered with the same particles under identical conditions. In other words, in contrast to systems at equilibrium which form crystals at high coverage, for sub-systems of finite area, the coverage in the jammed state fluctuates from one sub-system to another around its mean value θ_∞. The relative fluctuations are usually larger, the smaller the size of the sub-systems. This implies that for such systems, the reduced variance of the number of particles does not decrease to zero when the coverage reaches the saturation value.

3

Kinetic treatment of irreversible deposition processes by a master equation approach

The evolution of a small system S (a sub-system) which is part of a much larger one, R, can be described by a master equation [8,9]. In this approach, the evolution of the probability $q(n+1, N+1)$ to find $n+1$ particles in the sub-system S, when $N+1$ particles are deposited on R, is expressed as a function of the probabilities $q(n, N)$ and $q(n+1, N)$ by the relation:

$$q(n+1, N+1) = q(n, N)p(n+1, N+1|n, N) + q(n+1, N)p(n+1, N+1|n+1, N). \quad (3.1)$$

Note that the $(n+1)$ particles deposited on S are part of the $(N+1)$ particles deposited on R. In this equation, $p(n+1, N+1|n, N)$ and $p(n+1, N+1|n+1, N)$ represent respectively the conditional probabilities that when n (resp. $n+1$) particles are deposited on S and N particles on R, there will be $n+1$ particles adsorbed on S after the $(N+1)$th particle has adsorbed on R. For irreversible deposition processes, these conditional probabilities can be expressed in terms of the available surface function $\Phi(\theta)$. More specifically $p(n+1, N+1|n, N)$ is approximated by:

$$p(n+1, N+1|n, N) = \frac{a\Phi(\theta_a)}{A\Phi(\theta)} \quad (3.2)$$

where a (resp. A) is the area of the system S (resp. R) and θ_a (resp. θ) is the coverage of the system S (resp. R). The particles are assumed to be of unit area, therefore the coverages coincide with the number densities, $\theta = N/A$ and $\theta_a = n/a$. Expression (3.2) constitutes a mean field approximation because it is assumed that the deposition probability is only a function of the coverage of the system even for the small system S. This is certainly valid for systems of large area, but not for smaller systems, which can contain at the jamming limit less then a few tens of particles, where this probability becomes an explicit function of the "microscopic" configuration. In fact, the fluctuations of the available surface function, at a given coverage, from one configuration of deposited particles to another on the surface, become important once the exclusion surfaces associated with the deposited particles overlap. Then, Φ is no longer uniquely determined by θ.

Anyhow, in the following, we assume the mean field approximation to be valid, *i.e.*, we neglect the fact that configurations of adsorbed particles, corresponding to the same coverage, can have different available surface functions. We expect this hypothesis to be fairly correct as long as the jamming limit regime is not reached and the area a of the sub-systems not too small.

Using (3.2) and taking into account that

$$p(n, N+1|n, N) = 1 - p(n+1, N+1|n, N),$$

the master equation (3.1) can be rewritten as:

$$q(n+1, N+1) - q(n+1, N) = \frac{a}{A\Phi(\theta)} \left[q(n, N)\Phi\left(\frac{n}{a}\right) - q(n+1, N)\Phi\left(\frac{n+1}{a}\right) \right]. \quad (3.3)$$

The system R being assumed to be infinitely large, the addition of one particle produces an infinitesimal change of its coverage. The master equation can then be written in differential form:

$$\frac{\partial q(n,\theta)}{\partial \theta} = \frac{a}{\Phi(\theta)} \left[q(n-1,\theta)\Phi\left(\frac{n-1}{a}\right) - q(n,\theta)\Phi\left(\frac{n}{a}\right) \right]. \quad (3.4)$$

When the sub-system S is also large (but much smaller than R), the probability distribution $q(n,\theta)$ is expected to be strongly peaked around the average value $\langle n \rangle$ (proportional to a), and to have a width of order $a^{1/2}$. In these circumstances it is possible to make a large-system expansion of the master equation (3.4) [10]. The leading terms of that expansion yield a deterministic evolution equation for the average particle number, $\langle n \rangle$, and a linear Fokker-Planck equation for the distribution of the fluctuations. Consequently, in this limit the probability distribution becomes Gaussian and is completely characterized by its first and second moments.

The first moment of $q(n,\theta)$ gives the mean particle number, $\langle n \rangle = \sum_{n \geq 0} n q(n,\theta)$, and its evolution equation is easily obtained from (3.4):

$$\frac{d\langle n \rangle}{d\theta} = \frac{a}{\Phi(\theta)} \sum_{n \geq 0} q(n,\theta)\Phi\left(\frac{n}{a}\right) = \frac{a}{\Phi(\theta)} \left\langle \Phi\left(\frac{n}{a}\right) \right\rangle. \quad (3.5)$$

In the same way, for the second moment one obtains

$$\frac{d\langle n^2 \rangle}{d\theta} = \frac{a}{\Phi(\theta)} \left\langle (2n+1)\Phi\left(\frac{n}{a}\right) \right\rangle. \quad (3.6)$$

Provided that Φ is in general a non-linear function of θ, these equations cannot be solved analytically. However, if the area a is large enough, the fluctuations of n will be relatively small, and only values of n near $\langle n \rangle$ will contribute to the averages. In that case, one can expand $\Phi(n/a)$ as a Taylor series around $\langle n \rangle / a$:

$$\Phi\left(\frac{n}{a}\right) = \Phi\left(\frac{\langle n \rangle}{a}\right) + \left(\frac{n - \langle n \rangle}{a}\right) \Phi'\left(\frac{\langle n \rangle}{a}\right) + O\left[\left(\frac{n - \langle n \rangle}{a}\right)^2 \right], \quad (3.7)$$

where $\Phi'(x)$ denotes the derivative of $\Phi(x)$ with respect to x. Using this expansion in (3.5) one obtains the equation for the evolution of the mean particle number:

$$\frac{1}{a}\frac{d\langle n\rangle}{d\theta} = \frac{1}{\Phi(\theta)}\Phi\left(\frac{\langle n\rangle}{a}\right) + O\left(\frac{1}{a}\right). \tag{3.8}$$

The obvious solution, neglecting finite size effects, is $\langle n\rangle/a = \theta$, and expresses the fact that the mean coverage of the sub-system S is the same as the coverage of the large system R. In the same way, inserting the expansion (3.7) into equation (3.6) yields an equation for $\langle n^2\rangle$. From that equation, one can write the evolution equation for the variance $\sigma^2 = \langle n^2\rangle - \langle n\rangle^2$ (if the number ν of sub-systems is not infinitely large, refer to Eq. (2.5) for the definition of the variance):

$$\frac{1}{a}\frac{d\sigma^2}{d\theta} = 1 + 2\frac{\Phi'(\theta)}{\Phi(\theta)}\frac{\sigma^2}{a} + O\left(\frac{1}{a}\right). \tag{3.9}$$

This equation gives the relation between the variance of the adsorbed particle number and the available surface function. It is applicable, in principle, to all irreversible adsorption models whose kinetics can be described as a Markov process. Its validity is limited by the mean field assumption implied in the master equation (3.1), which fails near the jamming limit, while leading to good results for low and intermediate coverages.

For any value of the coverage, the solution of the first order differential equation (3.9), satisfying the proper initial condition for an empty surface, *i.e.*, $\sigma^2 = 0$ for $\theta = 0$, is:

$$\frac{\sigma^2}{\langle n\rangle} = \frac{\Phi^2(\theta)}{\theta}\int_0^\theta \frac{d\theta'}{\Phi^2(\theta')} \tag{3.10}$$

where $\langle n\rangle/a = \theta$ has also been used. Therefore, if $\Phi(\theta)$ is known, the variance of the number of deposited particles on sub-systems out of a large surface can be obtained by a simple quadrature. The comparison between the reduced variance determined directly from computer simulations and calculated by using the mean field relation (3.10) is shown in Figure 2a for the Random Sequential Adsorption and in Figure 2b for the Ballistic Deposition processes (these processes will be defined in the next section). These two examples illustrate the fact that the mean field approach is only valid at low to intermediate coverages and in particular that it is unable to predict the *non zero* value of $\sigma^2/\langle n\rangle$ at the jamming limit.

If the available surface function is of the form $\Phi(\theta) = 1 + a_1\theta + a_2\theta^2 + a_3\theta^3 + O(\theta^4)$, using (3.9) or (3.10) leads to the following expansion for the reduced variance:

$$\frac{\sigma^2}{\langle n\rangle} = 1 + a_1\theta + \frac{4}{3}a_2\theta^2 + \left(\frac{1}{6}a_1a_2 + \frac{3}{2}a_3\right)\theta^3 + O(\theta^4). \tag{3.11}$$

In the particular case where $a_1 = a_2 = ... = a_{k-1} = 0$ and $a_k \neq 0$, equation (3.11) takes the form:

$$\frac{\sigma^2}{\langle n\rangle} = 1 + \frac{2k}{k+1}a_k\theta^k + O(\theta^{k+1}). \tag{3.12}$$

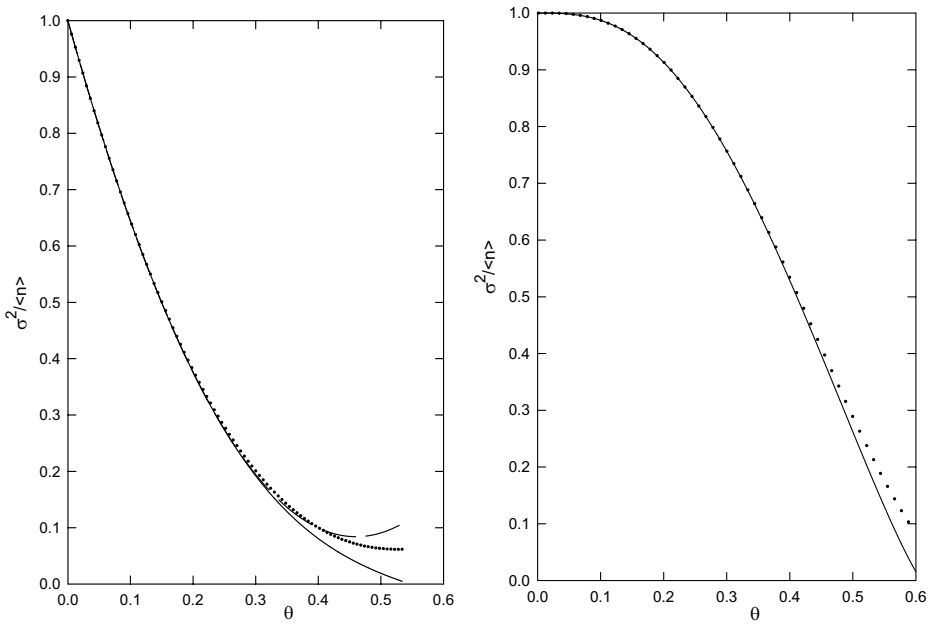

Figure 2. *(a) Reduced variance of the number of particles adsorbed as a function of the coverage in the framework of the RSA model: simulations (• • •), mean field approximation (—) calculated by using expressions (4.12, 4.13) for the available surface function and relation (3.10) between $\sigma^2/\langle n\rangle$ and Φ, third order expansion (Eq. (4.15)) (– – –). (b) Reduced variance of the number of particles adsorbed as a function of the coverage in the framework of the BD model: simulations (• • •), mean field approximation (—).*

Another demonstration of relation (3.12) based on the general relation (2.6) and on the evolution of the radial distribution function $g(r)$ due to the adsorption of a new particle can be found in the article of Bafaluy *et al.* [9]. Since this latter demonstration is rigourous, it appears that expression (3.12) is exact although it can be found by using the approximation (3.10).

The problem of the reduced variance of the number density has also been investigated by Adamczyk *et al.* [11, 12] by a method based on a combinatorial calculation of the number of possibilities that exist to deposit n particles on the sub-system S and N on the system R. They have also introduced a mean field approximation similar to that used in the master equation approach. They have found that:

$$\frac{\sigma^2}{\langle n\rangle} = \frac{\Phi(\theta)}{\left(\Phi(\theta) - \theta\dfrac{d\Phi}{d\theta}\right)} \cdot \tag{3.13}$$

This expression leads then to:

$$\frac{\sigma^2}{\langle n \rangle} = 1 + k a_k \theta^k + O(\theta^{k+1}) \tag{3.14}$$

in the particular case where $a_1 = a_2 = ... = a_{k-1} = 0$ and $a_k \neq 0$. This expression has been applied by the group of Adamczyk to the RSA case where $k = 1$. It is then equivalent to expression (3.12). For values of $k \neq 1$ it does, however, not agree with expression (3.12) so that the relation (3.13) cannot be correct in general.

4

Statistical geometry deposition models

All the models that have been developed to describe the irreversible deposition processes share a common property: the particles are deposited sequentially onto the surface and the initial location of the deposition trial is chosen randomly and uniformly above the adsorbing surface. One can then distinguish roughly between two types of models: (i) the models for which the initial position of the particle above the plane determines totally its final position if one takes the microscopic configuration of the already deposited particles into account. These models cannot account for the diffusion effects. They can be called "*statistical geometry models*" because they are exhaustively governed by the laws of statistics and geometry. The RSA and the Ballistic Deposition (BD) models are two examples of them. (ii) The "*diffusional models*" in which, even if the initial position of the trial particle is known, its final position can only be determined statistically. These models are usually developed to account for the diffusion of the particles in the bulk before reaching the deposition plane.

1. The simplest irreversible deposition model with excluded volume effect: the Random Sequential Adsorption (RSA) model

1.1. General results relative to the RSA of spheres

The simplest of all these models, which takes the irreversible nature of the adsorption process and the surface exclusion effects into account, is the Random Sequential Adsorption (RSA) model. We will now review some of the results relative to it. One must distinguish between RSA deposition processes on a lattice and RSA processes on a continuum surface. We will focus our attention mainly on this second category, the first one having been reviewed extensively by Evans [1]. The RSA model was first defined for hard spheres as follows: (i) particles are deposited sequentially; (ii) the first step of an adsorption trial consists in choosing the adsorption position of the new particle randomly over the deposition plane. If the incoming particle overlaps with an already deposited one the adsorption trial is rejected and a new trial is started, independent of the previous one; (iii) if the incoming particle does not overlap with already deposited ones it is irreversibly

fixed on the surface and can neither diffuse along the surface nor desorb from it. Adamczyk *et al.* [13,14] have proposed to extend the model to particles interacting through a repulsive potential $u(r)$. We will denote this model as the "repulsive soft core RSA". They modified the rule (ii) accordingly as follows: (ii') for the incoming particle labeled $n+1$, one calculates the total interaction potential between this particle and the n particles already deposited:

$$U_{n+1} = \sum_{j=1}^{n} u(r_{n+1,j}). \tag{4.1}$$

The probability for this adsorption trial to be successful is then given by the Boltzmann factor $\exp(-U_{n+1}/kT)$.

The RSA model was first introduced by Flory [15] to account for chemical reactions taking place along a polymer chain. The continuous version of the one dimensional RSA problem is also known under the name "car parking problem". As many other one-dimensional problems it can be solved exactly: the kinetic law, the structure of the system and the jamming limit coverage have been determined rigorously [16–19]. One of the first major contributions relative to the continuous RSA model in a space of dimension larger than one is due to Widom [3]. He showed that an RSA deposition process does not lead to the same configurations as the ones predicted by the laws of equilibrium statistical mechanics of hard spheres. He also introduced the concept of available surface function $\Phi(\theta)$ and showed that if the available surface function can be developed in a virial expansion:

$$\Phi(\theta) = 1 + a_1\theta + a_2\theta^2 + a_3\theta^3 + O(\theta^4) \tag{4.2}$$

the coefficients a_1 and a_2 are identical for RSA and for equilibrium configurations. It is only for the coefficients of order higher than 2 that differences between these two cases appear. We will give a quantitative demonstration for this result in the paragraph 1.3. One can however propose a rapid argument for the fact that a_1 and a_2 are identical for the RSA and the equilibrium cases. Let us illustrate it by the example of hard spheres. For the RSA, as well as for the equilibrium case, the available surface function is given by the mean value of the Boltzmann factor $\exp(-U(\mathbf{r})/kT)$ where $U(\mathbf{r})$ represents the interaction potential between a wandering particle on the surface and all the deposited particles (see Sect. 1 of Chap. 2). In the case of hard spheres, $U(\mathbf{r})$ is equal to either 0 or ∞. If the surface is empty, $\Phi = 1$ in both the RSA and equilibrium cases. When there is only one particle on the surface, in both cases the exclusion surface is equal to $4\pi R^2$, R being the radius of the particles so that in both cases a_1 is equal to -4 because $\theta = \pi R^2/A$ for an area A covered by only one particle. The minus sign comes from the fact that a particle excludes some area on the surface. From Figure 3 one sees that if there are two particles deposited on the surface, the exclusion area is not always equal to $8\pi R^2$, but it can be smaller because the overlapping area, denoted by $A_2(r)$, has been counted twice in the first order contribution. The coefficient

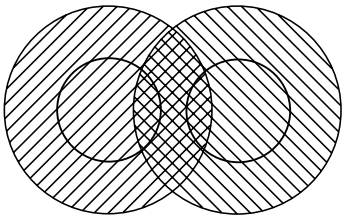

Figure 3. *Schematic representation of two particles adhering on a plane. The heavy circles represent the particles themselves. The crosshatched lens-shaped area represents the overlapping area of the two exclusion disks, noted $A_2(r)$.*

a_2 is thus given by:

$$a_2 = \frac{1}{2(\pi R^2)^2} \int_0^\infty g(r) A_2(r) 2\pi r dr. \tag{4.3}$$

In the equilibrium case, all the configurations are equiprobable so that $g(r) = H(r - 2R)$ at order zero in the particle density, $H(r - 2R)$ being the Heaviside step function equal to 0 for $r < 2R$ and equal to 1 for $r \geq 2R$. In the case of RSA, if only one particle is deposited on the surface all the positions in which a new incoming particle would not overlap with the one already present are equivalent. This implies that, when only two particles are present on the surface, $g(r)$ must also be equal to $H(r - 2R)$. Thus, according to relation (4.3), the coefficients a_2 are identical for the RSA and the equilibrium cases: $a_2 = 6\sqrt{3}/\pi$.

The fact that Φ_{RSA} becomes different from Φ_{EQ} only from the third order on in the coverage implies that experimentally it will not be possible to distinguish between the RSA and the equilibrium available surface functions at low coverages. Differences become significant for coverages larger than 25%. The coefficient a_3 has been determined for the RSA process of hard spheres [20, 21] and is equal to $\left(40/\pi\sqrt{3} - 176/3\pi^2\right) \approx 1.4069$. The expression of the available surface function for the RSA of hard spheres in the low to intermediate coverage range takes thus the form:

$$\Phi_{RSA}(\theta) = 1 - 4\theta + \frac{6\sqrt{3}}{\pi}\theta^2 + 1.4069\theta^3 + O(\theta^4). \tag{4.4}$$

Later on, Given found that the coefficient of the fourth order term was $a_4 = 0.720\,565$ [22]. Expression (4.4) is to be compared with the equilibrium virial expansion of Φ [21]:

$$\Phi_{EQ}(\theta) = 1 - 4\theta + \frac{6\sqrt{3}}{\pi}\theta^2 + 2.4243\theta^3 + O(\theta^4). \tag{4.5}$$

For particles interacting through a pair potential $u(r)$, the available surface

function is given in terms of a diagrammatic expansion by [23]:

$$\Phi_{RSA}(\theta) = 1 + \frac{\theta}{\pi d^2}\int_A d\mathbf{r} f(r) + \left(\frac{\theta}{\pi d^2}\right)^2 \int_A d\mathbf{r}_1 \int_A d\mathbf{r}_2 f(r_{01}) f(r_{02})[f(r_{12})+1] + \left(\frac{\theta}{\pi d^2}\right)^3 \Big\{ \frac{1}{3}\int_A d\mathbf{r}_1 \int_A d\mathbf{r}_2 \int_A d\mathbf{r}_3 f(r_{01}) f(r_{02}) f(r_{13}) f(r_{23})[f(r_{12})+1] + \frac{1}{3!}\int_A d\mathbf{r}_1 \int_A d\mathbf{r}_2 \int_A d\mathbf{r}_3 f(r_{01}) f(r_{02}) f(r_{03}) \times [f(r_{13})+1][f(r_{23})+1][f(r_{12})+1] \Big\} + O\left(\frac{\theta}{\pi d^2}\right)^4 . \quad (4.6)$$

In this expression $f(r)$ represents a Mayer function defined by

$$f(r) = \exp[-u(r)/kT] - 1.$$

The particle labeled 0 is fixed and all the integrations extend over the whole surface whose area is denoted by A. This expression will be derived in the paragraph 1.3.

The result of Widom proving that the RSA configurations are different from equilibrium ones is particularly well illustrated at the jamming limit. Indeed, one of the characteristic properties of an irreversible deposition process is to lead to a maximum coverage θ_∞ (the jamming limit coverage) above which one can no longer add new particles to the system and which is much smaller than the two dimensional random close packing coverage. For the two dimensional RSA case of hard spheres, θ_∞ is equal to 0.547 [24]. This value is found from computer simulations: no exact theory exists up to now to predict its value for two or higher dimensional RSA processes. Some approximate methods have been proposed to get an estimate of θ_∞. For example Dickman *et al.* [25] used a low coverage series in time in conjunction with the asymptotic power law to construct Padé approximants. This leads to a predicted value of the jamming limit coverage of 0.547 88 which is very close to the value found from computer simulations. This method, however, fails to predict the jamming limit coverage of the RSA of non spherical hard objects [26] which shows that the method is by far not general.

It has also been shown independently by Pomeau [27] and Swendsen [28] that, for hard spheres, the kinetic law describing the evolution of the coverage toward the jamming limit is a power law:

$$\theta_\infty - \theta(t) \approx K t^{-1/2} \quad (4.7)$$

where K is a constant ($K \approx 0.236$) determined from computer simulations [24]. Since the available surface function $\Phi(\theta)$ is related to the coverage by relation (2.3b), it follows that:

$$\Phi_{RSA}(\theta) \approx K_0(\theta_\infty - \theta)^3 \quad (4.8)$$

with $K_0 = 1/2K^2 \approx 8.98$. The proof of relation (4.7) is based on the fact that, once reaching a certain time t_s characterizing the beginning of the asymptotic

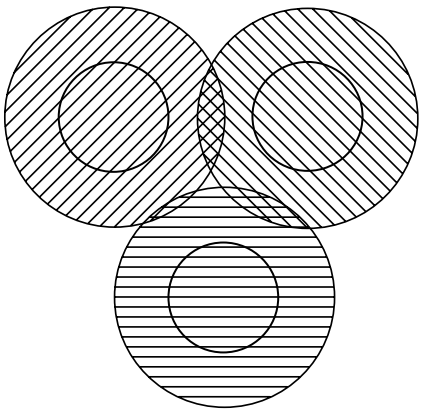

Figure 4. *Schematic representation of three particles adhering on a plane, with their exclusion disks delimiting a curvilinear triangle which may be occupied by the center of at most one new particle.*

regime, the area that remains available for the center of a new sphere consists only of isolated targets. These targets are disconnected and can be occupied by the center of only one particle each (see Fig. 4). Most of these targets are defined by three deposited particles and thus by one linear dimension, denoted by h, and by two angles. The areas of the targets characterized by the dimension h are proportional to h^2 and the kinetic equation describing the evolution of the number $n_s(h,t)$ of targets at time t characterized by h is:

$$\frac{d}{dt}n_s(h,t) = -\alpha\, h^2 n_s(h,t) \tag{4.9}$$

where α is a constant. The solution of this equation is:

$$n_s(h,t) = n_s(h,t=t_s)e^{-\alpha\, h^2(t-t_s)}. \tag{4.10}$$

Thus the coverage follows the kinetic law:

$$\theta_\infty - \theta(t) = a\int_0^{h_s}(h,t=0)e^{-\alpha\, h^2(t-t_s)}dh \tag{4.11}$$

where h_s is the largest value of h at time t_s. Finally, $n_s(h,t=t_s)$ must be a smooth function in h and since only small values of h are relevant, one can assume that $n_s(h,t=t_s) = n_s(h=0,t=t_s)$. After performing the integral in relation (4.11) one gets the kinetic law (4.7). We have given this demonstration of the relation (4.7) to emphasize the fact that it is of *purely statistical and geometrical nature*. It must be realized that the power law dependence comes from the fact that the area of the targets becomes infinitely small when $t \to \infty$. The behavior is then totally controlled by the probability that the center of a particle directly lands in such a target, which is of purely statistical and geometrical nature.

Experimentally, various attempts have been made to verify the power law kinetics and we will review these studies later. It must, however, already be pointed out that it is very difficult to verify this law due to the fact that in the asymptotic regime, near the jamming limit, the adsorption kinetics is very slow so that the experiments have to be performed over very long periods of time. Moreover, the asymptotic regime concerns only a very limited proportion of deposited particles and thus the deposition kinetic law has to be measured with great precision over a long period of time. This represents usually the worse experimental conditions.

On the other hand, one can follow quite easily kinetic laws over a very large range of coverage in the low to intermediate regime. The comparison of the experimental data to the RSA model then requires to know an expression of the available surface function over a large coverage range. This can be obtained by using an interpolation procedure between expressions (4.4, 4.8) which are valid at low and high coverage, respectively. One chooses Φ_{RSA} to be of the form:

$$\Phi_{RSA}(\theta) = (1-x)^3 f(x) \tag{4.12}$$

where $x = \theta/\theta_\infty$ and $f(x)$ is a function which depends on x and on adjustable parameters. The adjustable parameters are determined by imposing that the Taylor expansion of expression (4.12) is identical to expression (4.4). Choosing $f(x)$ of the form:

$$f(x) = 1 + c_1 x + c_2 x^2$$

allows both c_1 and c_2 to be determined. In addition, one can estimate the jamming limit coverage θ_∞. One finds $c_1 = 0.7877$, $c_2 = 0.3751$ and $\theta_\infty = 0.5531$ [29]. Note how accurate the jamming limit coverage is predicted by this procedure. This result seems to indicate that we thus possess a method to determine analytically the jamming limit coverages of RSA processes. Unfortunately, a similar method, applied to the 3-dimensional RSA case gives $\theta_\infty = 0.365$ compared to $\theta_\infty = 0.382$ determined from computer simulations [30]. In this case the method does not lead to a very accurate estimate of the jamming limit coverage.

One can also chose $f(x)$ to be of the form:

$$f(x) = (1 + c_1 x + c_2 x^2 + c_3 x^3)^{-1}. \tag{4.13}$$

One then imposes the value of θ_∞ to be equal to the value found from computer simulations (0.547). This leads to the following values of the adjustable parameters: $c_1 = -0.8120$, $c_2 = 0.2336$ and $c_3 = 0.0845$ [21].

The evolution of Φ_{RSA} as a function of the coverage θ is represented in Figure 5. One can see, in particular, the comparison between the function directly determined from computer simulations and the values calculated from expressions (4.4, 4.13). In Figure 6 one compares the adsorption kinetics determined by integration of equation (2.3b) for different expressions of Φ_{RSA}. From this figure one can point out that apparently small differences in the available surface functions can lead to large deviations in the adsorption kinetics. One can also get a good idea of the accuracy of expressions (4.4, 4.13) to describe the RSA kinetics.

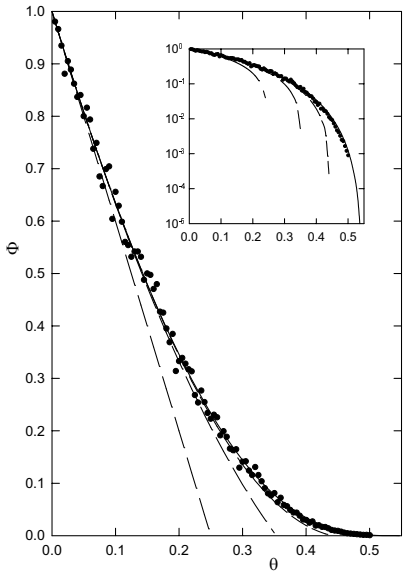

Figure 5. *Available surface function as a function of the coverage for the RSA model: simulation (• • •), rational function (Eqs. (4.12, 4.13)) (—), Taylor expansions of the first order (– – –), second order (- - -) and third order (...) (Eq. (4.4)). The inset shows the same results, except that Φ is given on a logarithmic scale.*

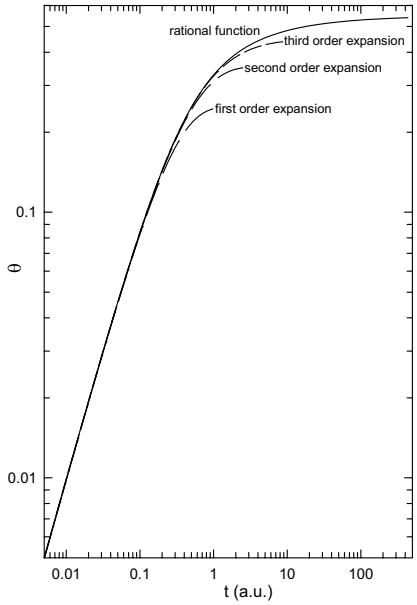

Figure 6. *RSA adsorption kinetics showing the evolution of the coverage as a function of time obtained by integration of the reciprocal (Eq. (2.4)) of the various approximations of the available surface function given in Figure 5.*

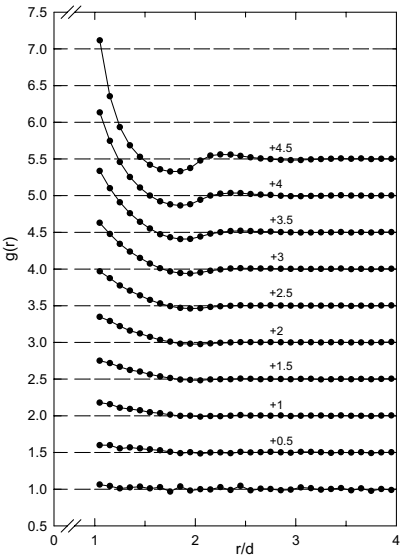

Figure 7. *Radial distribution function as a function of the center-to-center distance derived from RSA computer simulations ($d = 2R$). From bottom to top, the curves correspond to coverages of 0.05, 0.10, 0.15, ..., 0.50. Each curve is shifted by half a unit with respect to the preceding one for the sake of clarity.*

The determination of the kinetic law is one way to characterize the deposition process. It is often taken to analyze the adsorption of proteins or very small particles which are not visible by optical microscopy usually employed for larger particles. For such particles one determines also structural properties of the assembly of deposited spheres and in particular the evolution of the radial distribution function $g(r)$ with the coverage. For the RSA case it is usually obtained by computer simulations and some examples are shown in Figure 7. On this figure one can see that at low coverage almost no peak is visible. A first peak shows up for coverages of the order of 0.10 and, at coverages higher than 0.40, a second peak can be distinguished. However, the RSA deposition process never leads to correlation distances between the deposited particles exceeding two or three particle diameters. It has been shown theoretically and by computer simulations that at the jamming limit, the radial distribution function diverges at contact as $\ln(r/2R-1)$ [24]. This property is, however, very difficult to verify experimentally for various reasons such as the particle polydispersity or the precision in the measurements of the particle positions. Moreover, as we will discuss, such a behavior does certainly not exist in real physical situations due to hydrodynamic interactions between depositing and adsorbed particles.

Almost all these results have been determined from computer simulations. However, starting from a diagrammatic expansion of the kinetic equations on the n-particle distribution functions, Tarjus *et al.* [23] proposed an approximate integral equation equivalent to the equilibrium Percus-Yevick equation. This equation

can be written in the form:

$$\frac{1}{2\rho}\frac{\partial}{\partial\rho}\left[\rho^2 h(r_{12})\right] = C(r_{12}) + \rho\int d\mathbf{r}_3 C(r_{13})h(r_{32}) \tag{4.14}$$

with $h(r) = 1 - g(r)$ and $C(r)$ corresponds to the mixed correlation function [31]; r_{ij} represents the distance between particle i and particle j. This equation has also been derived for the RSA case by Given and Stell [32]. Introducing an additional closure condition relating $C(r)$ to the n-particle distribution functions, this equation could be solved numerically for the RSA of hard spheres in the 1, 2 and 3-dimensional cases [31] and provides a numerical approximation of $g(r)$. The $g(r)$ thus determined appears to be accurate in a large range of coverage. At the highest physically meaningful coverages, the approximate pair correlation function displays, however, a small dephasing compared to the exact result and does not show the logarithmic divergence at contact which is a characteristic feature of the RSA radial distribution function at the jamming limit.

As it was mentioned, the reduced variance of the number of particles deposited in sub-systems also constitutes a parameter which characterizes the deposition process and which can be determined experimentally. Inserting the third order expansion of Φ given by equation (4.4) into the general relation between σ^2 and Φ (expression (3.10)) leads to:

$$\frac{\sigma^2}{\langle n\rangle} = 1 - 4\theta + \frac{8\sqrt{3}}{\pi}\theta^2 + \left(\frac{16\sqrt{3}}{\pi} - \frac{88}{\pi^2}\right)\theta^3 + O(\theta^4). \tag{4.15}$$

In the low coverage regime, this expression reduces to $\sigma^2/\langle n\rangle \approx 1 - 4\theta$. It can be noticed that this means that the reduced variance decreases linearly with θ in this low coverage range, exactly as does Φ itself. This is a signature of a process where one particle deposited on the surface is sufficient to hinder a new one to adsorb. By using the expression (4.13) for the available surface function and again the relation (3.10) one can get an approximation of the evolution of the reduced variance of the number density over a large coverage range as shown in Figure 2a. From this figure one can also see that near the jamming limit, the approximation based on relation (3.10) fails because it predicts that $\sigma^2/\langle n\rangle$ vanishes at θ_∞, whereas for the real irreversible process it remains strictly positive. Indeed, the relation (3.10) implies that $\sigma^2/\langle n\rangle$ vanishes at the jamming limit as Φ^2. However, for irreversible deposition processes the jamming limit varies from one surface to another and thus, even at the jamming limit, the density fluctuation can never become zero. Thus, all the mean field approximations used to derive the evolution of $\sigma^2/\langle n\rangle$ with θ fail in the asymptotic regime. Similar conclusions can be drawn from the comparison between the value of $\sigma^2/\langle n\rangle$ determined from the general expression (2.6), the radial distribution function corresponding to the Percus-Yevick like $g(r)$ and the reduced variance directly determined from computer simulations [31].

1.2. Extension to non spherical hard objects

We have, up to now, described the RSA model of hard spheres. However, a large variety of molecules, especially proteins, are non spherical and can often, in first approximation, be considered as spherocylinders (*e.g.*, fibrinogen) or ellipsoids (*e.g.*, albumin). This constitutes one of the major reasons why the RSA model has been extended to non spherical but still hard objects. These objects can be characterized by a length and an aspect ratio α which is defined as the ratio of the longest to the shortest dimension of the particles in the case of ellipses and spherocylinders. Thus, an aspect ratio of 1 corresponds to spheres, whereas a large aspect ratio indicates that the particles are needle-like.

The methods developed for hard spheres to determine the available surface function have been extended to non-spherical hard objects. Ricci *et al.* [26] calculated the coefficients of the low coverage expansion (4.2) up to the third order. They found that, whereas the expression of Φ truncated at the third order term in the coverage provides a better approximation over a wider coverage range than the expression truncated at the second order term for values of $\alpha < 5$, the contrary is observed for $\alpha > 5$.

The asymptotic kinetic law of non spherical objects, first mentioned by Swendsen [28], has also been investigated. This author stated that, as for hard spheres, adsorption kinetics of hard ellipses, or more generally of elongated objects, should follow the power law (4.7). It has been shown later on, however, that an additional degree of freedom has to be taken into account during the adsorption of elongated particles: instead of two degrees of freedom corresponding to the two coordinates of the center of the particles, one has for elongated objects a third degree of freedom corresponding to the angular position of the object. The asymptotic power law thus becomes [33]:

$$\theta(\infty) - \theta(t) \propto t^{-1/d} \tag{4.16}$$

where d is the number of degrees of freedom which is equal to 3 in the case of elongated particles. Viot *et al.* [34] refined this analysis and found that, in fact, there exist two classes of targets in the asymptotic regime: non selective and selective targets. A target is said to be non selective if an object placed in this target can be freely rotated by any angle ranging from 0 to 2π with only slightly displacing the center of the particle. A selective target, on the other hand, is such that it is only in a limited range of orientations that the target can accommodate a particle. The first class of targets corresponds to the case $d = 2$ whereas for the selective targets $d = 3$. The non selective targets thus disappear much more rapidly than the selective ones, according to the asymptotic power law (4.7), whereas the selective targets disappear following the power law $t^{-1/3}$.

The asymptotic regime can thus also be roughly subdivided in two regimes. Viot *et al.* [34] have shown that the characteristic crossover time where the system changes from one behavior to the other goes as $(\alpha-1)^{-1/2}$. The $t^{-1/3}$ time domain

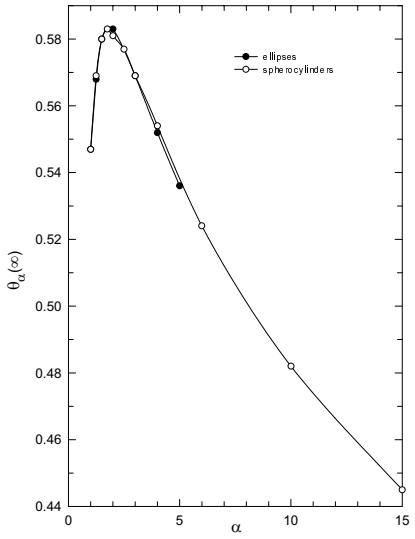

Figure 8. *Jamming limit coverage as a function of the elongation parameter α corresponding to an RSA process of spherocylinders and ellipses (taken from Refs. [26, 34]). See also Table 1.*

thus shrinks as $\alpha \to 1$. Finally, it has also been shown by these authors that the $t^{-1/2}$ term has an additional time dependence:

$$\theta(\infty) - \theta(t) \propto \frac{\exp\left[-(\propto -1)^2 t\right]}{\sqrt{t}} \,. \tag{4.17}$$

This additional exponential term is responsible for the fact that for $\alpha > 1.5$, the $t^{-1/2}$ behavior could not be observed in computer simulations.

The evolution of the jamming limit coverage with the aspect ratio α has also been investigated. It was found that $\theta_\alpha(\infty)$ passes through a maximum and decreases strongly when α becomes large. For spherocylinders and ellipses, this maximum is found at $\alpha \cong 1.75$ as can be seen in Figure 8. For rectangles, also studied by Viot *et al.* [34], the jamming limit coverage goes through a maximum for α equal to approximately 1.618. It may be interesting to mention that this value corresponds to the golden section but we have no explanation for this observation.

Finally, as for hard spheres, one can obtain an approximate expression for the available surface function by using an interpolation procedure between the low coverage and the asymptotic expressions of $\Phi(\theta)$. Due to the fact that in the final asymptotic regime the kinetic law is given by expression (4.16) with $d = 3$, one finds:

$$\Phi(\theta) = q\left[\theta_\alpha(\infty) - \theta_\alpha(t)\right]^4 \tag{4.18}$$

where q is independent of the coverage and varies slowly with the aspect ratio α.

Table 1. Jamming limit coverage $\theta_\alpha(\infty)$ for spherocylinders and ellipses as a function of the elongation parameter α [26, 34]. Note that when $\alpha = 1$, both spherocylinders and ellipses reduce to spheres or disks for which $\theta(\infty) = 0.547$.

spherocylinders			
α	simulation	equation (4.19) with exponent $+1$	equation (4.19) with exponent -1
1	0.547	0.553	0.503
1.25	0.569	0.644	0.624
1.5	0.580	0.633	0.613
1.75	0.583	0.620	0.605
2	0.581	0.607	0.596
2.5	0.577	0.579	0.569
3	0.569	0.552	0.547
4	0.554	0.504	0.501
6	0.524	0.426	0.440
10	0.482	0.326	0.348
15	0.445	0.252	0.274
ellipses			
α	simulation	equation (4.19) with exponent $+1$	equation (4.19) with exponent -1
1	0.547	0.553	0.503
1.25	0.568		
1.5	0.580		
2	0.583	0.606	0.589
3	0.569		
4	0.552	0.492	0.499
5	0.536	0.446	0.462

As for the hard sphere case, two fitting functions were proposed:

$$\Phi = (1-x)^4(1 + c_{\pm 1}x + c_{\pm 2}x^2)^{\pm 1} \tag{4.19}$$

where $x = \theta_\alpha/\theta_\alpha(\infty)$. The parameters $\theta_\alpha(\infty)$, $c_{\pm 1}$, $c_{\pm 2}$, are determined by matching the Taylor series of these fitting functions with the known low coverage expansion to third order. It was shown that both expressions provide a good estimate of the available surface function Φ over the whole coverage range. Nevertheless, the expression (4.19) with the exponent -1 constitutes a better approximation. We have seen that for the hard sphere case, this procedure allowed to get a good estimate of the jamming limit coverage. As can be seen in Table 1, this is no longer the case for elongated objects.

1.3. Diagrammatic treatment of the RSA adsorption kinetics

We will now give the diagrammatic treatment of the RSA adsorption kinetic of hard spheres. We will focus our attention only on the terms up to third order in the number density ρ of adsorbed particles, but the method is general and can be extended to higher order terms. We will make use in this paragraph of the n-particle distribution function [35] denoted by $\rho^{(n)}(\mathbf{r}_1, \mathbf{r}_2, \dots \mathbf{r}_n)$. The quantity $\rho^{(n)}(\mathbf{r}_1, \mathbf{r}_2, \dots \mathbf{r}_n) d\mathbf{r}_1 d\mathbf{r}_2 \dots d\mathbf{r}_n$ represents the probability to find the center of a particle in the surface element $d\mathbf{r}_1$ around the position $\mathbf{r}_1$, the center of a second particle in the surface element $d\mathbf{r}_2$ around the position $\mathbf{r}_2$, ..., the center of a nth particle in the surface element $d\mathbf{r}_n$ around the position $\mathbf{r}_n$. In order to simplify the notations, the following shorthand notation will be used:

$$\rho^{(n)}(\mathbf{r}_1, \mathbf{r}_2, ..., \mathbf{r}_n) d\mathbf{r}_1 d\mathbf{r}_2 ... d\mathbf{r}_n = \rho^{(n)}(1, 2..., n) d1 d2 ... dn.$$

Let us take a portion S of the adsorption surface. We will first derive a fundamental relation due to Reiss *et al.* [36] which relates the probability to find the surface S empty of particles to the mean number of particles, of pairs of particles, ... adsorbed on S. This relation will serve in the derivation of the master equation characterizing the kinetic process.

Let p_0 be the probability to find the surface S empty of particles, p_1 the probability to find *exactly* one particle in S, ... p_n the probability to find *exactly* n particles adsorbed on the surface S. One then has the trivial relation:

$$p_0 + \sum_{n=1}^{\infty} p_n = 1.$$

This relation can be rewritten as:

$$p_0 - \sum_{n=1}^{\infty} \{[1 + (-1)]^n - 1\} p_n = 1.$$

By applying the binomial formula one gets:

$$p_0 = 1 + \sum_{m=1}^{\infty} (-1)^m \sum_{n=m}^{\infty} C_n^p p_n.$$

This reads:

$$p_0 = 1 - (p_1 + 2p_2 + 3p_3 + \dots) + (p_2 + 3p_3 + 6p_4 + \dots) - (\dots). \qquad (4.20)$$

The second term of the right hand side of relation (4.20) represents the mean number of particles in the area S, the third term corresponds to the mean number of pairs of particles in $S \dots$ Relation (4.20) constitutes the fundamental relation that we were looking for.

Let us now turn to the kinetic equation of the adsorption process on a surface whose area we chose equal to unity without loss of generality. We will follow a

procedure which is discussed in more general terms in reference [23]. We will, in the first stage of this analysis, take into account the possibility of particle desorption from the surface. According to the generalization of the relation (2.3b) to the adsorption/desorption case, and using an appropriate time rescaling, the number density ρ of adsorbed particles follows the equation:

$$\frac{d\rho}{dt} = \Phi - k\rho \tag{4.21}$$

where k corresponds to the desorption constant. As shown in Chapter 2, the available surface function Φ represents the probability that, when a particle arrives randomly over the surface, it will find space to adsorb. Hence, to determine Φ one has to answer the question: by choosing a position $\mathbf{r}$ randomly over the adsorption surface, what is the probability that there is no center of a particle in a disk C of radius $2R$, centered on $\mathbf{r}$, R being the radius of the hard spheres? The available surface function Φ is then equal to p_0, where p_0 represents the probability that the disk C is empty of particles.

To calculate the probability p_0 let us place a virtual particle at the center of the disk C. We will choose the origin of the surface at this position. Each adsorbed particle whose center lies in the disk of radius $2R$ overlaps with this virtual particle. Let us introduce the Mayer function defined by $f(\mathbf{r}) = -1$ when $|\mathbf{r}| < 2R$ and $f(\mathbf{r}) = 0$ otherwise. The Mayer function associated with a particle is thus equal to -1 when the center of the particle lies in the disk of radius $2R$, and is equal to 0 otherwise. The fundamental relation (4.20) can then be written as:

$$p_0 = 1 + \int \rho^{(1)}(2) f(1,2) d2 + \frac{1}{2!} \iint \rho^{(2)}(2,3) f(1,2) f(1,3) d2 d3 + \frac{1}{3!} \iiint \rho^{(3)}(2,3,4) f(1,2) f(1,3) f(1,4) d2 d3 d4 + \ldots \tag{4.22}$$

where $f(1,2)$ stands for $f(\mathbf{r}_{12})$. The integrals extend over the whole adsorption surface of area unity and $\mathbf{r}_1$ corresponds to the position of the center of the disk C. The second term of the right hand side of relation (4.22) represents the mean number of particles in the disk C. The minus sign appearing in relation (4.20) is taken into account by the fact that the Mayer function is negative. The third term of the right hand side of relation (4.22) corresponds to the mean number of pairs in the disk $C \ldots$ It is clear from the expression (4.22) that one needs to know the distribution functions $\rho^{(1)}(1)$, $\rho^{(2)}(1,2) \ldots$ to determine the available surface function.

The equation (4.21) is in fact the kinetic equation for $\rho^{(1)}(1)$ because $\rho^{(1)}(1) = \rho$, the surface being assumed homogeneous, and p_0 in expression (4.22) corresponds to the available surface function Φ. Let us now write the kinetic equation for the two particle distribution function. One has:

$$\frac{d}{dt}\rho^{(2)}(1,2) = \rho^{(1)}(1) P_c(1|2) + \rho^{(1)}(2) P_c(2|1) - 2k\rho^{(2)}(1,2) \tag{4.23}$$

where $P_c(1|2)$ represents the conditional probability that knowing that there is a particle at position $\mathbf{r}_1$, a particle can adsorb at the position $\mathbf{r}_2$. Let us denote by $e(1,2)$ the function defined by:

$$e(1,2) = \exp[-u(\mathbf{r}_{12})/kT] = 1 + f(1,2).$$

By using the fundamental relation (4.20) to express the conditional probabilities $P_c(1|2)$ and $P_c(2|1)$, relation (4.23) can be rewritten as:

$$\begin{aligned}\frac{d}{dt}\rho^{(2)}(1,2) = \rho^{(1)}(1)\Bigg[e(1,2) + \int \frac{\rho^{(2)}(1,3)}{\rho^{(1)}(1)} f(2,3)e(1,2)d3 \\ + \frac{1}{2!}\iint \frac{\rho^{(3)}(1,3,4)}{\rho^{(1)}(1)} f(2,3)f(2,4)e(1,2)d3d4 + \dots\Bigg] \\ + \rho^{(1)}(2)\Bigg[e(1,2) + \int \frac{\rho^{(2)}(2,3)}{\rho^{(1)}(2)} f(1,3)e(1,2)d3 \\ + \frac{1}{2!}\iint \frac{\rho^{(3)}(2,3,4)}{\rho^{(1)}(2)} f(1,3)f(1,4)e(1,2)d3d4 + \dots\Bigg] - 2k\rho^{(2)}(1,2).\end{aligned} \tag{4.24}$$

Due to the fact that the different integrations are not performed over the variables $\mathbf{r}_1$ and $\mathbf{r}_2$, relation (4.24) can be rewritten as:

$$\begin{aligned}\frac{d}{dt}\rho^{(2)}(1,2) = e(1,2)\Bigg[\rho^{(1)}(1) + \int \rho^{(2)}(1,3)f(2,3)d3 \\ + \frac{1}{2!}\iint \rho^{(3)}(1,3,4)f(2,3)f(2,4)d3d4 + \dots \\ + \rho^{(1)}(2) + \int \rho^{(2)}(2,3)f(1,3)d3 + \dots\Bigg] - 2k\rho^{(2)}(1,2).\end{aligned} \tag{4.25}$$

The term $e(1,2)$ assures that the particles located at the position $\mathbf{r}_1$ and $\mathbf{r}_2$ do not overlap. One can write similarly the kinetic equation for the 3-particle distribution function. One finds:

$$\begin{aligned}\frac{d}{dt}\rho^{(3)}(1,2,3) = e(1,2)e(1,3)e(2,3)\Big\{\rho^{(2)}(1,2) + \rho^{(2)}(1,3) + \rho^{(2)}(2,3) \\ + \int \rho^{(3)}(1,3,4)f(2,4)d4 + \int \rho^{(3)}(1,2,4)f(3,4)d4 \\ + \int \rho^{(3)}(2,3,4)f(1,4)d4 + \frac{1}{2!}\iint \rho^{(4)}(1,3,4,5)f(2,4)f(2,5)d4d5 \\ + \dots\Big\} - 3k\rho^{(3)}(1,2,3).\end{aligned} \tag{4.26}$$

Similar kinetic equations exist for all the n-particle distribution functions. One thus ends-up with a hierarchy of kinetic equations which constitute the kinetic counterpart of the Kirkwood-Salzburg equations describing equilibrium configurations [23]. These Kirkwood-Salzburg equations are found from our hierarchy by assuming equilibrium, *i.e.*, $d\rho^{(n)}/dt(1,\dots,n) = 0$ as we will see later on.

Let us now first concentrate on the RSA case which corresponds to $k = 0$ (no desorption). Our goal is to derive the density expansion of the available surface function Φ. Let us introduce the function $y_n(1, \ldots, n)$ defined by:

$$\rho^{(n)}(1, \ldots, n) = \left(\prod_{1<j\leq n} e(i, j) \right) y_n(1, \ldots, n)\rho^n. \tag{4.27}$$

The advantage of the y_n functions is that they tend to 1 when $\rho \to 0$ whatever the positions $\mathbf{r}_1, \ldots, \mathbf{r}_n$ on the adsorption surface. The expression (4.22) can then be rewritten as:

$$\Phi = 1 + \rho \int f(1, 2)d2 + \frac{\rho^2}{2!} \int e(2, 3)y_2(2, 3)f(1, 2)f(1, 3)d2d3 + \ldots \tag{4.28}$$

In order to get the density expansion we have to determine the evolution of the n-particle distribution functions with the density and not with time. Using equation (4.25) one gets, for example for the two particle distribution function:

$$\begin{aligned} \Phi \frac{d}{d\rho} \left\{ \rho^2 y_2(1, 2) \right\} = 2\rho &+ \rho^2 \int y_2(1, 3)e(1, 3)f(2, 3)d3 \\ &+ \rho^2 \int y_2(2, 3)e(2, 3)f(1, 3)d3 \\ &+ \frac{\rho^3}{2!} \iint y_3(1, 3, 4)e(1, 3)e(1, 4)e(3, 4)f(2, 3)f(2, 4)d3d4 + \ldots \end{aligned} \tag{4.29}$$

Similar expressions can be found for the other n-particle distribution functions. Let us now define the functions $\beta_k^{(n)}(1, \ldots, n)$ by:

$$\Phi = \sum_{k=0}^{\infty} \beta_k^{(1)}(1)\rho^k \tag{4.30a}$$

and

$$y_n(1, \ldots, n) = \sum_{k=0}^{\infty} \beta_k^{(n)}(1, \ldots, n)\rho^k. \tag{4.30b}$$

By substituting these expressions into the equations (4.28, 4.29), and by using the fact that $\beta_0^{(n)}(1, \ldots, n) = 1$, one can determine all the β functions.

Let us determine the available surface function up to the third order in the coverage. By introducing the relation (4.30b) for $y_2(1, 2)$ up to the first order in

the density in expression (4.28) one gets:

$$\Phi = 1 + \rho \int f(1,2)d2 + \frac{\rho^2}{2!} \iint e(2,3)f(1,2)f(1,3)d2d3 + \frac{\rho^3}{3!} \iiint e(2,3)e(2,4)e(3,4)f(1,2)f(1,3)f(1,4)d2d3d4 + \frac{\rho^3}{2!} \iint e(2,3)\beta_1^{(2)}(2,3)f(1,2)f(1,3)d2d3 + \ldots \quad (4.31)$$

It remains to determine the function $\beta_1^{(2)}(2,3)$. This can be achieved by comparing the terms of second order in the density ρ in relation (4.29). One then obtains:

$$\left\{1 + \rho \int f(1,2)d2 + \ldots\right\}\left\{2\rho + 3\rho^2\beta_1^{(2)}(1,2) + \ldots\right\} = 2\rho + 2\rho^2 \int e(1,3)f(2,3)d3 + \ldots \quad (4.32)$$

which leads to:

$$\beta_1^{(2)}(1,2) = \frac{2}{3} \int f(1,3)f(2,3)d3. \quad (4.33)$$

This gives finally the following expression for the available surface function Φ:

$$\Phi = 1 + \rho \int f(1,2)d2 + \frac{\rho^2}{2!} \iint e(2,3)f(1,2)f(1,3)d2d3 + \frac{\rho^3}{3!} \iiint e(2,3)e(2,4)e(3,4)f(1,2)f(1,3)f(1,4)d2d3d4 + \frac{\rho^3}{3} \iiint e(2,3)f(2,4)f(3,4)f(1,2)f(1,3)d2d3d4 + \ldots \quad (4.34)$$

This expression is identical to (4.6) and all the coefficients appearing in it can be calculated and lead to the expression (4.4). It must be pointed out that expression (4.4) has first been obtained by a simpler, but in spirit equivalent, procedure as the one outlined here. On the other hand, this method is more general and gives, in principle, the full diagrammatic expansion of the available surface function relative to the RSA adsorption process. From this expression one could also derive the integral equation which has served in the derivation of the Percus-Yevick like distribution function.

One can now also perform a calculation of the available surface function for the equilibrium case when desorption is allowed. By setting the equations (4.21, 4.25, 4.26) to zero, one gets:

$$\rho e(1,2)\left\{2\rho + 2\int \rho^{(2)}(1,3)f(2,3)d3 + \ldots\right\} = 2\Phi\rho^{(2)}(1,2) \quad (4.35a)$$

and

$$\rho e(1,2)e(1,3)e(2,3)\Big\{\rho^{(2)}(1,2)+\rho^{(2)}(1,3) + \rho^{(2)}(2,3)+\int \rho^{(3)}(1,3,4)f(2,4)d4+\ldots\Big\} = 3\Phi\rho^{(3)}(1,2,3). \quad (4.35b)$$

Similar equations can be found for higher order distribution functions. This hierarchy of equations constitutes the Kirkwood-Salzburg equations which characterizes the equilibrium state [35]. One can then follow a procedure similar to that developed for the RSA case to calculate the expansion of Φ in the coverage. Relation (4.31) remains valid for this case. Let us determine, here too, the function $\beta_1^{(2)}(2,\,3)$. By using relations (4.35a, 4.35b) one gets:

$$2\rho^2+2\rho^3\int e(1,3)f(2,3)d3 = 2\left\{1+\rho\int f(1,2)d2+\ldots\right\}\left\{\rho^2+\rho^3\beta_1^{(2)}(1,2)+\ldots\right\}. \quad (4.36)$$

This leads to

$$\beta_1^{(2)}(1,2)=\int f(1,3)f(2,3)d3 \quad (4.37)$$

so that one finally gets the expression of the equilibrium available surface function:

$$\Phi = 1+\rho\int f(1,2)d2+\frac{\rho^2}{2!}\iint e(2,3)f(1,2)f(1,3)d2d3 + \frac{\rho^3}{3!}\iiint e(2,3)e(2,4)e(3,4)f(1,2)f(1,3)f(1,4)d2d3d4 + \frac{\rho^3}{2!}\iiint e(2,3)f(2,4)f(3,4)f(1,2)f(1,3)d2d3d4+\ldots \quad (4.38)$$

Comparing the expressions (4.34, 4.38) one finds, as it was stated previously, and proven by Widom [3], that Φ_{RSA} is equal to Φ_{EQ} up to the second order in the density (or coverage). It is only from the third order term on that differences appear. As for the RSA case, all the terms appearing in relation (4.38) can be calculated to give the expression (4.5) for the equilibrium available surface function.

2. Generalized RSA models

2.1. Random site model

The usual random sequential adsorption model can further be extended to account for non homogeneous adsorbing surfaces. In other words, in contrast with one of the basic rules of the RSA model, a given point on the surface is not equivalent to

any other point [37]. Point sites, separated by at least a distance $d' \geq 0$, are first distributed randomly over the surface. Then, one of these points is selected at random and receives the orthogonal projection of the center of a spherical particle if this latter does not overlap with a preadsorbed particle. If overlap occurs the trial is rejected and a new site is chosen. The adsorption is considered as irreversible as in the usual RSA model. This model is aimed at the description of affinity chromatography, where ligands immobilized on the adsorbent bind selectively with a desired solute.

Clearly, the number of available sites decreases when the number of adsorbed particles increases and becomes eventually zero. Then, as for the usual RSA, the jammed state is reached. It must be realized that, in general, only part of the sites are the locations of particle centers, but all the others are inhibited due to the volume excluded by other adhering particles. In the limit of an infinite surface density of sites (which can only be achieved if $d' = 0$), this model (called RSA-RS) is identical with the classical RSA (or continuous surface RSA). Note also that if the minimum site spacing d' is larger than the particle diameter d, the process follows simply the Langmuir model.

In the case where $d \gg d'$, one of the striking results found by Jin *et al.* [37] is that the kinetics of the coverage process in RSA-RS is connected to the kinetics of RSA by a so-called mapping. More specifically, the coverage $\theta(\tau)$ reached in RSA after a time τ, is obtained in RSA-RS after a time t, these times being related by:

$$\tau = \alpha(1 - e^{-t/\alpha}). \tag{4.39}$$

In this relation, the parameter α is the dimensionless site density defined by:

$$\alpha = \frac{\pi d^2}{4}\rho_s \tag{4.40}$$

where ρ_s is the number of sites per unit surface area.

2.2. RSA of soft spheres. The equivalent hard sphere concept

The hard core interaction constitutes a first approximation to capture the essential features of the deposition process. However, particles, and even molecules, do never behave exactly as hard spheres but interact for example through electrostatic or van der Waals forces. It is to take the influence of these forces during the deposition process into account that Adamczyk *et al.* [13, 14] have extended the definition of the RSA process to "soft particles" (repulsive soft core RSA). As mentioned in paragraph 1.1, in the repulsive soft core RSA model, the deposition probability of a particle at a position $\mathbf{r}$ characterized by a potential energy $\phi(\mathbf{r})$ is proportional to the Boltzmann factor $\exp[-\phi(\mathbf{r})/kT]$. Studies relative to this extended RSA model have been extensively reviewed in reference [2] and we will only mention its essential features.

In the studies of the RSA of soft particles, the interaction potential between particles has always been an exponentially decaying Yukawa potential originating

from the double layer interactions:

$$\phi(r) = \frac{2\phi_0}{x} \exp(-\kappa R(x-2)) \tag{4.41}$$

with $x = r/R$ where R corresponds to the radius of the particles and r to the center-to-center distance of two spheres. In addition, it has been assumed that the potentials are additive. The parameter κ corresponds to the inverse of the Debye length of the fluid and ϕ_0 represents the interaction potential energy between two particles at contact. The comparison between experimental results and the predictions of this model is, however, not easy because there exist neither analytical results for the first coefficients of the coverage expansion of the available surface function nor an estimate of the jamming limit coverage as a function of the parameters entering in the potential (*i.e.*, ϕ_0 and κR). To circumvent these difficulties, Adamczyk *et al.* [2,13,14,38] introduced the concept of equivalent hard sphere radius r^*. To this end they introduced the dimensionless effective interaction range defined by:

$$r^* = R(1 + H^*). \tag{4.42}$$

They have given an estimate of H^* by assuming that r^* corresponds to the interparticle distance at which the potential (4.41) reaches a critical value ϕ_{ch} that they have taken equal to $10kT$. The estimate of H^* is given by:

$$H^* = \frac{1}{\kappa R} \ln \xi - \frac{1}{\kappa R} \ln \left(1 + \frac{1}{2\kappa R} \ln \xi \right) \tag{4.43}$$

where $\xi = \phi_0/\phi_{ch}$ [2]. The repulsive soft core RSA model is then approximated by a hard sphere RSA model of particles interacting through a hard core potential, the radius being r^*. The coverage of the surface is, however, estimated with the geometric radius R. In particular, the first and second coefficients of the coverage expansion of the available surface function are given by:

$$a_1 = a_{1,H^*=0}(1 + H^*)^2 \tag{4.44}$$

$$a_2 = a_{2,H^*=0}(1 + H^*)^4 \tag{4.45}$$

where $a_{1,H^*=0}$ and $a_{2,H^*=0}$ correspond to the coefficients at $H^* = 0$. The jamming limit coverage θ_{mx} is also estimated by a simple scaling:

$$\theta_{mx} = \frac{\theta_\infty}{(1 + H^*)^2} \cdot \tag{4.46}$$

Furthermore, this model predicts that for long adsorption times the kinetic law is of the form:

$$\theta(\infty) - \theta(t) = \frac{\alpha t^{-1/2}}{(1 + H^*)^2} \tag{4.47}$$

where α is a constant independent of H^*.

This approach seems, at first sight, very crude and there is no theoretical basis for its validity. Nevertheless, it can constitute a first empirical approach whose validity can only be tested by comparing its predictions to those determined directly from computer simulations using the repulsive hard core RSA. Using the repulsive soft core RSA, Adamczyk *et al.* have indeed shown that $\theta(t)$ varies linearly with $t^{-1/2}$ over a significant range of time. However, for very long adsorption times, the adsorption kinetics deviates systematically from this power law. Moreover, they have compared the jamming limit coverage relative to the repulsive soft core RSA to the predictions given by expression (4.46) relative to the equivalent hard sphere concept. A problem emerges at this point: in the repulsive soft core RSA model, like in any other model devised to describe the irreversible adsorption, the available space for adsorbing new particles consists in small targets, when the adsorbing surface approaches the jammed state. Even the lowest (repulsive) potential in these targets can be very high. As a consequence, the adsorption probability in these targets becomes extremely small. From the experimental point of view, an infinite (hence unrealistic) experimental time would be required to have these targets filled. This problem is related to the fact that there exists an additional parameter, *i.e.*, the maximum adsorption time, which should be introduced for this model to become complete. This problem will also be found in the diffusional models discussed in the next paragraph. Adamczyk *et al.* [13] have chosen to define the jamming limit coverage by extrapolating the $t^{-1/2}$ law of the coverage with time up to $t = \infty$. This coverage was compared over a large domain of values of κR to expression (4.46). A fairly good agreement was observed for values of $\kappa R > 10$, whereas for smaller values ($\kappa R < 10$) the value predicted by (4.46) was systematically smaller than the value found by means of computer simulations, the difference being of the order of 10% for $\kappa R = 4$. On the other hand, as far as the radial distribution function is concerned, one can expect that the two models (repulsive soft core RSA and equivalent hard sphere RSA) will give different results, the $g(r)$ being sensitive to the short range interactions. Such a comparison has, however, not been published to our knowledge. The equivalent hard sphere concept thus seems to appear as a useful, but empirical, first approach to analyze experimental results relative to irreversible deposition processes of small particles.

Recently, Oberholzer *et al.* [39] extended this generalized RSA algorithm to take not only the interactions between the depositing particle and the particles already adsorbed on the surface into account but also the interactions between the depositing particles and the adsorption plane into account. To do so they define an adsorption trial as follows: they select a random position over the deposition plane. They then assume that the particles follow a straight line toward the surface. At each position of the particle they calculate the interaction energy between the depositing particle and the adsorbed particles as well as the deposition surface. They assume pairwise additivity of the interaction potentials to determine the maximum U_{max} of this potential. Two procedures are then proposed. In a first one, if $U_{max} < U_b$ the particle is irreversibly adsorbed at the surface at the position of contact between the depositing particle and the surface. Otherwise the particle is rejected and a new trial is started. The value of U_b constitutes a parameter

which can be varied when comparing the simulation results to experimental data. In a second procedure, the adsorption trial is rejected as previously if $U_{max} > U_b$ whereas if $U_{max} < U_b$ it is accepted with a probability $\exp(-\Delta U/kT)$ where $\Delta U = U_{max} - U_b$. They have determined for both algorithms radial distribution functions and have shown that in first approximation both lead to a power law dependence for the asymptotic kinetic regime which goes as $t^{-1/2}$.

One can thus conclude that, even if these approaches are neither rigorous nor based on firm theoretical grounds, they constitute a first practical approximation to predict the behavior of irreversible deposition processes of soft particles. The validity of these extended RSA models has, however, also to be proven. We will discuss this point in Chapter 5 dealing with the influence of the diffusion of the particles in solution on the deposition process.

2.3. Particle spreading – conformational change

All the models discussed so far assumed explicitly that the particles deposited on a surface were rigid bodies. However, in some cases (*e.g.*, proteins) it may be desirable to account, not only for the deposition itself, but also for the configurational change that the particles may undergo due to their strong interaction with the adsorbent. In particular, spreading at the surface renders desorption less probable and constitutes an argument in favor of models of irreversible adsorption.

The classical RSA, taking into account both the irreversibility and the geometrical exclusion effects, can be extended to account also for conformational changes of the particles once in contact with the collector [40]. Three variants of this model (symmetric spreading, asymmetric spreading, tilting) were elaborated and discussed in the one-dimensional case where, as often, the problem is exactly solvable. Nevertheless, in order to stay within the scope of the present paper, we restrict the discussion to the two-dimensional case [41]. This is all the more justified since many similarities exist between one and two dimensions, as suggested by van Tassel *et al.* themselves.

On the basis of experimental evidence, van Tassel *et al.* proposed a model capable of interpreting the effects of symmetric spreading on the adsorption kinetics, saturation coverage and particle distributions. This model rests on the rules defining the standard RSA model, with the additional feature which consists in allowing an adsorbed particle to grow to a larger size on the surface if enough space is available. In the following, particles with their original diameter, d_α, are called α-particles. Those that can grow up to a preset diameter d_β become β-particles. If this size transition is not possible (*i.e.*, if the full spreading up to the diameter d_β is not possible), they stay α-particles with the corresponding diameter d_α. This means explicitly that each particle can *a priori* exist only in one of two mutually exclusive states (α or β). It is important to realize that adsorbed particles (whether α or β) serve to block both the adsorption of new particles (α) and the spreading of neighboring particles ($\alpha \rightarrow \beta$).

The spreading occurs at a rate characterized by the rate constant k_s. For instance, the increase of the number density ρ_β of β-particles as a function of time

t is given by:

$$\frac{\partial \rho_\beta}{\partial t} = k_s \rho_\alpha \Psi_\alpha \tag{4.48}$$

where ρ_α is the number density of unspread particles at time t and Ψ_α denotes the probability for a given α-particle to have space available to spread. In the most general case where the spreading is not instantaneous, an exponentially distributed "life time" t_s is assigned to each newly adsorbed particle; this time is evidently related to the spreading rate k_s. This means that the particle tries to spread at the time t_s after its arrival on the surface. But during this waiting time, other particles may have reached the collector and may hinder the transition from the α- to the β-state. Therefore, in the model where spreading is not instantaneous, less particles can spread than in the case where the spreading is attempted as soon as the particle touches the surface.

Remarkably the asymptotic behavior of the density of α-particles is identical to that of the standard RSA of monodisperse disks, *i.e.*, the saturation is approached as $t^{-1/2}$. In contrast, the β-particle density tends much faster to its limit, namely it approaches its limit essentially in an exponential way. In the model based on an instantaneous spreading, the total coverage, as well as the relative contributions of the α- and β-particles to this total coverage, depend on the single parameter $\Sigma = d_\beta/d_\alpha$, as in the case of the filling of a surface with a binary mixture of disks or spheres [42–44]. In the more general case of a finite spreading rate, the kinetics, as well as the total and partial coverages, depend on Σ as well, but also on the spreading rate or, more precisely, on the ratio of the spreading rate to the adsorption rate per unit area.

Finally, it may be mentioned that one step further has been made very recently by van Tassel *et al.* [45] who combined spreading and desorption. An adsorbed particle either desorbs or attempts to spread at prescribed rates. Successful spreading events lead to irreversibly bound particles. Obviously, a supplementary parameter (*i.e.*, three parameters instead of two) is needed to completely specify the kinetic profiles.

2.4. Random adsorption/desorption process

An interesting extension of the classical RSA model can be obtained by allowing the particles to desorb. As a consequence the process thus described becomes a reversible one. The kinetic equation (2.3b) must then be rewritten as a generalized Langmuir equation including a desorption term:

$$\frac{d\theta}{dt} = \Phi(\theta) - p_d\theta \tag{4.49}$$

where p_d is proportional to the probability per time unit for any particle to desorb from the surface, while $\Phi(\theta)$ retains its usual meaning but is not identical to Φ_{RSA} [46]. Such a process leads eventually to equilibrium unless p_d is strictly zero [47]. The coverage θ_{EQ} characterizing this equilibrium state is *a priori* not

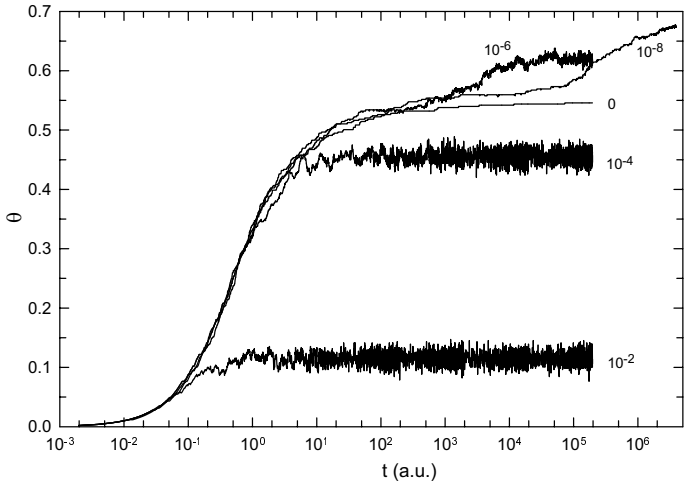

Figure 9. *RSA adsorption/desorption kinetics showing the evolution of the coverage as a function of time for different values of the desorption probability p_d (indicated on each curve). The case $p_d = 0$ corresponds to the RSA case.*

equal to the jamming coverage predicted by the RSA model (0.547), but depends on p_d. Note also that $d\theta/dt = 0$ implies $\Phi(\theta_{EQ}) > 0$ when $p_d > 0$, whereas in RSA $\Phi = 0$ when $d\theta/dt = 0$, *i.e.*, at saturation. This is a particular case illustrating the general rule which states that, in a reversible disordered system at equilibrium, the available surface function is larger than its RSA counterpart at the same coverage [48].

In practice, after each adsorption trial, whether successful or not, any particle present on the surface has a probability p_d to desorb. It is, however, faster from the computational point of view to consider only one "candidate" desorbing with the probability p_1. Strictly speaking, this is not equivalent for the simple reason that in this latter case exactly 0 or 1 particle is removed from the collector, whereas in the former case several particles may desorb at a time. Nevertheless, if p_d is small, and if we define p_1 by

$$p_1 = 1 - (1 - p_d)^{n_{ads}} \tag{4.50}$$

where n_{ads} is the number of particles corresponding to the current coverage θ, both methods tend to be equivalent because multiple desorptions become highly improbable.

Simulation results using the multiple desorption algorithm are displayed in Figure 9 which illustrates the prime importance of the choice of p_d. For "high" values of p_d (10^{-2} and 10^{-4} in this example), the kinetics level off at an equilibrium coverage smaller than that predicted by the RSA ($p_d = 0$). For very small, though non zero, desorption probabilities (10^{-6} and 10^{-8}), the kinetics follows that of the RSA model over a relatively long period of time. But, for even longer times, the coverage rises above the RSA jamming limit. This means that over the period of time where the kinetics with and without desorption are practically

identical to the RSA case, we have $\Phi(\theta) - p_d\theta \approx \Phi_{RSA}(\theta)$. Furthermore, $p_d\theta$ being of the order of 10^{-6} or even 10^{-8}, it appears that $\Phi \approx \Phi_{RSA}$ until θ begins to increase to its final plateau value. This somewhat surprising observation originates from the fact that locally one particle may block a target which can receive two particles after the desorption of the former one. The replacement of one particle by two particles occurs seldom, but over very long times it is efficient enough to significantly increase the coverage if compared to the RSA. The results shown here were obtained on only one surface and are therefore not very accurate. However, the principle is clearly revealed. It may be stressed that the equilibrium coverage increases continuously when p_d decreases as long as p_d stays strictly positive [47]. Setting $p_d = 0$ leads to an abrupt drop to the RSA jamming coverage. In other words, turning a reversible process into an irreversible one can show up a discontinuity in the evolution of the coverage with respect to the desorption probability at a given time.

2.5. Irreversible adsorption with surface diffusion

In all the examples discussed up to now, once the particles are adsorbed on the surface they cannot diffuse along the surface. This is of course an approximation which is valid as long as the characteristic adsorption time τ_a is small compared to the characteristic diffusion time τ_d. The characteristic adsorption time τ_a is given by:

$$\tau_a = [k_a \Phi(\theta, t)]^{-1} \tag{4.51}$$

where $\Phi(\theta, t)$ corresponds to the available surface function at the coverage θ at time t. Indeed, the major difference between irreversible deposition processes with and without surface diffusion is that in the latter case the available surface function is only a function of the coverage whereas in the former case it depends also upon the time: at a given coverage the system can evolve through the particle diffusion. The characteristic diffusion time τ_d is given by:

$$\tau_d = (D\rho)^{-1} \tag{4.52}$$

where D represents the self diffusion coefficient and ρ corresponds to the number density of adsorbed particles. This problem in which, once adsorbed, particles can no longer desorb but diffuse along the surface has been investigated in reference [46]. The dimensionless parameter ζ defined by:

$$\zeta = \frac{\tau_a}{\tau_a + \tau_d} \tag{4.53}$$

has been introduced in order to characterize the process. This parameter lies always between 0 and 1. Small values of ζ correspond to an RSA-like deposition process. However, when the surface coverage increases, the available surface decreases so that at the end of the adsorption process, even if the surface diffusion is small, the characteristic diffusion time becomes of the order of or smaller than

τ_a. The system thus relaxes to equilibrium configurations. It has been shown in reference [46] that the available surface function $\Phi(\theta)$ is in fact a function of θ and ζ. If one expands Φ in a power series as given by equation (4.2), the coefficients a_1 and a_2 are identical to the RSA (and equilibrium) coefficients and $a_3(\zeta)$ is a function of the parameter ζ only.

3. The simplest irreversible deposition model taking excluded volume effects and gravity into account: the Ballistic Deposition (BD) model

For large particles, the deposition process is mainly governed by the gravitational field provided that the density of the particles exceeds that of the fluid. It is described in first approximation by the Ballistic Deposition (BD) model. This model is defined as follows: (i) as for the RSA model the particles are deposited sequentially on the surface. (ii) For each deposition trial, a starting position is chosen randomly over the adsorption plane. The particle then follows a vertical trajectory until it reaches the adsorption plane or contacts a previously deposited particle. In this latter case, it follows the path of steepest descent until it reaches a stable position. (iii) If this position lies on the deposition plane, the particle is irreversibly fixed on it. Otherwise the particle is removed from the system and a new trial is started. This model was first introduced by Jullien and Meakin [49] who determined, through computer simulations, the jamming limit coverage which is equal to approximately 0.61. This value is larger than its RSA counterpart indicating a more compact structure at the jamming limit. This observation can be interpreted as follows: due to the rolling mechanism in a virtually infinitely intense gravitational field, the probability to find two particles in contact is much larger than in the RSA case. The one-dimensional BD problem has been solved exactly by Talbot and Ricci [50]. The kinetics in the low to intermediate coverage range for the two dimensional case has first been analyzed by Thompson and Glandt [51] who found that the available surface function $\Phi(\theta)$ varies as:

$$\Phi(\theta) = 1 + a_3\theta^3 + O(\theta^4). \tag{4.54}$$

The value -9.612 of a_3 given by Thompson and Glandt has been corrected later by Choi *et al.* [52] and is in fact equal to $-9.949\,78$. The asymptotic kinetic law has also been analyzed and is given by:

$$\theta_\infty - \theta(t) \propto \frac{e^{c_1 t}}{t^{c_2}} \tag{4.55}$$

with $c_1 = 2\sqrt{3}/\pi$ and $c_2 = 2$. The origin of this law is, as in the RSA case, again of purely statistical and geometrical nature. The exponential decrease is due to the fact that the evolution of the coverage is not so much due to the evolution of the mean size of the targets which, in contrast to the RSA case, remains different from zero near the jamming limit, than to the evolution of the number of targets.

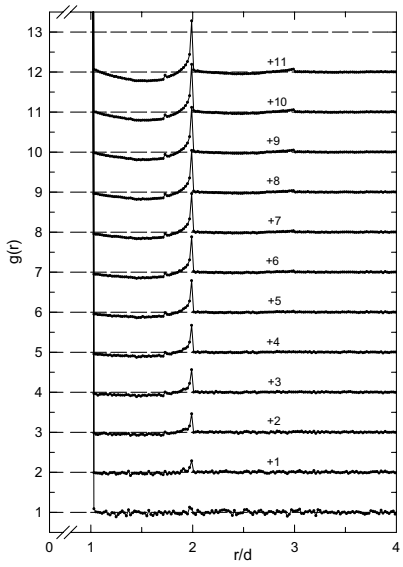

Figure 10. *Radial distribution function as a function of the center-to-center distance derived from BD computer simulations ($d = 2R$). From bottom to top, the curves correspond to coverages of 0.05, 0.10, 0.15, ..., 0.60. Each curve is shifted by one unit with respect to the preceding one for the sake of clarity.*

As for the RSA case, the knowledge of the low and high coverage behavior allows the interpolation between both regimes and thus to obtain an approximate expression of the available surface function or of the kinetics over the whole coverage range. It has been shown that the expression:

$$\theta_\infty - \theta(t) = \frac{c_0 e^{-4/\pi S_m t}(1 + c_4 t)}{1 + c_1 t + c_2 t^2 + c_3 t^3} \tag{4.56}$$

with $c_0 = \theta_\infty = 0.6105$, $c_1 = 0.714\,18$, $c_2 = 1.580\,56$, $c_3 = 2.474\,24$, $c_4 = 0.178\,84$ and $S_m = \sqrt{3}/2$, provides an accurate approximation for the evolution of the coverage with time over the whole coverage range [52].

In contrast to the RSA case where one deposited particle can already hinder the deposition of a new one, at least three particles need to be present on the surface to hinder a new one to touch the deposition plane in the BD model. This explains that the first non vanishing term in expression (4.54) is of order 3 in the coverage and implies that the reduced variance $\sigma^2/\langle n \rangle$ varies as $1 + (3/2)\ a_3\theta^3$ at low coverage (following relation (3.12) where $k = 3$, in contrast to RSA for which $k = 1$) and thus presents an horizontal tangent at the origin. Finally the radial distribution function has also been investigated as a function of the coverage. As shown in Figure 10, it leads to much better defined peaks than does the RSA process. However, as for the RSA case, there is no long range positional correlation: the correlation length remains for all coverages of the order of two

particle diameters. Since in both models particles interact only if they come into mutual contact, no long range order can appear in the configurations build up at the surface, which always are disordered ones, even at high coverage.

4. Generalized ballistic-deposition (GBD) model

Up to now we have discussed two geometrical models, RSA and BD, widely used in the literature. These two models may be considered in fact as particular cases of a unique random irreversible deposition model (generalized ballistic-deposition model, GBD) as was shown by Viot *et al.* [53] in the one-dimensional case and Choi *et al.* [54] in the two-dimensional case. Whether one- or two-dimensional, the GBD model contains a parameter a, called tuning parameter, which measures the efficiency of the restructuring due to the rolling mechanism. If $a = 0$, the RSA model is recovered, whereas for $a = 1$, the GBD model reduces to the usual BD model.

We focus from now on to the two dimensional problem. The basic idea is the following: spheres start from positions uniformly distributed above the adsorbing plane and follow vertical trajectories, unless they touch a preadsorbed particle. If the new particle touches directly the plane it is adsorbed with a probability $(1 - p)$ and, conversely, removed with a probability p. If the new particle touches first one preadsorbed particle, it follows the path of steepest descent. If this path leads the particle into a trap, it is removed since no multilayer formation is allowed. Otherwise, *i.e.*, if the rolling particle succeeds in reaching the plane, it is permanently fixed on it at the contact point with a probability p, or discarded with the complementary probability $(1 - p)$. The tuning parameter a is then simply defined by $a = p/(1 - p)$ and the kinetic equation has the form:

$$\frac{d\theta}{dt} = \Phi^{DD}(\theta) + a\Phi^{RM}(\theta) \tag{4.57}$$

where DD stands for direct deposition and RM for rolling mechanism.

Obviously, for $a = 0$, the above equation coincides with the RSA kinetic equation where, by definition, only direct deposition contributes to the formation of the particle layer. If $a = 1$, direct deposition and rolling mechanism have the same *a priori* statistical weight. This corresponds to the definition of the BD model. While p approaches 1 or, equivalently, a tends to infinity, the GBD model privileges more and more the adsorption after rolling to the expense of the direct adhesion. Finally, when p is strictly equal to 1, deposition occurs exclusively *via* the rolling mechanism and makes the GBD model an aggregation model. The saturation coverage increases monotonically with a from 0.547 ($a = 0$) up to 0.691 ($a = \infty$). The latter case corresponds to a unique cluster of particles, each of which being connected to at least one other particle.

5

Diffusional models

1. Extended RSA model taking diffusion into account

If one observes the deposition of particles on a surface with a microscope one realizes an important aspect which is not taken into account in the RSA model: the Brownian motion of the particles in the vicinity of the adsorbing plane plays an important role. This diffusion process implies that, even if a depositing particle interacts with an already deposited one, it is not rejected from the system but, due to the Brownian motion, it can diffuse around its initial position and eventually still adhere to the surface by keeping the memory of its initial position. To account for these observations computer simulation models and a theoretical approach have been proposed [55–58].

1.1. Computer simulations

1.1.1. Diffusion RSA-like models

In the historically first model, called Diffusion RSA (DRSA) model, particles are adsorbed randomly and sequentially on the surface [56, 57]. The initial position of the particle (more precisely of its center) is chosen randomly in a plane parallel to the adhesion surface and located above it. The distance between this starting plane and the plane of deposition must at least be equal to one particle diameter. The particle then undergoes a Brownian motion and all the deposited particles behave as hard spheres. The diffusion process can take place on a lattice, the mesh size of the lattice being small compared to the size of the particles (typically $R/100$ where R represents the radius of the particles), or can be considered as continuous, the mean displacement at each step being again small compared to R. If the diffusing particle touches the deposition plane, it is irreversibly fixed on it. In addition, a third plane parallel to the deposition plane must be introduced. It lies at a distance h above the starting plane. If the diffusing particle touches this third plane, it is removed from the system. This plane had to be introduced in order to avoid that the simulations become prohibitively long. This is a characteristic feature of the diffusional models and will be discussed in Section 5 of this chapter.

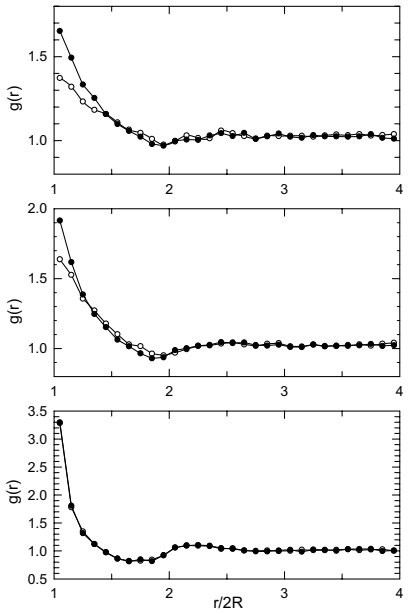

Figure 11. *Radial distribution function as a function of the center-to-center distance derived from RSA* (○) *and DRSA* (●) *computer simulations. From top to bottom, the curves correspond to coverages of 0.24, 0.35, and* θ_∞*, respectively.*

As far as the structure of the deposited layers is concerned, the simulations lead to the following conclusions: (i) the structures of the deposited layers generated by taking the diffusion process of the particles in the solution into account are different from their RSA counterparts for coverages smaller than the jamming limit coverage. This is illustrated in Figure 11 representing the radial distribution functions for two coverages different from jamming, obtained with the RSA and DRSA models. (ii) The coverage at the jamming limit is almost indistinguishable from the RSA jamming limit. Extensive computer simulations were performed in the one dimensional case for the DRSA model to verify this result and it came out that $\theta_\infty = 0.7483 \pm 0.0011$ in the RSA case and $\theta_\infty = 0.7529 \pm 0.0010$ in the DRSA case [58]. Both values are thus not identical but indistinguishable from an experimental point of view. (iii) In addition, the structures of the layers at jamming in the two cases are also indistinguishable (Fig. 11). These two effects can be understood in the following way: at small coverages the diffusion plays its full role in the deposition. However, near the jamming limit only a small number of available spaces still remain and they are all of very small size. Over these small areas, the deposition probability becomes uniform and the filling of the spaces depends only upon geometrical constraints.

The deposition kinetic law has also been investigated [57]. It is, however, no longer clear how to define the available surface function Φ. Indeed, if the available surface function at a given coverage θ corresponds to the ratio of the adsorption

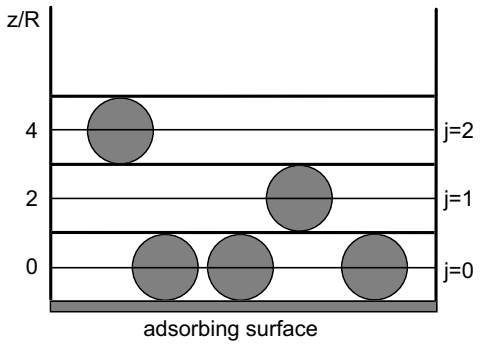

Figure 12. *Schematic representation of the slab model. The particles start from the mid-plane of slab 1 (i.e., at altitude $2R$) and diffuse on a fine mesh lattice until they are adsorbed at $z = 0$. Once a particle reaches the altitudes $z = 4R$ or $z = 0$ it is rejected. This allows the transition rates $W_{1,0}$ and $W_{1,2}$ to be determined.*

flux in the presence and in the absence of particles on the surface, it is not clear at which distance from the surface one assumes the particle concentration in the bulk to be constant. This problem is intimately connected to the fact that the available surface function will depend, not only upon intrinsic properties of the surface, but also upon an additional parameter which, in computer simulations, is often the time allowed to a particle to deposit. This aspect will be discussed extensively in the Section 5. The first attempt to overcome this problem was to propose a master equation approach in which the space is divided into slabs parallel to the adsorbing surface and of thickness equal to the diameter of the particles (Fig. 12). The lowest slab, labeled 0, corresponds to the diffusion layer of the particles between the already adsorbed ones. One introduces then transition rates $W_{j,j\pm1}$ from slab j to slab $j \pm 1$. These transition rates are independent of j for $j \geq 2$. Only $W_{1,0}$ and $W_{1,2}$ are functions of the structure and thus of the coverage of the interface. The rate $W_{1,0}$ corresponds in fact to the transition rate of adsorption. The values of these rates could be determined from computer simulations on a fine mesh grid as functions of the coverage, which allowed the whole master equation system to be solved and thus to have access to the adsorption kinetics.

1.1.2. Cellular automaton

A more recent approach is based on Cellular Automaton (CA) modeling [59]. In this approach the particles in the solution diffuse on a square lattice whose mesh size is equal to $4R$. This lattice extends from the surface up to a distance L of the order of $250R$. The simulation is carried out in such a way that many particles move on the lattice at the same time, the particle concentration being kept constant at the border plane of the solution located at the distance L from the adsorbing plane. The adsorption is performed on a plane in a continuous way: this is achieved by shifting the boundary lattice next to the surface of deposition

by a value chosen randomly in an interval $[-R, R]$. On the lattice in the solution the particles have a probability p_1 to move toward the surface, a probability p_2 to move in the direction opposite to the surface and a probability p_3 to move in either direction parallel to the surface. Once a particle touches the surface without overlapping with an already deposited sphere, it has a probability q to remain adsorbed. If it is not adsorbed, it is taken back to its former position and continues its diffusion. Once a particle is deposited it remains indefinitely fixed in its position. The major differences between the CA model approach and the DRSA approach are the following: (i) in the CA modeling many particles can diffuse simultaneously in the volume and this can influence the deposition process; (ii) once a particle touches the surface, even if it does not overlap a previously deposited particle, it does not automatically adsorb on the surface; in the same way, if an overlap occurs, the incoming particle is not automatically rejected from the system, which is an improvement with respect to the RSA model; (iii) the adsorption step does not, in the CA model, take the diffusion process of the particle in the solution near already deposited once in a fine way into account: it is a compromise between an RSA like adsorption and a diffusion process. It is for this reason that one expects for the asymptotic kinetics of the process predicted by the CA model a behavior similar to that of the RSA dynamics. In contrast, in the DRSA model, the particle diffuses on a fine mesh grid (mesh size $\ll R$). This feature gives the DRSA model the ability to imitate quite accurately the diffusion in a continuous space not only in the bulk solution but also in the vicinity of adsorbed particles and of the adsorbing plane. This higher degree of accuracy of the description of the motion is of course obtained to the expense of the computer time.

1.2. Theoretical approach

Widom introduced the concept of the function Φ for equilibrium systems [3]. This function corresponds, in the cases discussed up to now, to the available surface function. He showed that Φ is simply related, in that case, to the chemical potential μ of the particles in the system by the relation:

$$\mu = \mu_0(T) + kT\ln(\rho) - kT\ln(\Phi) \tag{5.1}$$

where ρ represents the number density of particles in the system. Let us now apply this concept in the bulk but in the vicinity of the adsorption plane, when the particles can still diffuse and have thus not interacted with the adsorption plane. Divide the whole space into small slabs of thickness δ much smaller than the radius R of the particles. Each slab is considered to be a system on its own. A particle is defined to be part of a slab if its center lies in the slab. It is defined as "adsorbed" on the surface if its center lies on the plane $z = 0$, *i.e.*, at a distance R from the adsorbing surface (Fig. 13). Each slab is characterized by its height z and the function $\Phi(z)$ which can be evaluated according to the procedure introduced by Widom: freeze all the particles in all the slabs. Let then a probe particle wander in the slab z. At each point, this particle feels a potential $U(\mathbf{r})$. Φ is then defined

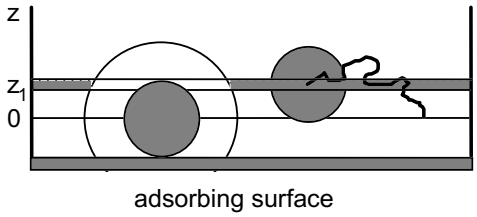

Figure 13. *Schematic representation of the available volume in an infinitely thin slab located at altitude z_1. The ratio of the dashed volume to the total volume of the slab represents the available volume function $\Phi(z)$ for the case of hard spheres.*

as the mean value of $\exp[-U(\mathbf{r})/kT]$ taken over the whole slab. For the case of hard spheres, $\Phi(z)$ represents the available volume for a particle in slab z. We will now generalize the treatment of reference [55] to describe the equations allowing the adsorption kinetics to be determined.

Let us assume that the diffusion process coupled with the adsorption phenomenon can be described by a one-dimensional Markovian process obeying the master equation:

$$\frac{\partial}{\partial t}P_n = W_{n+1,n}P_{n+1} + W_{n-1,n}P_{n-1} - (W_{n,n+1} + W_{n,n-1})P_n \tag{5.2}$$

where n is given by $n = z/\delta$. P_n represents the probability that a particle is in the slab $z = n\delta$ at a given time t and $W_{n,n+1}$ represents the probability that a particle located in this slab will diffuse to the slab $n+1$ per unit time. If reflecting boundary conditions would hold on the planes $z = 0$ and $z = z_0$ (where z_0 is arbitrary), equilibrium would be attained in which $P_n = P_n^e$ where P_n^e is given by $P_n^e(z) = \rho^e(z)\delta$. Moreover, at equilibrium, assuming detailed balance between the different slabs, one finds the following relations:

$$\frac{P_{n+1}^e}{P_n^e} = \frac{\rho^e(n+1)}{\rho^e(n)} = \frac{W_{n,n+1}}{W_{n+1,n}} = \frac{\Phi(n+1)}{\Phi(n)} \tag{5.3}$$

where $\Phi(n)$ stands for $\Phi(n\delta)$. The last equality is a direct consequence of the fact that Φ represents the available space for the center of the particles if they behave as hard spheres. The equality remains however valid even if the particles interact through other interaction potentials. The equality between the second and fourth members is equivalent to say that the chemical potential of the particles in the slab n and $n+1$ as given by expression (5.1) are equal. On the other hand, $W_{n,n+1}$ represents the ease with which a particle from slab n can diffuse to slab $n+1$.

Let us now assume that $W_{n,n+1}$ is only a function of $\Phi(n)$ and $\Phi(n+1)$. One can then write the general form of $W_{n,n+1}$ as:

$$W_{n,n+1} = \frac{D}{R^2}\frac{\Phi(n+1)}{f(\Phi(n), \Phi(n+1))} \tag{5.4}$$

where D represents the diffusion coefficient of the particles in the bulk at the height z. This coefficient depends certainly on z. From equation (5.3) it follows that $f(\Phi(n), \Phi(n+1))$ must be symmetric in $\Phi(n)$ and $\Phi(n+1)$. Moreover, if Φ does not vary with z, $W_{n,n+1}$ will become independent of Φ. This implies that $f(\Phi, \Phi) = \Phi$. It can be shown that these properties imply that:

$$\left(\frac{\partial}{\partial \Phi} f(\Phi, \Phi')\right)_{\Phi=\Phi'} = \left(\frac{\partial}{\partial \Phi'} f(\Phi, \Phi')\right)_{\Phi=\Phi'} = \frac{1}{2}\cdot \tag{5.5}$$

Expanding the relation (5.2) up to second order, taking relation (5.5) into account and going to the limit $\delta \to 0$, one obtains, after a lengthy but straightforward calculation, a Smoluchowski equation:

$$\frac{\partial P}{\partial t} = \frac{\partial}{\partial z}\left[D\left(\frac{\partial P}{\partial z} - P\frac{\partial \ln \Phi}{\partial z}\right)\right]. \tag{5.6}$$

This is the fundamental diffusion equation of the particles through the adsorption plane. It shows that the particle distribution is evolving in a medium having an effective potential equal to $\ln \Phi$. Equation (5.6) has also been obtained recently through irreversible thermodynamic arguments, starting from the expression (5.1) of the chemical potential and knowing that $-\nabla(\mu/T)$ corresponds to the thermodynamic force conjugated to the flux of particles through a plane located at a height z above the adsorption plane [60]. To get the deposition rate, this equation must be solved with the correct boundary conditions. If the adsorption plane is perfectly adsorbing, the boundary condition at the adsorption plane is:

$$P(z=0) = 0. \tag{5.7}$$

One has also to give the boundary conditions in the solution. Usually one assumes that the concentration of particles at $z = 2R$ is known. Moreover, the flux of particles through the layer of particles at a height z is equal to:

$$J_S = -\frac{D}{R^2}\left[\frac{\partial}{\partial \gamma}\rho - \rho\frac{\partial \ln \Phi}{\partial \gamma}\right] \tag{5.8}$$

where $\gamma = z/2R$. Assuming steady state conditions, J_S becomes independent of z and can be integrated by the classical method of variation of the constant. One then gets:

$$J_S = -\frac{1}{R^2}\rho_B I(x) \tag{5.9}$$

with

$$I(x) = \frac{1}{\displaystyle\int_0^1 \frac{1}{D(\gamma)\Phi(x,\gamma)} d\gamma} \tag{5.10}$$

where $x = \theta/\theta_\infty$ and ρ_B corresponds to the number density of particles in the bulk. Relation (5.10) is a generalization of the result of Wojtaszczyk *et al.* [60] to the case where the diffusion constant can vary with the position z. One can thus write a kinetic equation of the form:

$$\frac{\partial\theta}{\partial t} = K_a \rho_B I(x) \tag{5.11}$$

where K_a represents a kinetic adsorption constant. This relation constitutes a generalization of the Langmuir equation, which would be defined by $I(x) = 1 - x$ in equation (5.11), and had first been proposed in reference [60].

A few remarks are necessary at this point.

(i) This approach does not provide the evolution of the function $\Phi(x, z)$ with the reduced coverage θ/θ_∞ and the height z. This function must be found by another method. A first and reasonable approximation is to assume that the structure of the adsorbed layer is similar to that of an RSA system of adsorbed particles. We have seen that one possesses good approximate expressions for $\Phi_{RSA}(x)$ over the whole coverage range. These expressions thus constitute an approximation for $\Phi(x, z = 0)$. Wojtaszczyk *et al.* [60] have assumed the following form of the function $\Phi(x, z)$:

$$\Phi(x, z) = \Phi_{RSA}\left[x\left(1 - \left(\frac{z}{2R}\right)^2\right)\right]. \tag{5.12}$$

This, however, cannot describe correctly the evolution of the function Φ with the height z even at low coverage. Indeed, for $1 \leq z/2R \leq \sqrt{3}/2$, the wandering particle of Widom can only interact with at most one particle for each position. This implies that $\Phi(x, z)$ is directly proportional to the coverage in this range of z. The scaling law postulated in relation (5.12) can thus not be correct as soon as second order terms appear in the available surface function at the adsorbing plane.

(ii) This approach, as it is presented, is not valid near the jamming limit. Indeed, near the jamming limit the available space on the adsorption surface is constituted of small targets. The diffusion layer is thus formed of independent channels each characterized, in first approximation, by its area at the adsorption plane. All the channels can then be classified according to their area and the diffusion equation (5.6) must be applied to each class of channels. The rate of adsorption then corresponds to the rate of disappearance of the channels. This rate depends upon the area characterizing the channel. It has been shown that for each channel a scaling law as the one postulated in relation (5.12) applies approximately because, for these channels, it is the diffusion of the particles in the vicinity of the adsorption plane which dominates the deposition kinetics. The overall deposition kinetics is then given by the average of the deposition kinetics for each class of channels, averaged over all the classes. This procedure leads to the following deposition law [55]:

$$\theta(\infty) - \theta(t) \propto t^{-2/3}. \tag{5.13}$$

(iii) The approach presented in this section can be extended to the case where the particles are also submitted to an external field deriving from a potential such as the gravitational field. In this case the chemical potential of a molecule is given by:

$$\mu(z) = \mu_0(T) + kT\ln[\rho(z)] - kT\ln[\Phi(z)] + V(z) \tag{5.14}$$

instead of expression (5.1). $V(z)$ represents the potential energy of a molecule at the position z. One can thus extend the definition of the function Φ to include the effect of external forces: one has to replace $\Phi(z)$ by $\varphi(z) = \Phi(z)\exp[-V(z)/kT]$ and the whole analysis remains valid.

2. Extended RSA model taking diffusion and gravity into account

By taking not only diffusion but also gravity into account, one extends the previous DRSA model and gets the DRSAG model (DRSA with gravity) [61]. In the cellular automaton model approach this corresponds to an increase in the ratio p_1/p_2. The hydrodynamic interactions are still neglected. One can then show that the structure of the layer at a given coverage is uniquely determined by the reduced radius R^*, which depends notably on the buoyancy $\Delta\rho$ of the particles with respect to the bulk fluid and the acceleration g of the gravity. When colloidal particles are of density different from the bulk fluid in which they diffuse, prior to their adhesion to an interface, the movement results from the influence of the random (Brownian) diffusion, the deterministic vertical displacement due to the gravity, and the hard core repulsion between the particles. The mean maximum coverage θ_∞ depends also on the single parameter R^*. The origin of this parameter is shown up below.

The movement of spherical particles, of radius R, in a fluid can be described by the Langevin equation which relates the position $\mathbf{r}'(t' + \Delta t')$ of a particle at time $t' + \Delta t'$ to its position $\mathbf{r}'(t')$ at time t':

$$\mathbf{r}'(t' + \Delta t') = \mathbf{r}'(t') + \frac{D\mathbf{F_g}}{kT}\Delta t' + \Delta\mathbf{r}'_B \tag{5.15}$$

where D is the Stokes-Einstein diffusion coefficient. The vector $\mathbf{F_g}$ represents the gravitational force, *i.e.*, the only deterministic force acting on the particles assumed in the present study; it is given by:

$$\mathbf{F_g} = \frac{4}{3}\pi R^3 \Delta\rho\mathbf{g} \tag{5.16}$$

where $\mathbf{g}$ represents the acceleration of the gravity. The vector $\boldsymbol{\Delta}\mathbf{r}'_B$ represents the random (Brownian) displacement during the time interval $\Delta t'$. As usual, it is assumed that each component of the random movement $(\Delta x'_B, \Delta y'_B, \Delta z'_B)$ is a

normal deviate with mean equal to zero and standard deviation equal to $\sqrt{2D\Delta t'}$. As a consequence

$$\Delta x'_B = \gamma_x\sqrt{2D\Delta t'}; \quad \Delta y'_B = \gamma_y\sqrt{2D\Delta t'}; \quad \Delta z'_B = \gamma_z\sqrt{2D\Delta t'} \tag{5.17}$$

where γ_x, γ_y and γ_z are normal deviates, with mean equal to zero and standard deviation equal to one. Langevin's equation, corresponding to a diffusion in a three-dimensional space, separates into three independent equations:

$$x'(t' + \Delta t') = x'(t') + \Delta x'_B \tag{5.18a}$$
$$y'(t' + \Delta t') = y'(t') + \Delta y'_B \tag{5.18b}$$
$$z'(t' + \Delta t') = z'(t') - \frac{DF_g}{kT} + \Delta z'_B \tag{5.18c}$$

where $F_g = (4/3)\pi R^3 \Delta\rho g$ appears only in the third component. The minus sign in equation (5.18c) accounts for the fact that when $\Delta\rho > 0$, the gravitational force tends to decrease the altitude of the particle. Applying the transformations $x = x'/R$, $y = y'/R$, $z = z'/R$, $t = Dt'/R^2$, and using the definitions (5.17), leads to three equations describing the time evolution of the dimensionless Cartesian coordinates (x, y, z) of the center of a diffusing particle:

$$x(t + \Delta t) = x(t) + \gamma_x\sqrt{2\Delta t} \tag{5.19a}$$
$$y(t + \Delta t) = y(t) + \gamma_y\sqrt{2\Delta t} \tag{5.19b}$$
$$z(t + \Delta t) = z(t) - R^{*4}\Delta t + \gamma_z\sqrt{2\Delta t} \tag{5.19c}$$

where

$$R^* = R\left(\frac{4\pi\Delta\rho g}{3kT}\right)^{1/4} \tag{5.20}$$

is a dimensionless parameter which contains all relevant physical characteristics of the diffusion. Note that R^{*4} can be interpreted as the work of the gravitational force necessary to elevate the particle by R, expressed in units of the thermal energy kT. Equations (5.19a–5.19c) clearly demonstrate that the diffusion depends on the unique parameter R^*. Note also that R^* is involved in the relation between the horizontal and vertical displacements as follows. In the time interval Δt, the mean horizontal square displacement $\langle(\Delta x)^2 + (\Delta y)^2\rangle$ equals $4\Delta t$, and the mean vertical displacement $\langle\Delta z\rangle$ equals $-R^{*4}\Delta t$ when $\Delta\rho > 0$. If $\Delta\rho < 0$, R^{*4} must be changed into $-R^{*4}$. Eliminating Δt from these two expressions leads to:

$$\langle(\Delta x)^2 + (\Delta y)^2\rangle = -\frac{4\langle\Delta z\rangle}{R^{*4}}\,. \tag{5.21}$$

Approximate analytical solutions for the radial distribution function and for the jamming limit coverage $\theta_\infty(R^*)$ have been obtained for the $(1 + 1)$-dimensional case [62]. For the $(2 + 1)$-dimensional case, the jamming limit coverage has been

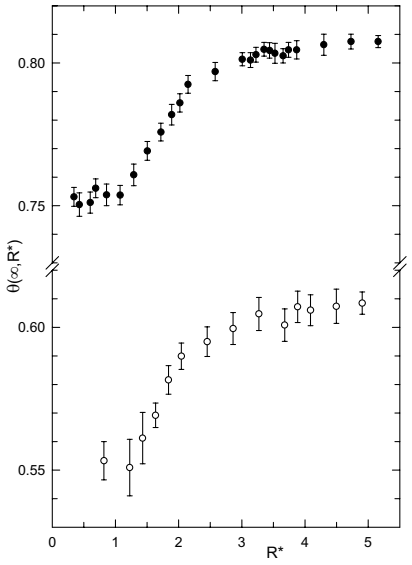

Figure 14. *Jamming limit coverage as a function of the reduced radius R^* (Eq. (5.20)) obtained by simulation of the deposition of hard spheres on a line (•) and on a surface (○) in a gravitational field. The error bars represent 95% confidence intervals.*

determined from computer simulations as a function of R^* and is represented in Figure 14. This figure shows that $\theta_\infty(R^*)$ varies from its ballistic value to its RSA value when R^* varies approximately from 4 to 1. It can thus be assumed that a system characterized by a value of R^* larger than 4 behaves almost ballistically whereas a system characterized by R^* smaller than 1 behaves almost as predicted by the DRSA model at least as far as the jamming limit coverage is concerned. Interestingly, it has been shown [63] that by a suitable normalization, the values of $\theta_\infty(R^*)$ follows a unique curve as a function of R^* for one- and two-dimensional collectors (Fig. 15). The renormalized jamming limit $\theta_{N,\infty}(R^*)$ is defined by the following relation:

$$\theta_{N,\infty}(R^*) = \frac{\theta_\infty(R^*) - \theta_{DRSA,\infty}}{\theta_{BD,\infty} - \theta_{DRSA,\infty}} \tag{5.22}$$

where $\theta_{DRSA,\infty}$ and $\theta_{BD,\infty}$ correspond respectively to the DRSA and the ballistic deposition model jamming limit coverage. This result has been confirmed analytically in the limit of large values of R^* [62]. In addition, it has been shown that the jamming limit coverage varies with R^* for large R^* as:

$$\frac{\theta_\infty(R^*)}{\theta_{BD,\infty}} \cong 1 - \beta_d R^{*-8/3} \tag{5.23}$$

where β_d is a parameter depending only upon the dimension of the collector, whereas the exponent $-8/3$ is invariable.

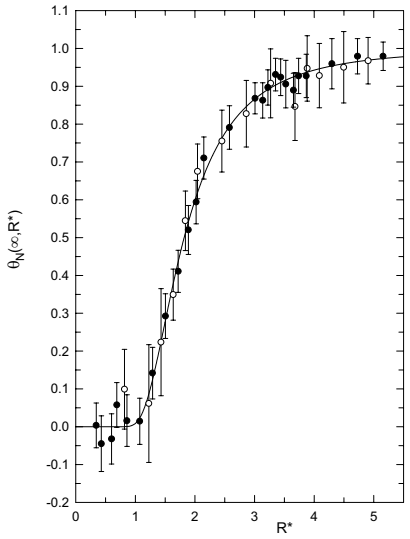

Figure 15. *Normalized jamming limit coverage (Eq. (5.22)) as a function of the reduced radius R^* obtained by simulation of the deposition of hard spheres on a line (•) and on a surface (○) in a gravitational field. The error bars represent 95%-confidence intervals. The solid line is a least squares fit of an empirical function to the data, i.e., $\theta_N(\infty, R^*) \approx \exp(-1.32R^{*-4} - 3.44R^{*-3})$.*

3. Models taking interparticle forces deriving from a potential into account

In all the models described up to now the particles were treated as hard spheres. However, the group of Adamczyk [13,64] has shown that electrostatic interactions between particles can also play an important role in the deposition process. To account for these effects Adamczyk *et al.* have proposed the modified RSA model discussed previously, which is based on the rule that an adsorption trial is accepted with a probability proportional to the Boltzmann factor $\exp[-U(\mathbf{r})/kT]$ where $U(\mathbf{r})$ represents the potential energy that the particle feels at the position $\mathbf{r}$. An extension to take the forces in three dimensions into account has been introduced more recently by Oberholzer *et al.* [39] but it corresponds in its spirit to the same kind of approach as proposed by the group of Adamczyk. In order to verify the validity of the rule of Adamczyk, Brownian Dynamics simulations were performed with an extended DRSAG algorithm which takes interparticle interactions into account during the deposition process [65,66]. The gravitational field was always included in the simulations in order to assure that the particles will eventually reach the surface in a reasonable computer time. The interaction potential between particles was taken from the DLVO theory. A first study [65] led to the conclusion that the ratio of the adhesion probabilities at a given location $\mathbf{r}$, for the particles subject to weak gravitation, in the presence and in absence of the interparticle

interaction follows approximately a Boltzmann law. However, further studies [66] in which the strength of the interaction potential was varied were less conclusive. It seems, nevertheless, that the weaker the gravitational field, the closer is the ratio to the Boltzmann factor. Further studies are still needed to investigate this problem.

More recently, the group of Lenhoff [39] performed an interesting Brownian dynamics simulation in which the authors followed the evolution of a whole assembly of particles in a volume in contact with the adsorbing surface. The chemical potential of the particles was kept constant in the volume at a given distance from the surface. They took both particle/particle and particle/surface interactions into account. The particle motion along the plane was subject to either unrestricted diffusion or zero diffusion. In this latter case, once the particles were adsorbed on the adsorption plane, the components of the forces acting on the particles and parallel to the surface were set equal to zero, the component perpendicular to the surface keeping its full value. Hydrodynamic interactions were not taken into account. It was found that, due to the interplay between the repulsive particle/particle and the attractive particle/surface electrostatic interactions, different behaviors can be observed by changing the ionic strength, *i.e.*, the value of κR where κ corresponds to the inverse of the Debye length. They found that, as is predicted by the generalized RSA model described by Adamczyk, for colloidal particles, in which κR is usually large, the jamming limit coverage decreases with the ionic strength. An opposite conclusion emerges for small κR as it could be the case for proteins. They found that the kinetics in the asymptotic regime seems to follow the power law (5.13) [55]. The simulation results were also compared to experimental results, especially the radial distribution function, and fairly good agreement was found between simulation and experimental data. Unfortunately no systematic comparison between these results and the extended RSA model predictions was performed. Such a comparison would be very useful because, even if these more realistic simulations are very valuable, it is difficult to perform them for each experimental system whereas from an extended RSA model, some aspects can be calculated directly without turning to extensive computer simulations.

4. Models taking hydrodynamic forces into account

Up to now we have discussed models in which the hydrodynamic interactions (HI) were restricted to those between the depositing particles and the fluid in a virtually unlimited space. We shall describe models which take into account in the HI not only the ambient fluid but also the deposited particles and the adsorbing plane. The presence of these HI play an important role in sedimentation and adsorption processes because (i) they are of long range and (ii) they can never be suppressed. The HI between spheres and planar surfaces or between two spheres have been extensively studied for a long time both theoretically and experimentally [67, 68]. In contrast, their influence on the structure of the assembly of the deposited particles has only been taken into account recently. This originates partly from the

difficulty to handle these interactions due to their non-additive character. Their long range interaction also implies that the computer simulations which generate assemblies of deposited particles become prohibitively time consuming.

The simulations taking HI into account are similar to the generalized DRSA simulations in which one takes all kind of forces into account, apart from the fact that the diffusion coefficient has no longer the constant value corresponding to the Stokes law, but varies with the position of the depositing particle. More precisely, the trajectory of the particle is simulated by using the classic algorithm of Ermak and McCammon [69]. The diffusion coefficient becomes a diffusion tensor. In order to take the HI between the depositing particle, the deposition plane and the already deposited particles into account, one uses the approximation of the additivity of the friction tensors:

$$\xi(\mathbf{r}) = \xi_{sp}(z) + \sum_i (\xi_{ss,i}(\mathbf{r}_i) - \xi_0) \tag{5.24}$$

where $\xi(\mathbf{r})$ corresponds to the friction tensor of the particle at the position $\mathbf{r}$, $\xi_{sp}(z)$ represents the friction tensor relative to the particle/plane interaction of the spherical particle suspended at a height z above the deposition plane. $\xi_{ss,i}(\mathbf{r}_i)$ corresponds to the friction tensor relative to the interaction between the depositing particle and the ith deposited particle located at the position $\mathbf{r}_i$ and ξ_0 corresponds to the Stokes friction tensor. Bossis and Brady have shown that this approximation takes properly into account lubrication forces, which act when objects are close together, and lead also to the correct behavior at long distances [70].

The first attempt to analyze this problem is due to Bafaluy *et al.* [71] who investigated the deposition probability $q(\mathbf{r})$ of a Brownian particle at a position $\mathbf{r}$ in the presence of one or two particles on the surface. The simulations have shown that the deposition probability $q(\mathbf{r})$ becomes almost independent of $\mathbf{r}$ (Fig. 16). This finding contrasts with the predictions relative to the DRSA model in which $q(\mathbf{r})$ is maximum near the already deposited particles due to the diffusion process around this particle. This behavior originates from the fact that the components of the diffusion tensor describing the motion of the particle perpendicular to the plane of adhesion decreases more rapidly than the component of the diffusion tensor describing the motion parallel to this plane. This result seems to indicate that the RSA model should account correctly for the structure of the assembly of deposited particles. Indeed, even if from the simulations one can only draw a conclusion up to a coverage of 0.30, where at most three body interactions are important, at higher coverage the geometrical constraints become increasingly important so that the RSA rules should remain valid as far as the deposition location is concerned.

Hydrodynamic interactions have also been introduced in the BD model, by simulating the trajectories of the particles until they reach the surface. This has first been done by Pagonabarraga and Rubí for the $(1+1)$-dimensional case [72]. The spheres were constrained to fall in a vertical plane onto a line but the HI were calculated as if the particles were in the three dimensional space. This approach was extended to the $(2+1)$-dimensional case [73]. The conclusions which can be

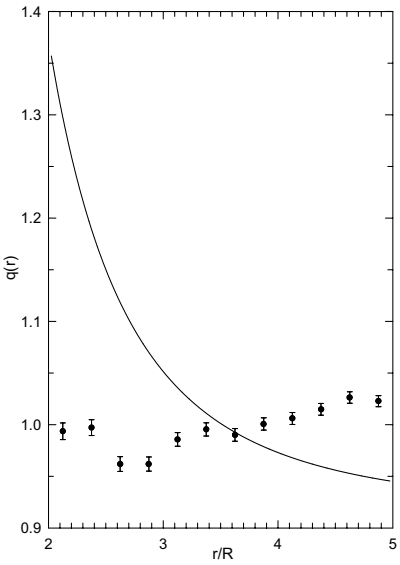

Figure 16. *Results of the simulation of the diffusion of a particle near an adsorbed one showing that the introduction of the hydrodynamic forces* (•) *in the algorithm renders the probability of adsorption practically independent from the distance between the spheres. In contrast, the DRSA (diffusion in the absence of HI) predictions (—) indicate a preferential adhesion near the fixed particle.*

drawn from this study are the following: (i) HI modify only slightly the radial distribution functions of the assemblies of deposited particles (Fig. 17). This is particularly the case at low to intermediate coverages where the peaks in the $g(r)$ become smaller and broader. This comes from the fact that HI act in the presence of a gravitational field as a repulsive interaction. Indeed, during the deposition, the particles have more difficulty to diffuse toward the fixed sphere than to diffuse along this sphere. However, the higher the coverage the smaller are the differences between the BD radial distribution functions with and without HI. This feature is similar to that observed for the DRSA case in the presence and absence of HI. This result seems even to be quite general: *at high coverages, the geometrical constraints play a leading role in the position of adhesion of the new incoming particles.* (ii) HI also modify the first non vanishing term a_3 in the expansion of the available surface function in the coverage. It has been shown that $a_3^{BHD}/a_3^{BD} \approx 0.5$ where BHD stands for Ballistic Hydrodynamic Deposition. But overall, the differences induced in the available surface function by the HI are still small. (iii) Finally, as a general conclusion one can say that, as far as average quantities such as the density fluctuations, the available surface function, *etc.*, are concerned, the BD model without HI constitutes a good approximation. It is only for the detailed analysis of the structure of the layer of deposited particles that HI play a significant quantitative role.

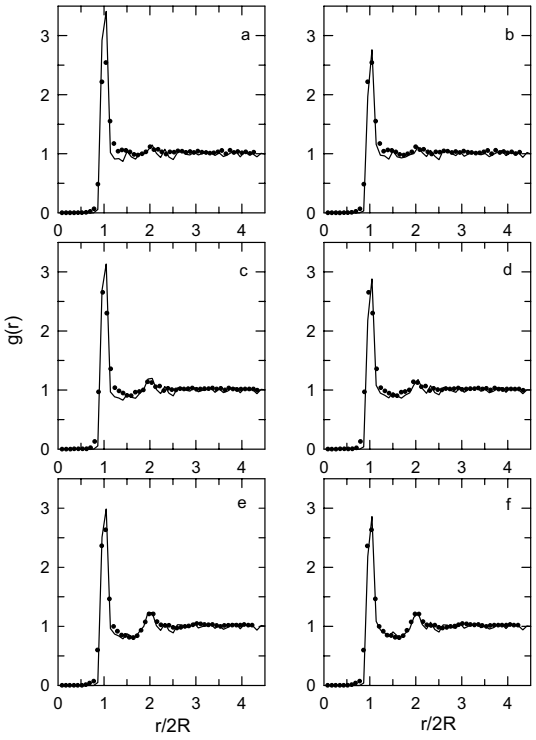

Figure 17. *Comparison of the experimental (•) radial distribution functions corresponding to melamine spheres, with simulation data. Figures a, c, e correspond to the ballistic model, whereas figures b, d, f correspond to the ballistic model including the hydrodynamic forces. Coverage: 0.15 (a, b), 0.35 (c, d), 0.50 (e, f).*

It has been stated previously that, in the absence of HI, for a given coverage the structure of an assembly of deposited particles, interacting through a hard sphere potential, is only a function of the parameter R^*. It has been shown that the *same* parameter R^* given by relation (5.20) also characterizes, at a given coverage, the structure of a system of hard spheres sedimenting toward the surface *by taking the HI into account* [74]. This result is based on the approximation that the friction tensor of a particle interacting with different spheres and with the deposition plane is given by relation (5.24). Two demonstrations have been proposed for this result. One demonstration is based on the resolution of the Langevin equation and on the relation between the random displacement of the particle due to thermal motion and the diffusion tensor. The second demonstration is based on the Smoluchowski equation for the diffusion-sedimentation process, the boundary conditions being the following: the flux is zero perpendicularly to the deposited particles and the particle concentration is zero at the surface (perfectly absorbing barrier). Moreover, using this approach it could be shown that the

deposition kinetics are only functions of the parameters R^* and R^2/D_S where D_S corresponds to the Stokes-Einstein diffusion tensor. It can be pointed out that, at a given coverage, the structure of the deposited layer of hard spheres is a function of R^* only. In particular, it is independent of the viscosity of the fluid supporting the particles. This, however, does not mean that this structure is the same as the one obtained without taking HI between the moving particle and the adsorbed ones and the adsorbing plane into account. Indeed, in one case the diffusion is anisotropic, whereas in the other case it is isotropic. It may be stressed that even if the viscosity tends to zero (as long as the concept of viscosity keeps its significance), one does not recover the case in which HI are omitted. The viscosity only changes the time scale of the deposition process as it comes out from equation (7) of reference [74].

5. Problems related to diffusional models

Consider a particle in a semi-infinite fluid, initially located at the distance z_0 from the adsorbing empty plane. It can be shown that the probability P_{ads} for this particle to adsorb after a diffusion time t is given by [75]:

$$P_{ads}(z_0,t) = \mathrm{erfc}\left(\frac{z_0}{2\sqrt{D_S t}}\right) \tag{5.25}$$

where D_S is the Stokes-Einstein diffusion coefficient and "erfc" the complementary error function. From this probability one can derive the mean time needed to adsorb:

$$\begin{aligned}\langle t\rangle &= \int_0^\infty t\frac{\partial P_{ads}}{\partial t}dt \\ &= \frac{z_0}{2\sqrt{\pi}}\int_0^\infty e^{-z_0^2/4D_S t}\frac{dt}{\sqrt{D_S t}} \\ &= \frac{z_0^2}{2\sqrt{\pi}D_S}\int_0^\infty \frac{e^{-u^2}}{u^2}du.\end{aligned} \tag{5.26}$$

This integral does not converge and therefore the mean adsorption time is infinite. This justifies from the theoretical point of view the introduction in the DRSA simulations of the upper rejection plane evoked in Section 1. Moreover, if the particle, before touching the deposition plane, diffuses over a long distance, which is possible if the height h of the rejection plane is chosen not too small, it looses the memory of its initial position. In the simulations that were performed in reference [57], the height of the rejection plane was usually fixed to five diameters.

Furthermore, even though $\langle t\rangle = \infty$, one can define the time $t_{1/2}$ after which, on the average, half of a collection of particles, all starting from altitude z_0 above the adsorbing plane at time $t = 0$, will reach this plane. This median time is simply defined by $P_{ads}(t_{1/2}) = 1/2$, hence by $\mathrm{erfc}(z_0/(2\sqrt{D_S t_{1/2}}) = 1/2$. It follows from this definition that $t_{1/2} \approx z_0^2/0.909\,89 D_S$.

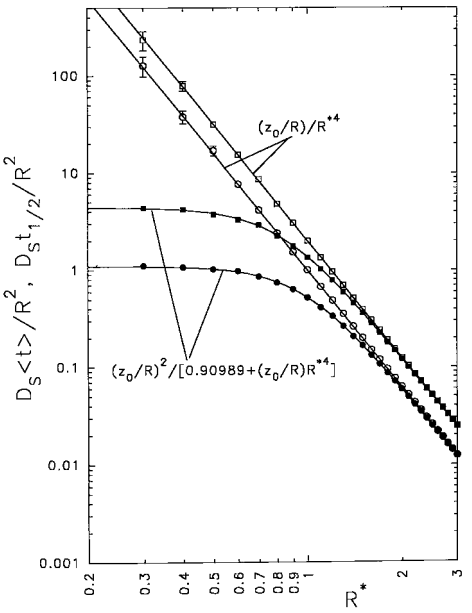

Figure 18. *Simulated mean (white symbols) and median (black symbols) sedimentation times as a function of the reduced radius R^* for two starting heights: $z_0/R = 1$ (circles), $z_0/R = 2$ (squares). The lines correspond to equation (5.27) for the mean time and to equation (5.28) for the median time.*

If the model takes diffusion and gravity into account, the deterministic gravitational force leads to the adsorption of the first particle with probability equal to 1 and the average adsorption (or sedimentation) time is equal to z_0/ν_s, where ν_s is the sedimentation velocity (or Stokes velocity). In terms of dimensionless quantities, this average time is given by

$$\frac{D_S\langle t\rangle}{R^2} = \frac{z_0/R}{R^{*4}}\,. \tag{5.27}$$

Pure diffusion corresponds to $R^* = 0$, hence the average time goes to infinity, as already mentioned. As to the median time $t_{1/2}$, it tends to coincide with the average time when $R^* \to \infty$, for then the distribution of the adsorption time tends to a Dirac distribution centered on $\langle t\rangle$. In contrast, when $R^* = 0$, the dimensionless median time is given by $D_S t_{1/2}/R^2 \approx (z_0/R)^2/0.909\,89$. An interpolation formula, spanning the whole range of R^* from zero to infinity, is obtained by defining the median time as the harmonic average of both its limiting values:

$$\frac{D_S t_{1/2}}{R^2} \approx \frac{(z_0/R)^2}{0.909\,89 + (z_0/R)R^{*4}}\,. \tag{5.28}$$

Figure 18 compares the predictions of equations (5.27, 5.28) with simulation results as a function of R^*, for $z_0/R = 1$ and 2.

Following equation (5.25), it appears that the adsorption probability tends to 1 when the time tends to infinity. That is, on an empty surface, the adsorption probability equals 1 when the diffusion time is unlimited. Since any of the following particles continues its diffusion even after collisions with preadsorbed particles, the probability of adhesion is also equal to one if the allowed duration of diffusion is assumed to be unlimited. This holds as long as at least one target is available on the surface, *i.e.*, as long as the jammed state is not reached. Once the last possible particle has adhered, the probability drops abruptly to zero by definition of the jammed state. This reasoning is true in the presence of gravity also. A particle falling in a trap has a strictly positive probability to escape unless the particle is infinitely heavy (BD model), hence will escape after an infinite time. The adhesion probability is therefore simply a step function when represented as a function of the coverage. Such a step function, however, gives no information on the kinetics of the filling process, whereas it is intuitively evident that, on the average, the time needed by a particle to adhere increases when the surface coverage increases.

Again following Landau and Lifchitz [75], the flux at an empty surface is given by:

$$J(\theta = 0) = \frac{z_0}{2t\sqrt{\pi D_S t}} e^{-z_0^2/4D_S t} \tag{5.29}$$

for a particle starting from $z = z_0$ at time $t = 0$. This means that, on the average, if n_0 particles start at $z = z_0$ there are Jn_0 particles which will reach the adsorbing surface per unit of time at time t. The integral of J over time leads to the adsorption probability given by equation (5.25). As a consequence, if we wish to use the definition of the available surface function given in Section 1 of Chapter 2, *i.e.*, the ratio of the adsorption flux to the surface, at a given coverage θ, to the adsorption flux on the empty surface ($\theta = 0$), we see that we have to specify, on the one hand, the initial distance of the particles from the adsorbing wall and, on the other hand, the time at which the flux is measured:

$$\Phi(\theta, z_0, t) = \frac{J(\theta, z_0, t)}{J(0, z_0, t)} \tag{5.30}$$

In practice, can we determine the kinetics of the process in the absence of gravity by computer simulations of sequential processes (see also paragraph 1.1)? Strictly speaking, this seems to be impossible because $\langle t \rangle = \infty$ at $\theta = 0$, hence *a fortiori* at $\theta > 0$. Therefore, for practical purposes, we have to impose a limit somewhere. There are two main possibilities: either the diffusion time or the distance at which the particle can diffuse away from the adsorbing plane must be limited. An alternative to the time limitation is a limitation of the number of collisions. Time and distance limitations are not mutually exclusive. The first criterion which is met leads to the rejection of the particle, hence to a new adsorption attempt. In case of rejection, the wasted time can be incorporated in the kinetics, but this biased method causes an uncontrolled error in the estimation of the time actually needed to reach a given coverage. What is $\Phi(\theta)$ in these circumstances? If we still wish to write $d\theta/dt = \Phi(\theta)$, we have to realize that Φ depends on the one hand on the

geometrical structure of the surface and on the other hand on the limitation(s) imposed to the simulation procedure as indicated above. This suggests immediately that Φ must depend on the longest diffusion time allowed and/or on the farest point a particle can reach before being withdrawn from the system, in addition to the distance of the starting plane to the adsorbing plane.

A way to get around these conceptual difficulties was suggested in reference [57]. The diffusion cell was subdivided into horizontal slabs, each of height $2R$ (Fig. 12), and the diffusing particles moved on a fine mesh three dimensional lattice. A particle was located in a given slab if its center lay in the mid plane of this slab. Assume that at a given time t, N_0, N_1, N_2, *etc.*, particles are located in slabs 0, 1, 2, *etc.*, respectively. Note that slab 0 corresponds to the lowest one, *i.e.*, the one immediately above the adsorbing plane. Therefore N_0 represents the number of irreversibly adhering particles. During the time interval Δt, all these numbers N_j change by an amount ΔN_j depending on the transition rates $W_{j,j\pm1}$ from slab j to one neighboring slab, according to the following series of equations:

$$\begin{cases} \Delta N_0 = W_{1,0} N_1 \Delta t \\ \Delta N_1 = [(-W_{1,0} - W_{1,2}) N_1 + W N_2] \Delta t \\ \Delta N_2 = [-2W N_2 + W_{1,2} N_1 + W N_3] \Delta t \\ \ldots \\ \Delta N_j = [-2N_j + N_{j-1} + N_{j+1}] W \Delta t, \text{ for } j \geq 3 \\ \ldots \end{cases} . \tag{5.31}$$

Note that $W_{j,j\pm1}$ is independent from the coverage when $j \geq 2$ and is then simply denoted by W. In contrast, $W_{1,0}$ and $W_{1,2}$ depend on the coverage. Note also that $W_{0,1} = 0$ since no particle can desorb. For a finite number of slabs, the system of equations can be solved numerically starting from an arbitrary initial particle distribution in the slabs. This leads in particular to the time evolution of N_0. Taking the derivative of N_0 with respect to time leads then in principle directly to the available surface function, up to a scaling constant.

However, as indicated in paragraph 1.1, it is not clear at which distance from the surface one has to assume the particle concentration in the bulk to be constant. If we chose to keep N_1 fixed, *i.e.*, to keep the average number of particles in the slab located just above the adsorbing slab constant, the available surface is simply proportional to the transition rate $W_{1,0}$. In this latter case the numerical solution of the system is even not necessary. The transition rate $W_{1,0}$ was obtained by simulation as explained in reference [57]. This transition rate is shown in Figure 19 together with the best fit of the function:

$$W_{1,0}^{fit} = \frac{a_0 (1-x)^p}{1 + a_1 x + a_2 x^2 + a_3 x^3} \tag{5.32}$$

to the simulated data, where $x = \theta / 0.547$. It may be mentioned that one obtains $p \approx 2.43$ which is to be compared to 2.5 as can be deduced from the asymptotic

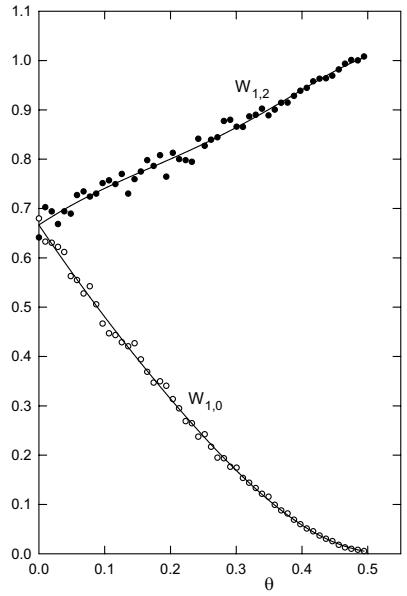

Figure 19. *Transition rates from slab 1 to slab 0, and from slab 1 to slab 2. Symbols indicate simulation data, whereas lines represent least squares fits to these data (Eq. 5.32).*

behavior of $\theta(t)$ established by Schaaf *et al.* [55]. This should stress the resemblance between $W_{1,0}$ and Φ.

In order to emphasize the importance of the choice of the distance at which the bulk concentration is supposed to be constant, we have solved the system (5.31) in the case where the diffusing cell has a height of $12R$ and is hence subdivided into six slabs, with the initial occupation numbers $N_0 = 0$, $N_1 = N_2 = N_3 = N_4 = N_5 = 1$. The last slab plays the role of a reflecting barrier, *i.e.*, particles can diffuse up to it and come back afterward. The first time the numerical solution of (5.31) was obtained upon fixing $N_1 = 1$, the second time $N_5 = 1$ throughout the iterative resolution procedure. The resulting kinetic evolution of the number of particles in slabs 0 and 1 are shown in Figure 20. Obviously, the choice of the slab where the occupancy is kept constant influences significantly the time evolution of N_0 (and of the other numbers as well, but this is less important); however, as could be anticipated, after long enough an adsorption time, both kinetics converge toward the same saturation number of particles on the surface.

6. Mixtures

A first step toward the description of polydispersed particle systems has been made by studying the case of bidispersed mixtures [42, 43, 76] or mixtures of objects of different shapes [77]. The more complicated situation provided by polydispersed mixtures was analyzed by Tarjus and Talbot [78] and Meakin and Jullien [43].

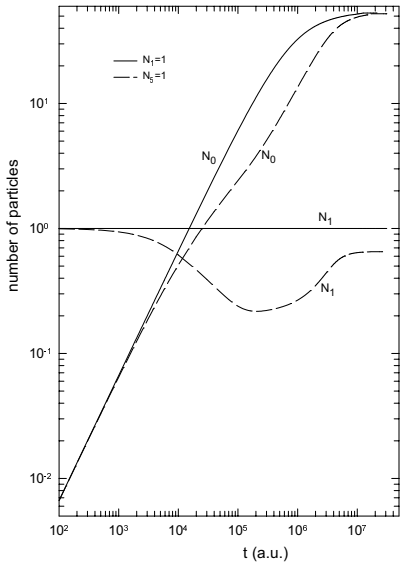

Figure 20. *Number of particles located in slabs 0 and 1 as a function of time, as determined by solving the system of coupled equations (5.31) (for details, see text).*

In the particular case of a binary mixture of disks, deposited following the rules of the RSA model, one species having a much smaller (or larger) radius than the other species, the jamming limit could be determined on the basis of two coupled first-order differential equations [42]. Moreover, the kinetics of the deposition of the small disks proved to follow the usual RSA law, *i.e.*, $\theta_S(t) = \theta_S(\infty) - kt^{-1/2}$ (where the subscript "S" stands for small), whereas the kinetics of the deposition of the large disks follows an exponential law.

For arbitrary particle radii, however, no precise prediction on the respective contributions of the small and large particles to the total coverage can be made. Therefore, only simulations can lead to the estimation of these respective contributions, as well as to the kinetics of deposition of both species involved. Meakin and Jullien [43] studied extensively the case of binary mixtures of hard disks according to the RSA deposition rules. Let $r = R_L/R_S$ be the ratio of the large disk radius to the small disk radius. For various values of r, in the range 1.125–8, simulations were carried out using several values between 0 and 1 of the composition parameter p which is the fraction of small disks selected for trial deposition onto the substrate (note that the particle reservoir is assumed to be infinite which means that the proportion p does not vary over the duration of the deposition process). Meakin and Jullien [43] confirmed that θ_S follows the RSA power law in the asymptotic regime, while θ_L approaches its limiting value exponentially, *i.e.*, much more rapidly than does θ_S.

On the other hand, the jamming limit contributions $\theta_S(\infty)$ and $\theta_L(\infty)$, as well as the total jamming limit coverage $\theta_T(\infty)$, depend on both r and p. The highest

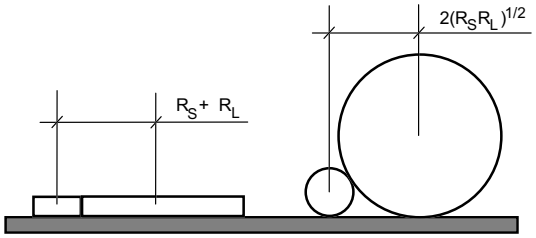

Figure 21. *Schematic representation of the deposition of two unequal disks at contact (left) and two unequal spheres at contact (right). Although the small disk and the small sphere have the same radius, and similarly for the large particles, the center-to-center distance projected on the adsorption plane is smaller in the case of the spheres if compared to the case of the disks.*

total coverage is obtained for $p \to 0$. In this case, practically only large disks are drawn from the reservoir until their own jamming limit is reached; then, the gaps formed by the large disks can only be filled by the small ones. This is obviously the most efficient way to cover the surface as much as possible at fixed ratio r. When the radius ratio r tends to infinity while p tends to zero but remains strictly positive, the total coverage $\theta_T(\infty)$ is given by:

$$\theta_T(\infty) = \theta_L(\infty) + [1 - \theta_L(\infty)]\theta_L(\infty) \tag{5.33}$$

where $\theta_L(\infty) = 0.547$ is the coverage obtained with monodisperse disks in RSA. Clearly, the small disk contribution is given by the second term on the right hand side: $\theta_S(\infty) = (1 - 0.547)0.547 \approx 0.248$, hence $\theta_T(\infty) \approx 0.795$. Note also that if p is set to exactly zero, $\theta_T(\infty)$ drops abruptly to the RSA limit equal to 0.547. The process is therefore not continuous with respect to p at $p = 0^+$.

The study of the deposition of spheres constituting a binary mixture was carried out in the framework of the DRSAG model [66, 79]. The results are qualitatively the same as in RSA as far as the jamming limit is concerned. Here, however, the jamming coverages are slightly higher due to the influence of the gravitational force which tends to form configurations more compact than those obtained with the RSA model. Also, diffusion allows a small particle to reach a position in contact with a large particle such that the projected center-to-center distance is only $2\sqrt{R_S R_L}$ which is always smaller than the sum $R_S + R_L$ of the radii, hence smaller than the RSA counterpart for disks (Fig. 21). As an example, Figure 22 shows the contributions of the small and large spheres, as well as the total coverage, at the jamming limit for a mixture of spheres of 4 and 6 μm in radius and a buoyancy of 0.045 g/cm^3, as a function of the composition parameter p.

Muralidhar and Talbot studied the kinetics of the adsorption of polydisperse mixtures, assuming a continuous distribution of the radius [80]. They restricted the analysis to the initial adsorption kinetics, *i.e.*, to the small coverage of the collector. This approach was devised for the description of both irreversible and

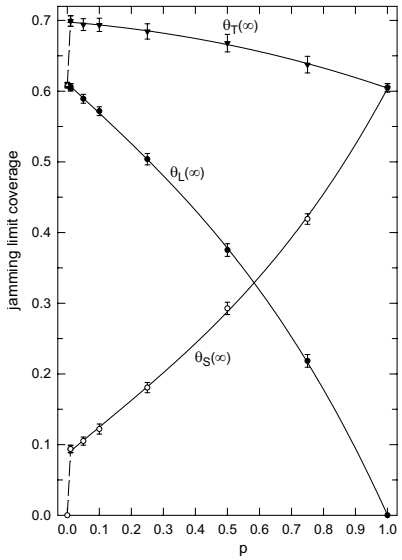

Figure 22. *Jamming limit coverage as a function of the composition parameter p for a bidispersed mixture of spheres of 4 and 6 μm in radius. The particles are deposited according to the DRSAG model. The buoyancy of the particles is $\Delta\rho = 0.045$ g/cm^3. θ_S and θ_L represent the contribution of, respectively, the small and large spheres to the total coverage θ_T. Note that the total coverage has a discontinuity when p becomes zero (indicated by the dashed line). The symbols (dots and triangles) represent simulation results and the lines are drawn to guide the eye.*

reversible processes. The generalized kinetic equation is written:

$$\frac{\partial\rho(R,t)}{\partial t} = k_a(R)c_0(R)\Phi(R,t) - k_d(R)\rho(R,t) \tag{5.34}$$

where $\rho(R,t)dR$ is the surface density of adsorbed molecules of radius between R and $R+dR$, $c_0(R)dR$, is the corresponding bulk concentration, $k_a(R)$ and $k_d(R)$ are the adsorption and desorption rates for particles of radius R, respectively. Furthermore, $\Phi(R,t)$ is the available surface function for an incoming molecule of radius R. The authors determine analytically the moments of the particle radius distribution on the surface and relate them to the moments of the radius distribution in the bulk phase, this latter being of the form Re^{-R}. In particular, it is shown how the surface distribution moments deviate progressively with time from the bulk moments in the case where the adsorption coefficients are size dependent. The range of validity of the theoretical expressions derived for the size distribution moments is established using computer simulation. Finally, it may be stressed that this theory, although restricted to the small coverage regime, is considerably more accurate than the multicomponent Langmuir equation, where it is assumed that $\Phi_i = 1 - \Sigma\theta_i$.

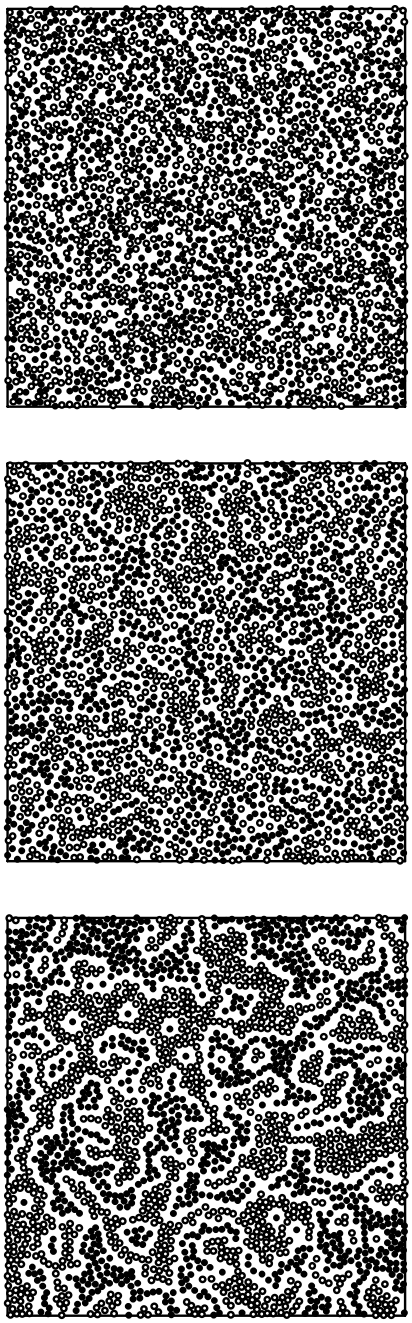

Figure 23. *Typical configurations formed by a mixture of particles with short range (hard core) repulsion (white-white and black-black) or long range repulsion (white-black) adhering irreversibly on a surface, for increasing values of the repulsion parameter f ($f = 1$, 1.5 and 2 from top to bottom).*

Brilliantov *et al.* [81] have considered the RSA deposition process of a mixture of hard particles having a continuous distribution of radii $P(R)$ ranging from zero up to some maximum size. They studied the case of a power law size distribution:

$$P(R) = \alpha R^{\alpha-1} \tag{5.35}$$

and found that such a process gives rise to fractal structures characterized by the fractal dimension D_f depending on the exponent α. For low values of α, these authors proposed the series expansion:

$$D_f = 2 - \pi\alpha - (\pi^{3/2} + \pi/2)\alpha^2 + O(\alpha^3). \tag{5.36}$$

However, this expansion seems to not correspond to the values of D_f reported in Figure 3 of reference [81]. Indeed, another small-α expansion, which seems to be more correct, is proposed in an article to be published by the same authors in *Physical Review E*.

Up to now we have implicitly considered that a suspension was a mixture if it contained two or more species of particles differing by their sizes. A mixture may be defined in several other ways. As an example, consider a two-component mixture of particles (particles a and b) identical from the geometrical point of view (disks of equal diameter) but with different mutual interaction. Assume that any a-particle interacts with any other a-particle through a hard core potential and similarly for the b-particles. In contrast, an a-particle and a b-particle repel each other. In practice, in the RSA-like simulation, this is obtained using the diameter d as the minimum distance between identical particles as usually in models dealing with hard particles, but a minimum distance $f \times d$, larger than the diameter, for nonidentical particles. As in the non equally sized particle case discussed above, the process is defined by two parameters: the composition parameter p and the repulsion factor f (≥ 1). Obviously, when $f = 1$ one recovers exactly the classical RSA. Figure 23 displays typical configurations obtained with $f = 1,\ 1.5$ and 2 (from top to bottom) for $p = 1/2$. In the three cases the total coverage equals approximately 0.374. When f increases it is apparent that the configurations become more and more inhomogeneous with, in particular, the formation of "islands" of b-particles surrounded by a "sea" of a-particles (the reversed interpretation is equally valid) and only a few isolated particles.

6

Experimental results

1. Is there a need for other adsorption models than the Langmuir model?

Adsorption kinetics of macromolecules or colloidal particles on solid surfaces have been and are still usually described by the Langmuir model. A Langmuir system follows the kinetic law:

$$\frac{d\theta}{dt} = k_a c_b \left(1 - \frac{\theta}{\theta_{max}}\right) - k_d \theta \tag{6.1}$$

where k_a and k_d represent respectively the adsorption and the desorption constant, θ_{max} corresponds to the maximum attainable surface coverage and c_b represents the concentration of adsorbing species in the bulk but in the vicinity of the adsorption plane. For this system, the available surface function $\Phi(\theta)$ is given by:

$$\Phi(\theta) = 1 - \frac{\theta}{\theta_{max}} \cdot \tag{6.2}$$

The first question that has to be answered from experiments is the following: is there a need for other adsorption models than the Langmuir model? A negative answer to this question would clearly mean that the theoretical studies concerning the RSA-like models are pure academic speculations!

This question has only started to be addressed rigorously over the last few years. This is mainly due to the difficulties to determine precise kinetic curves with all the boundary conditions well defined. For proteins, Jin *et al.* [48] have clearly demonstrated that a Langmuir model cannot accurately describe breakthrough chromatographic curves of lysozyme. A similar conclusion emerges out of the breakthrough curves of colloidal particles obtained by Johnson and Elimelech [82]. Analyzing kinetic experiments of colloidal particles on planar surfaces, Adamczyk *et al.* found that the Langmuir model cannot account for their experimental data [14,38] over a long time scale. The Langmuir model accounts correctly for the initial adsorption times but leads rapidly to adsorption kinetics which are much faster than the observed ones. Experimental adsorption kinetics of colloidal particles on solid surfaces near saturation also clearly exhibit a behavior different

from the one predicted by the Langmuir model [2]. Ramsden *et al.* have also observed that the adsorption rate of cytochrome P450 onto a lipid bilayer [83] and of apotransferrin onto $Si(Ti)O_2$ surfaces [84] cannot be correctly described by the Langmuir model which predicts a linear decrease of the adsorption rate with the coverage. Such a linear behavior is, however, not observed. The Langmuir model would also imply that the reduced variance of the number of adsorbed particles on solid surfaces should, according to relation (3.10), follow the law:

$$\frac{\sigma^2}{\langle n \rangle} = 1 - \frac{\theta}{\theta_{max}} \tag{6.3}$$

and thus vary linearly with the coverage. This is, however, usually not observed experimentally [8, 85].

These experimental observations thus clearly demonstrate that the Langmuir equation cannot account correctly for the various adsorption behaviors of colloidal particles or macromolecules on solid surfaces. The limitations of the Langmuir model stem mainly from the fact that it does not account correctly for the surface exclusion effect. This has certainly contributed to trigger the interest of the scientific community to study the RSA model over the past years.

2. Validity of the RSA model

2.1. Experimental results relative to colloidal particles

The first experimental study in which the RSA model was proposed to describe the adsorption process is due to Feder and Giaever [86, 87]. They investigated the adsorption of ferritine (an iron-storage protein) on a carbon surface. They measured a maximum surface coverage of 0.518. Feder also determined the radial distribution function $g(r)$ near jamming which he found compatible with the RSA model predictions. Onoda and Liniger [88] determined the maximum surface coverage for spherical latex particles irreversibly fixed on a solid surface and found for θ_∞ a value of 0.55 ± 0.01 which is in good agreement with the value predicted by the RSA model ($\theta_\infty = 0.547$).

Since these pioneering works, several studies concerning the adsorption kinetics of colloidal particles on solid surfaces and the structure of these surfaces covered by the irreversibly adsorbed latex particles have been reported. The effects of the ionic strength were in particular first investigated by the group of Adamczyk [2,13,14,38] who compared its experimental results with the predictions of the extended RSA model taking the double layer repulsive forces into account. To analyze their results, Adamczyk *et al.* compared them not only to the extended RSA model, but they also introduced the concept of "equivalent hard sphere radius" as discussed in paragraph 2.2 of Chapter 4. Lenhoff *et al.* [39, 89] also investigated the effect of ionic strength on the deposition process of positively charged amidine latex particles on mica sheets. They determined the structure of the deposited particle configurations through AFM imaging. Johnson and Elimelech [82] also

investigated the effect of the ionic strength on the particle deposition by chromatographic means. Finally, Wojtaszczyk *et al.* [85, 90] performed a systematic study of the statistical properties (structure and density fluctuations) of assemblies of deposited particles as a function of the coverage in the case where the screening length of the electrostatic interactions between particles is small compared to their radius ($\kappa R \gg 1$). The main conclusions that can be drawn from these studies are the following.

(i) The jamming limit coverage increases with the ionic strength. However, a quantitative comparison between experimental data with the relations (4.44, 4.46) is still lacking.

(ii) The adsorption kinetics seem also to be compatible with the extended RSA predictions. A few remarks are necessary at this point. To analyze the kinetic results in the low to intermediate coverage range the experimental data were often compared to kinetic functions obtained by the integration of the kinetic equation (2.3b) by keeping only the terms up to the second order in expression (4.5) of the available surface function modified according to the equivalent hard sphere concept [2, 14, 38]. Since Widom, one knows, however, that the RSA available surface function is indistinguishable from its equilibrium counterpart up to the second order in the coverage. The group of Adamczyk also found that, near the jamming limit, the adsorption rate of colloidal particles seems to vary linearly with $t^{-1/2}$ [14] as predicted by the RSA model. A similar behavior was observed by the group of Lenhoff [89] who studied the adsorption of positively charged amidine latex particles on mica sheets. Recently, however, this group reanalyzed its data and claimed that the asymptotic kinetic behavior is more compatible with a $t^{-2/3}$ power law as predicted by Schaaf *et al.* [55]. Unfortunately, no comparison between the experimental curves and the theoretical predictions was provided.

(iii) Radial distribution functions have also been determined for such systems and compared to the predictions of the repulsive soft core RSA model (see paragraph 1.1 of Chap. 4) obtained from computer simulations. Again it was shown that the experimental results are compatible with the repulsive soft core RSA model. Unfortunately the experimental $g(r)$ are usually compared to the RSA predictions at only *one* coverage which is, in addition, often low [2, 13, 38, 39, 89]. This agreement between experiments and theory is mainly due to the experimental systems which were investigated, at low ionic strength the maximum coverage being itself low. However, at low coverage, no great difference exists between RSA-like and equilibrium structures. For this reason Wojtaszczyk *et al.* [85, 90] have investigated the evolution of $g(r)$ with the coverage. They found that the $g(r)$ relative to an assembly of deposited sulphate latex particles of radius 0.77 μm ($R^* = 0.66$) with a Debye length small compared to the radius ($\kappa R \gg 1$) is in good agreement with an RSA $g(r)$ at intermediate and high coverages (coverages larger than 0.30). On the other hand, at coverages of the order of, or smaller than

0.15 slight differences between the RSA and the experimental $g(r)$ appear. As we will see later, such a behavior seems to be valid for other systems too. These differences can have different origins such as the polydispersity of the medium, the influence of the hydrodynamic interactions during the deposition process, *etc.*

(iv) The reduced variance of the number density has also been determined as a function of the coverage. Adamczyk *et al.* found that $\sigma^2/\langle n\rangle$ varies with the coverage in accordance with the predictions of the extended RSA model [11, 12]. In particular, at low coverages the reduced variance decreases linearly with θ. Such a behavior has not been observed by Wojtaszczyk *et al.* [85] with the particles exhibiting a $g(r)$ close to the RSA $g(r)$. They found that $\sigma^2/\langle n\rangle$ starts with an horizontal tangent at low coverage before decreasing in a more or less linear way down to its jamming limit value. In addition, they found that the available surface function for this system behaves similarly to that of larger particles in which gravity plays an important role; in first approximation, this finding corresponds to a ballistic behavior.

How can these radically different behaviors observed by Wojtaszczyk *et al.* and by the group of Adamczyk be explained? As we know from expression (3.12), the first non vanishing term in the expansion of $\sigma^2/\langle n\rangle$ with the coverage is of the same order as the first non vanishing term in the expansion of Φ with respect to θ. This order corresponds to the minimum number of deposited particles on the surface which is required to eventually forbid a new particle to reach the plane and thus to adhere on it [9]. It must be stressed that the adhesion experiments were performed by the two groups following two different ways: Wojtaszczyk *et al.* performed a sedimentation experiment with small particles ($R^* \approx 0.7$). In this case the Brownian motion dominates over the deterministic gravitational motion. However, even if the influence of gravity is small, it is not completely absent and if only one particle is deposited on the surface a new incoming sphere cannot be excluded from the surface. Due to the influence of gravity, it will thus, ultimately, still adhere on the surface. The situation is radically different for the experiments performed by the group of Adamczyk in which the impinging jet method is used. In principle, at the center of the cell, the particles feel – in spite of the flow – no force toward the surface. However, even for particles in the micron size domain, the gravity can play a small role. Furthermore the particles have to adhere on the bottom of a mica sheet, which renders R^* negative though near zero. With these conditions it becomes clear that the presence of one particle can affect the adhesion probability of a new one so that the reduced variance becomes linear in the coverage. Finally, it can be pointed out that, in the experiments of Wojtaszczyk *et al.*, $\sigma^2/\langle n\rangle$ varies differently from what is expected from the RSA model in spite of the fact that the radial distribution function of the system is close to the RSA $g(r)$ at intermediate and high coverages. This is at first sight in contradiction with the exact relation (2.6) between $\sigma^2/\langle n\rangle$ and $g(r)$. This apparent paradox has been explained in reference [91]. It comes from the fact that very slight differences in the

$g(r)$, which cannot be detected on the experimental radial distribution function itself, once integrated over space, lead to a large contribution to $\sigma^2/\langle n\rangle$.

The adsorption probability of a particle on a solid surface, and thus the available surface function, plays also a great role in chromatography. Johnson and Elimelech [82] have used this technique to investigate the dynamics of charged colloidal particles in porous media as a function of the ionic strength and thus of the screening length. They showed that their breakthrough curves cannot be predicted by the Langmuir model but are, on the other hand, recovered when the RSA expressions (4.4, 4.8) are used, the coverage θ being replaced by $\theta(\infty)\beta\theta$ where $\theta(\infty)$ corresponds to the RSA jamming limit and β is a rescaling parameter. They have thus used the equivalent hard sphere concept. They have also determined from their experiments the evolution of the coverage θ as a function of time. Figure 2 of reference [82] seems to indicate that at long times, in the jamming limit regime, the coverage varies linearly with $t^{-1/2}$ as observed by other authors. These experiments seem thus to demonstrate the validity of the RSA model to describe the explored system. It is however not clear if other deposition processes, more specifically if an equilibrium rescaled hard sphere available surface function would not have lead to a similar accordance between experiment and theory. A partial answer to this question would have been obtained if the experimental curves had been compared to the predictions obtained by assuming an expression of the form (4.12) for the available surface function over the entire coverage range.

2.2. Experimental results relative to the irreversible deposition of spherocylindrical particles

Very recently, Ramsden and Máté [92] have reported a study of the irreversible deposition of monodisperse spherocylindrical iron (III) hydroxide particles on a hydrophilic silica-titania surface. To our knowledge, this constitutes the first experimental study of irreversible deposition processes of spherocylindrical particles. They have shown that the Langmuir equation does not account for their experimental results. These latter, in contrast, could be interpreted by introducing the available surface function relative to an RSA process of spherocylinders, as well as three parameters which had to account for the influence of the electrostatic and hydration interactions. These parameters were the particle surface potential, the silica surface potential and the polar (hydration) interaction energy between the particles and the surface. Unfortunately, the values found for the three parameters are far different from the values of these quantities measured in solution by other means and no explanation was given for these large discrepancies. Additional experiments would be of interest to verify if their model can account for a large range of experimental conditions with these particles.

2.3. Experimental results relative to macromolecules

We have up to now discussed the experimental results relative to colloidal particles but the interest for the RSA model has really started from the experiments of Feder and Giaever on the adsorption of ferritin on solid surfaces [86, 87]. More recently, the group of Pefferkorn [93] also used the RSA model to describe the adsorption kinetics of macromolecules on solid surfaces. They constructed a function $K(N)$, where N is the number of adsorbed macromolecules on the surface, which is a specific adaptation of the available surface function to their experimental set-up. This function becomes equivalent to Φ when the characteristic time of their experiment (time of integration of the radioactive counting) is short compared to the characteristic adsorption time. They have compared their experimental values of $K(N)$ directly to the values predicted by RSA simulations. They found a good agreement between the RSA predictions and the experimental results for non-charged polymers such as polystyrene adsorbing on silica. On the other hand, for polyelectrolytes, they found that the model had to be adapted in such a way as to allow for the possibility of some diffusion of the adsorbing particles in the vicinity of their initial position before adsorbing irreversibly on the surface. They attributed this difference in the behavior to the possibility for non-charged macromolecules to relax rapidly once touching the surface and thus to create rapidly a great number of links with the surface. On the other hand, polyelectrolytes are more rigid entities than neutral polymers. At the beginning of their interaction with the surface, polyelectrolytes act more or less as hard entities and thus interact with the surface only through a limited number of links which still allow for some mobility on the surface. Unfortunately, here too, the experimental results have not been compared to the Langmuir model so that it is difficult to get an idea on the sensitivity of the results with respect to the deposition model. This group also investigated, by a similar method, the adsorption of poly(vinyl-4-pyridine) on polystyrene latex particles [94]. For this study the authors compared their results to an extended RSA model which allowed for the relaxation of the macromolecules on the surface by increasing the area that they cover. Here too, they found good agreement between experiments and simulations. They could even get access to the relaxation time of the polymers.

The group of Ramsden used an integrated optic technique to determine the adsorption kinetics of various proteins on a solid substrate. These authors compared their results to the adsorption rates determined by integrating equation (2.3b) in which the RSA available surface function up to third order (4.4) in the coverage has been used. The only fitting parameters that they introduced in their treatment were an adsorption constant (which is equivalent to a time rescaling) and the area covered by a molecule on the surface which is equivalent to the use of the hard sphere concept. They found that their experimental rates were all compatible with the theoretical predicted rates according to the RSA model extended by the hard sphere concept. The system investigated was iron-free transferrin [84, 95] adsorbed onto $Si(Ti)O_2$ surfaces. For this system they investigated the effect of the ionic strength on the area occupied by an adsorbed protein. For the adsorption of two

proteins belonging to the family of cytochrome P450 on a lipid bilayer, Ramsden *et al.* [96] found that at low bulk concentrations the system behaves according to the Langmuir model, whereas at higher bulk concentrations the adsorption kinetics become more RSA-like. This seems to come from the fact that the proteins can slowly diffuse along the surface and have the tendency to aggregate. At low bulk concentration the characteristic adsorption time τ_a is long compared to the characteristic diffusion time τ_d of the protein along the surface. The adsorbed proteins have thus the time to form large clusters on the surface before a new protein adsorbs. For this kind of configurations the available surface function should, indeed, be given by $\Phi = 1 - \theta$. On the other hand, at high bulk concentrations, τ_a becomes short compared to τ_d so that the system behaves as predicted by the RSA model. Such a crossover between an RSA and an equilibrium behavior has been predicted theoretically by Tarjus *et al.* [46] which introduced the dimensionless parameter ζ as already discussed in paragraph 2.5 of Chapter 4. This parameter has also been used by Ramsden *et al.* in their study. A similar behavior has been observed for the adsorption of metallodendrimers at silica-titanium surfaces [97]. For other systems such as human and bovine serum albumin adsorbing on $SiTiO_2$ surfaces [98] they used adsorption equations in which they allowed desorption:

$$\frac{d\Gamma}{dt} = k_a c_b \Phi - k_d f(\Gamma) \tag{6.4}$$

where Γ represents the adsorbed amount (mass) per unit area and $f(\Gamma)$ is a function of this adsorbed amount. c_b represents the concentration of the proteins in the bulk in the vicinity of the surface and k_a and k_d correspond respectively to the adsorption and the desorption constants. Usually $f(\Gamma)$ is taken equal to Γ, but Kurrat *et al.* [98] indicated that they had to use the function $f(\Gamma) = \Gamma^{-1/2}$ in order to be able to fit their data. Although they took the desorption into account, they used the RSA available surface function in equation (6.4) to account for their experimental data and found reasonable agreement between the experimental data and the predicted rates. It must be pointed out that, from a strict theoretical point of view, the use of equation (6.4) is incompatible with the use of the RSA available surface function. However, due to the fact that Φ_{RSA} differs from Φ_{EQ} only by the terms of order larger than 2 in the coverage expansion, it becomes impossible from an experimental point of view to discriminate between the two expressions of the available surface function. Differences between an adsorption process in which desorption can take place and an irreversible adsorption process can only become apparent in the asymptotic behavior (Fig. 9). To analyze this behavior, Ramsden plotted the adsorption rate in the asymptotic regime as a function of $t^{-1/2}$ [95] and he claimed that this rate varies linearly with $t^{-1/2}$. A careful inspection of his data reveals, however, that the rate does not vary exactly linearly with $t^{-1/2}$. One can speculate if another time dependence (such as $t^{-2/3}$) would not have led to a better agreement with the experimental data.

The RSA concepts have also been used by Jin *et al.* [47] who analyzed breakthrough curves of lysozyme obtained by Mao *et al.* [99]. They also used a kinetic equation of the type (6.4) to compare experimental breakthrough curves to the

theoretical prediction. They adapted both the RSA and the equilibrium available surface function to the case of an adsorption on discrete sites distributed randomly on the surface. They found, here too, good agreement between the experimental results of Mao *et al.* and the predicted breakthrough curves. They also used an RSA-like available surface function due to the fact that they could not evaluate the equilibrium counterpart over the whole coverage range.

2.4. Discussion

From all these experimental results relative to the adsorption of macromolecules or small colloidal particles on solid surfaces it clearly comes out that the major achievement of the introduction of the RSA concept has been to demonstrate that the available surface function entering in the adsorption kinetic equation can usually not be approximated by the Langmuir type function but that RSA or hard sphere equilibrium available surface functions are of great use. The experiments seem not to be able to discriminate between both functions so that the knowledge of the precise adsorption mechanism is not required to correctly account for the adsorption rates. It is only in the asymptotic regime that differences should emerge and more experimental data on a large number of systems are needed to be able to get a better picture of the behavior of the systems in this regime.

Due to the interplay between the diffusion process of particles in the vicinity of the adsorption plane and the hydrodynamic interactions, it is not really surprising that the RSA model predicts accurately the structure of the deposited layer and in particular the radial distribution function when the particles do not diffuse once adsorbed. However, what is, in our opinion, more surprising is the fact that this model predicts accurately the adsorption kinetics. Indeed, hydrodynamic interactions should, at least for colloidal particles, influence strongly the adsorption rate. This is especially expected at high coverage near the jamming limit. The adsorption power law $t^{-1/2}$ is of purely geometrical and statistical origin and has, in our opinion, no reason at all to be followed by experimental systems. The power law $t^{-2/3}$ takes the diffusion process into account and is thus more likely to be observed. However, it does not take hydrodynamic interactions into account. The fact that experimentally these laws seem to be observed thus constitutes a real mystery. However, before spending more effort to understand this observation, more experiments are needed to verify this result. In particular, if possible, the experimental data in the asymptotic regime should not be directly compared to a given power law but one should plot $\ln[\Gamma(t) - \Gamma(\infty)]$ as a function of $\ln(t)$, where $\Gamma(t)$ represents the adsorbed amount at time t and $\Gamma(\infty)$ corresponds to the adsorbed amount at infinite time. This quantity must be estimated experimentally and the eventual dependence of the slope of this curve on $\Gamma(\infty)$ should be investigated.

3. The case of the deposition of large spherical particles

Up to now we have discussed experimental results relative to the adsorption of particles or proteins in which gravitational effect should not play a significant role. We will now focus on the irreversible deposition of large colloidal particles in which gravity is of importance. Wojtaszczyk *et al.* [8, 85, 90] investigated the statistical properties of surfaces covered by such particles. The evolution of the radial distribution function $g(r)$, and of the reduced variance of the number of particles was investigated as a function of the coverage for various systems characterized by values of R^* ranging from 0.66 to 3.4. The evolution of the number of deposited particles on the surface was investigated as a function of the bulk concentration which is directly related to the available surface function Φ. The range of R^* investigated covers the transition from an RSA to a ballistic behavior according to Figure 14. As already mentioned, a fairly good agreement between the RSA-like radial distribution functions and the $g(r)$ relative to the system characterized by $R^* = 0.66$ was found. A fairly good agreement between the ballistic-like $g(r)$ and the radial distribution functions relative to the system characterized by $R^* = 3.4$ was also observed. However, at low coverages the deposition probability seemed to be slightly, but systematically, larger for values of the interparticle distance r corresponding to the minimum in $g(r)$ appearing after the first peak. These differences were first attributed for example to the hydrodynamic interactions between the adsorbed and the deposited particles or to short range repulsive interactions. Computer simulations taking hydrodynamic interactions into account in the ballistic deposition model have been performed and the radial distribution functions have been compared to the experimental $g(r)$ relative to the system characterized by $R^* = 3.4$. The hydrodynamic interactions reduced the differences between experiment and theory but could not lead to a perfect agreement between them (Fig. 17). For the systems characterized by R^* between 3.4 and 0.66 one could see that the $g(r)$ evolve continuously from a ballistic behavior to an RSA behavior. In contrast, such a continuous evolution was observed neither for the variation of the reduced variance of the number of particles with the coverage (Fig. 24), nor for the available surface function. For both entities a universal evolution with the coverage was observed by varying R^*. As already discussed in paragraph 2.1 such a behavior can be explained by the fact that in all these systems, even if slight, gravity always plays a role so that one deposited particle can never hinder a new one to adhere on the surface: the presence of at least three deposited particles is required on the surface to forbid a new one to reach it. Both $\sigma^2/\langle n\rangle$ and Φ thus vary at small to intermediate coverages as $1 - \alpha\theta^3$. It would be interesting to understand how the systems behave in the limit $R^* \to 0$ and even when R^* becomes slightly negative which can be achieved experimentally by adsorbing the particles on the bottom of a surface. In particular, will $\sigma^2/\langle n\rangle$ and Φ behave as predicted by the RSA model? In case of a positive answer to this question, how will the systems evolve from a ballistic behavior to an RSA behavior by varying R^*?

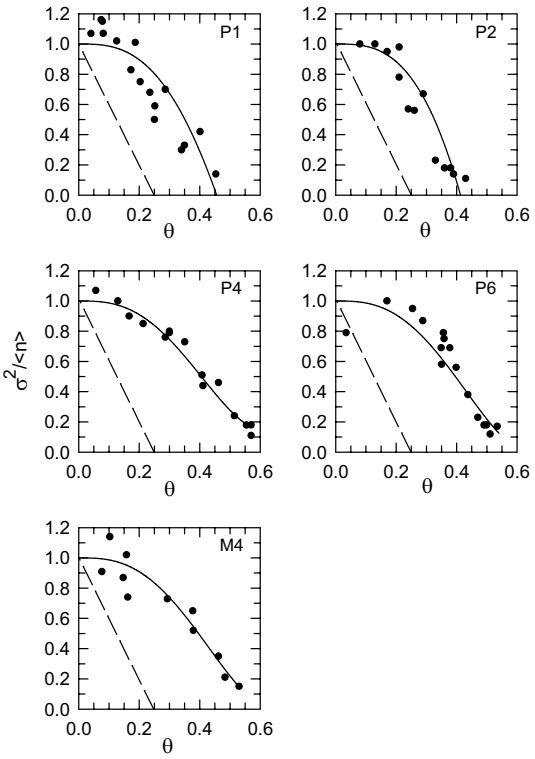

Figure 24. *Reduced variance of the number of particles deposited on a surface as a function of the coverage, for five types of particles: P_1, P_2, P_4 and P_6 correspond to polystyrene spheres of radius equal to 0.77, 1.02, 2.10 and 3.38 μm, respectively, whereas M_4 corresponds to melamine particles of radius 2.23 μm. Note that R^* ranges from 0.66 up to 3.43. The continuous line represents the least squares fit to the experimental data (•) of the polynomial $1-(3/2)9.949\,78\theta^3+b_4\theta^4$ where b_4 is a free parameter. The dashed line represents the RSA first order expansion, i.e., $1-4\theta$.*

Adamczyk *et al.* [100] determined the deposition kinetics of particles under strong influence of gravity. Surprisingly they found a deposition rate which, at intermediate coverages is faster than the rate predicted by the ballistic model, whereas at coverages exceeding 0.50 it levels off more rapidly than predicted by the BD model. This result is surprising because one expects the ballistic deposition rate to be the upper limit of the deposition rate. On the other hand, the BD model does not take the formation of multilayers into account. The presence of such a layer can eventually lead to an increase in Φ due to the fact that when a trap formed out of three deposited particles is filled by a fourth particle it can no longer act as a trap. The hypothesis of this result is currently under investigation in a collaborative work between the groups of Adamczyk and the group of Strasbourg.

4. Adhesion of red blood cells to a solid surface

In this section, we present experiments and simulations dealing with the sedimentation of red blood cells (RBC) in a liquid, and their adhesion to a horizontal solid surface. This constitutes a first example of the study of the adhesion of a system of *non ideal particles*. Indeed RBCs are neither spherical nor perfect disks. In addition, one cell differs slightly from its neighbors. However, this example shows how useful the concepts introduced by the RSA-like models are even for such non ideal systems.

In particular, the modeling of the adhesion of RBCs on a solid/liquid interface by the ballistic deposition (BD) model will be outlined. Indeed, this model, although appropriate for spherical particles only, hence in principle not applicable to the deposition process of disk-shaped RBCs, allows to reproduce our experimental data. This quite surprising observation will be discussed and analyzed, especially in respect to another irreversible deposition model specifically developed for the deposition of disks [101].

Suspensions of human RBCs previously fixed with glutaraldehyde were injected in a diffusion cell. The buoyancy of the RBCs may be estimated to 0.06–0.07 g/cm^3. Once all RBCs had deposited, ν non overlapping pictures ($\nu \approx 100$) were taken. This experiment was repeated for different values of the cell concentration, C_{RBC}, of the injected suspension in order to determine the mean $\langle\eta\rangle$, as well as the variance σ_η^2 of the relative area η covered by the RBCs. In the image analysis of the pictures, RBCs located in higher layers were eliminated by a threshold procedure, hence only RBCs in contact with the glass slide were retained.

If no overlap occurred between RBCs, the relative area covered by RBCs would be equal to:

$$\omega = \langle n\rangle \frac{\langle \pi R^2\rangle_b}{a} \tag{6.5}$$

where $\langle \pi R^2\rangle_b$ represents the mean area of an isolated deposited RBC and $\langle n\rangle$ the average number of RBCs per picture directly proportional to C_{RBC}. In fact, the relationship between ω and $\langle\eta\rangle$ is only linear for small concentrations (*i.e.*, small ω), where overlaps occur seldom (Fig. 25). To study the fluctuation of the relative area covered by RBCs, a normalized relative area variance was defined by:

$$z = \frac{\nu}{\nu - 1} \frac{a}{\langle \pi R^2\rangle_b} \sigma_\eta^2 \tag{6.6}$$

which is equivalent to that of the reduced variance already introduced, but adapted to the area covered by the particles rather than to their number. In spite of the scattering of the experimental data (Figs. 26a and 26b), it appears that z is approximately equal to $\langle\eta\rangle$ at low coverage where all the RBCs deposit without mutual overlaps. Then $\langle\eta\rangle = \omega = z$, which is characteristic of a binomial law from the statistical point of view. However, as $\langle\eta\rangle$ increases, z deviates significantly from its binomial counterpart all the more as $\langle\eta\rangle$ is large.

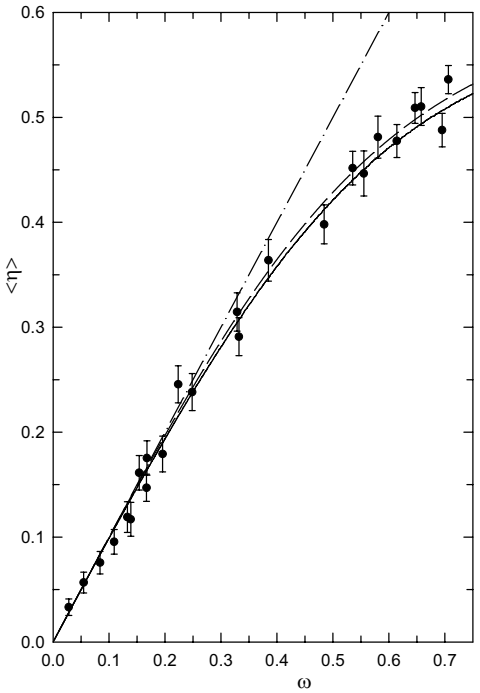

Figure 25. *Mean relative coverage as a function of the coverage which would be obtained if no overlap between particles occurred and if no rejection took place. Without overlap and rejection, the data points would align on the dot-dashed line which represents* $\langle\eta\rangle = \omega$*. The error bars on the experimental data* (•) *represent* $\pm$ *one standard deviation. The solid line corresponds to the simulation carried out with the RSA-MO model and the dashed line to the BD model.*

The deposition of the RBCs can be depicted by a model derived from the random sequential adsorption (RSA) model where the RBCs are approximated by monodisperse disks of radius R. In contrast to the classical RSA, this model accounts for overlaps between deposited particles. Moreover, hydrodynamic interactions of an incoming RBC with preadsorbed ones can phenomenologically be taken into account by minimizing the overlap areas between the particles.

In the RSA-MO model (where MO stands for minimized overlaps), an impact point is chosen *a priori*, at random, over the adsorbing surface for each new particle. If no overlap occurs with a preadsorbed particle, the incoming particle is permanently fixed at this point. Otherwise, a minimum area search procedure is started within a disk of radius δ centered on the initially selected impact point. The new particle will be fixed at the point of lowest total overlap area. If the contribution of a particle is lower than a given minimum, the particle is not taken into account for the evaluation of the relative area covered. This minimum contribution is quantified by the parameter f which represents the ratio of the supplementary area covered by the new particle to its own area πR^2. This algorithm mimics

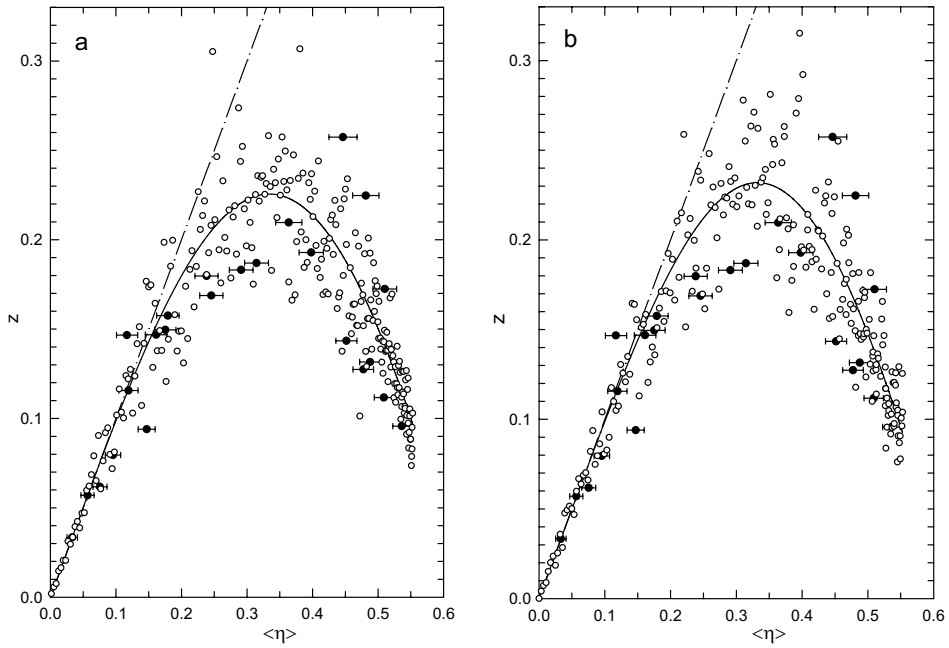

Figure 26. *(a) Normalized variance of the relative covered area η as a function of the mean relative coverage. The dot-dashed line corresponds to the binomial law ($z = \langle\eta\rangle$). Experimental data (•). Results of the simulation with the RSA-MO model (○). The solid line is the fit of the polynomial $x(1 + a_1x + a_2x^2 + a_3x^3 + a_4x^4 + a_5x^5)$ to the simulated values (x stands for $\langle\eta\rangle$). (b) Normalized variance of the relative covered area η as a function of the mean relative coverage. The dashed line corresponds to the binomial law ($z = \langle\eta\rangle$). Experimental data (•). Results of the simulation with the BD model (○). The solid line is the fit of the polynomial $x(1 + b_1x + b_2x^2 + b_3x^3 + b_4x^4 + b_5x^5)$ to the simulated values (x stands for $\langle\eta\rangle$, $b_1 = b_2 = 0$ and $b_3 \approx -14.92$ [9, 101]).*

the threshold procedure used in the image processing of the experimental pictures: particles located on the top of one or, more probably, several preadsorbed particles are withdrawn from the evaluation of $\langle\eta\rangle$ and of σ^2_η.

The Ballistic Deposition (BD) model has also been used as a complementary tool aimed at a better understanding of our experimental results [102]. For a description of this model the reader is referred to Section 3 of Chapter 4. In spite of the impossibility of mutual overlaps in the BD model and of the rolling mechanism which is a property of spherical particles, it may be interesting to confront data derived from it to data derived from the RSA-MO model or obtained experimentally. It may be noted that in the BD model, ω is defined by:

$$\omega = \langle n_b \rangle \frac{\pi R^2}{a} \tag{6.7}$$

where $\langle n_b \rangle$ represents the average number of particles, originally located in the

bulk fluid, used to reach a given mean coverage $\langle\eta\rangle$ of the surface. Therefore ω coincides with the dimensionless time usually defined in "geometrical" models such as the RSA and BD models.

For the BD model, where particle rejection exists, $\langle n_b\rangle$ is not equal to the average number $\langle n\rangle$ of deposited particles, in contrast to the RSA-MO model where $\langle n_b\rangle = \langle n\rangle$ since no particle is rejected. In fact, the BD model leads to a binomial distribution of the particles over the sub-systems, as does any other hard particle model, as long as the probability of interaction between the particles stays negligible. Once the trapping mechanism sets on, the curve representing $\langle\eta\rangle$ *vs.* ω displays a negative curvature, and reaches a plateau corresponding to the saturation of the surface. As shown in Figure 25, the data derived from the BD model are very close to those obtained with the RSA-MO model after optimization of the parameters appearing in this latter ($\delta/R = 1.2$, $f = 0.88$), and both models describe well the experimental data. As a consequence, we may assume that the particles rejected after trapping in the BD model play roughly the same role as the particles eliminated in the threshold procedure used in the processing of the experimental pictures. An equivalent process occurs with the RSA-MO model where particles that do not contribute a minimum increment to the coverage are eliminated from the estimation of $\langle\eta\rangle$. In addition, in this latter case, among the particles kept for the estimation of $\langle\eta\rangle$, relatively small mutual overlaps exist and tend also to reduce $\langle\eta\rangle$ in respect to $\langle\eta\rangle = \omega$ (binomial law). They are probably responsible for the slight difference with the predictions of the BD model.

Figures 26a and 26b present the fluctuation of the relative area covered by RBCs, expressed by z, as a function of $\langle\eta\rangle$, on the one hand derived from the two models and on the other hand determined experimentally. The data corresponding to both models have been obtained on the basis of samples of sub-systems (*i.e.*, of pictures) of size equal to the experimental one ($\nu = 100$ sub-systems or pictures). This relatively small number explains the large scattering observed. The fluctuations provided by the BD simulation behave like those predicted by the RSA-MO model and agree likewise with the experimental results. It is remarkable that not only the general trend of z is nearly identical for the two models (compare Figs. 26a and 26b), but also the scattering of the simulated data which, in addition, is in a reasonable agreement with the experimental scattering.

References

[1] J.W. Evans, Rev. Mod. Phys. **65**, 1281 (1993).

[2] Z. Adamczyk, B. Siwek, M. Zembala, P. Belouschek, Adv. Colloid Interf. Sci. **48**, 151 (1994).

[3] B. Widom, J. Chem. Phys. **39**, 2808 (1963).

[4] B. Widom, J. Chem. Phys. **44**, 3888 (1966).

[5] M. Toda, R. Kubo, N. Saitô, *Statistical Physics I: Equilibrium Statistical Mechanics* (Springer, Berlin, Heidelberg, New York, Tokyo, 1983).

[6] B. Senger, P. Schaaf, J.-C. Voegel, P. Wojtaszczyk, H. Reiss, Proc. Natl. Acad. Sci. USA **91**, 10029 (1994).

[7] F.L. Roman, J.A. White, S. Velasco, J. Chem. Phys. **106**, 4196 (1997).

[8] P. Wojtaszczyk, P. Schaaf, B. Senger, M. Zembala, J.-C. Voegel, J. Chem. Phys. **99**, 7189 (1993).

[9] J. Bafaluy, P. Schaaf, B. Senger, J.-C. Voegel, I. Pagonabarraga, J. Chem. Phys. **107**, 2089 (1997).

[10] N. van Kampen, *Stochastic Processes in Physiscs and Chemistry* (North-Holland, Amsterdam, 1981).

[11] Z. Adamczyk, L. Szyk, Bull. Pol. Acad. Chem. **43**, 243 (1995).

[12] Z. Adamczyk, B. Siwek, L. Szyk, M. Zembala, J. Chem. Phys. **105**, 5552 (1996).

[13] Z. Adamczyk, M. Zembala, B. Siwek, P. Warszynski, J. Colloid Interf. Sci. **140**, 123 (1990).

[14] Z. Adamczyk, B. Siwek, M. Zembala, J. Colloid Interf. Sci. **151**, 351 (1992).

[15] P.J. Flory, J. Am. Chem. Soc. **61**, 1518 (1939).

[16] A. Rényi, Publ. Math. Inst. Hung. Acad. Sci. **3**, 109 (1958).

[17] A. Rényi, Sel. Trans. Math. Stat. Prob. **4**, 205 (1963).

[18] J.K. MacKenzie, J. Math. Phys. **37**, 723 (1962).

[19] J.J. Gonzalez, P.C. Hemmer, J.S. Hoye, Chem. Phys. **3**, 288 (1974).

[20] P. Schaaf, J. Talbot, Phys. Rev. Lett. **62**, 175 (1989).

[21] P. Schaaf, J. Talbot, J. Chem. Phys. **91**, 4401 (1989).

[22] J.A. Given, Phys. Rev. A **45**, 816 (1992).

[23] G. Tarjus, P. Schaaf, J. Talbot, J. Stat. Phys. **63**, 167 (1991).

[24] E.L. Hinrichsen, J. Feder, T. Jøssang, J. Stat. Phys. **44**, 793 (1986).

[25] R. Dickman, J. Wang, I. Jensen, J. Chem. Phys. **94**, 8252 (1991).

[26] S.M. Ricci, J. Talbot, G. Tarjus, P. Viot, J. Chem. Phys. **97**, 5219 (1992).

[27] Y. Pomeau, J. Phys. A **13**, L193 (1980).

[28] R.H. Swendsen, Phys. Rev. A **24**, 504 (1981).

[29] J.W. Evans, Phys. Rev. Lett. **62**, 2126 (1990).

[30] J. Talbot, P. Schaaf, G. Tarjus, Mol. Phys. **72**, 1397 (1991).

[31] D. Boyer, G. Tarjus, P. Viot, J. Talbot, J. Chem. Phys. **103**, 1607 (1995).

[32] J.A. Given, G.R. Stell, *The XVIth International Workshop on Condensed-Matter Theories, June 1992* (Plenum, New York, 1993).

[33] J. Talbot, G. Tarjus, P. Schaaf, Phys. Rev. A **40**, 4808 (1989).

[34] P. Viot, G. Tarjus, S.M. Ricci, J. Talbot, J. Chem. Phys. **97**, 5212 (1992).

[35] T.L. Hill, *Statistical Mechanics: Principles and Selected Applications* (McGraw-Hill, NewYork, 1956).

[36] H. Reiss, H.L. Frisch, J.L. Lebowitz, J. Chem. Phys. **31**, 369 (1959).

[37] X. Jin, N.-H. Linda Wang, G. Tarjus, J. Talbot, J. Phys. Chem. **97**, 4256 (1993).

[38] Z. Adamczyk, B. Siwek, M. Zembala, P. Weronski, Langmuir **8**, 2605 (1992).

[39] M.R. Oberholzer, N.J. Wagner, A.M. Lenhoff, J. Chem. Phys. **107**, 9157 (1997).

[40] D. Boyer, J. Talbot, G. Tarjus, P. van Tassel, P. Viot, Phys. Rev. E **49**, 5525 (1994).

[41] P. van Tassel, P. Viot, G. Tarjus, J. Talbot, J. Chem. Phys. **101**, 7064 (1994).

[42] J. Talbot, P. Schaaf, Phys. Rev. A **40**, 422 (1989).

[43] P. Meakin, R. Jullien, Phys. Rev. A **46**, 2029 (1992).

[44] B. Senger, R. Ezzeddine, F.J. Bafaluy, P. Schaaf, F.J.G. Cuisinier, J.-C. Voegel, J. Theor. Biol. **163**, 457 (1993).

[45] P. van Tassel, P. Viot, G. Tarjus, J. Chem. Phys. **106**, 761 (1997).

[46] G. Tarjus, P. Schaaf, J. Talbot, J. Chem. Phys. **93**, 8352 (1990).

[47] X. Jin, Ph.D. thesis, Purdue University, West Lafayette, 1994.

[48] X. Jin, J. Talbot, N.-H. Linda Wang, AIChE J. **40**, 1685 (1994).

[49] R. Jullien, P. Meakin, J. Phys. A **25**, L189 (1992).

[50] J. Talbot, S.M. Ricci, Phys. Rev. Lett. **68**, 958 (1992).

[51] A.P. Thompson, E.D. Glandt, Phys. Rev. A **46**, 4639 (1992).

[52] H.S. Choi, J. Talbot, G. Tarjus, P. Viot, J. Chem. Phys. **99**, 9296 (1993).

[53] P. Viot, G. Tarjus, J. Talbot, Phys. Rev. E **48**, 480 (1993).

[54] H.S. Choi, J. Talbot, G. Tarjus, P. Viot, Phys. Rev. E **51**, 1353 (1995).

[55] P. Schaaf, A. Johner, J. Talbot, Phys. Rev. Lett. **66**, 1603 (1991).

[56] B. Senger, J.-C. Voegel, P. Schaaf, A. Johner, A. Schmitt, J. Talbot, Phys. Rev. A **44**, 6926 (1991).

[57] B. Senger, P. Schaaf, J.-C. Voegel, A. Johner, A. Schmitt, J. Talbot, J. Chem. Phys. **97**, 3813 (1992).

[58] B. Senger, J. Talbot, P. Schaaf, A. Schmitt, J.-C. Voegel, Europhys. Lett. **21**, 135 (1993).

[59] P.O. Luthi, J.J. Ramsden, B. Chopard, Phys. Rev. E **55**, 3111 (1997).

[60] P. Wojtaszczyk, J. Bonet Avalos, J.M. Rubí, Europhys. Lett. **40**, 299 (1997).

[61] B. Senger, F.J. Bafaluy, P. Schaaf, A. Schmitt, J.-C. Voegel, Proc. Natl. Acad. Sci. USA **89**, 9449 (1992).

[62] J. Faraudo, F.J. Bafaluy, Phys. Rev. E **54**, 3725 (1996).

[63] R. Ezzeddine, P. Schaaf, J.-C. Voegel, B. Senger, Phys. Rev. E **51**, 6286 (1995).

[64] Z. Adamczyk, P. Warszynski, Adv. Colloid Interf. Sci. **63**, 41 (1996).

[65] B. Senger, P. Schaaf, F.J. Bafaluy, F.J.G. Cuisinier, J. Talbot, J.-C. Voegel, Proc. Natl. Acad. Sci. USA **91**, 3004 (1994).

[66] R. Ezzeddine, Ph.D. thesis, University Louis Pasteur, Strasbourg, 1995.

[67] J. Happel, H. Brenner, *Low Reynolds Number Hydrodynamics* (Martinus Nijhoff, Dordrecht, 1986).

[68] T.G.M. van de Ven, *Colloidal Hydrodynamics* (Academic Press, London, 1989).

[69] D.L. Ermak, J.A. McCammon, J. Chem. Phys. **69**, 1352 (1984).

[70] G. Bossis, J.F. Brady, J. Chem. Phys. **80**, 5141 (1984).

[71] J. Bafaluy, B. Senger, J.-C. Voegel, P. Schaaf, Phys. Rev. Lett. **70**, 623 (1993).

[72] I. Pagonabarraga, M. Rubí, Phys. Rev. Lett. **73**, 114 (1994).

[73] I. Pagonabarraga, P. Wojtaszczyk, J.M. Rubí, B. Senger, J.-C. Voegel, P. Schaaf, J. Chem. Phys. **105**, 7815 (1996).

[74] P. Schaaf, Ph. Carl, J.-C. Voegel, E.K. Mann, B. Senger, Phys. Rev. E **54**, 6962 (1996).

[75] L. Landau, E. Lifshitz, *Physique théorique, Mécanique des fluides* (Mir, Moscou, 1989), tome 6.

[76] B. Bonnier, Y. Leroyer, E. Pommiers, J. Phys. I France **2**, 379 (1992).

[77] G.C. Barker, M.J. Grimson, Mol. Phys. **63**, 145 (1988).

[78] G. Tarjus, J. Talbot, J. Phys. A: Math. Gen. **24**, L913 (1991).

[79] B. Senger, R. Ezzeddine, F.J. Bafaluy, P. Schaaf, F.J.G. Cuisinier, J.-C. Voegel, J. Theor. Biol. **163**, 457 (1993).

[80] R. Muralidhar, J. Talbot, AIChE J. **39**, 1322 (1993).

[81] N.V. Brilliantov, Y.A. Andrienko, P.L. Krapivsky, J. Kurths, Phys. Rev. Lett. **76**, 4058 (1996).

[82] P.R. Johnson, M. Elimelech, Langmuir **11**, 801 (1995).

[83] J.J. Ramsden, Chem. Soc. Rev. **24**, 73 (1995).

[84] J.J. Ramsden, J.E. Prenosil, J. Phys. Chem. **98**, 5376 (1994).

[85] P. Wojtaszczyk, E.K. Mann, B. Senger, J.-C.Voegel, P. Schaaf, J. Chem. Phys. **103**, 8285 (1995).

[86] J. Feder, I. Giaever, J. Colloid Interf. Sci. **78**, 144 (1980).

[87] J. Feder, J. Theor. Biol. **87**, 237 (1980).

[88] G.Y. Onoda, E.G. Liniger, Phys. Rev. A **33**, 715 (1986).

[89] C.A. Johnson, A.M. Lenhoff, J. Colloid Interf. Sci. **179**, 587 (1996).

[90] P. Wojtaszczyk, Ph.D. thesis, University Louis Pasteur, Strasbourg, 1995.

[91] E.K. Mann, P. Wojtaszczyk, B. Senger, J.-C. Voegel, P. Schaaf, Europhys. Lett. **30**, 261 (1995).

[92] J.J. Ramsden, M. Máté, J. Chem. Soc. Faraday Trans. **94**, 783 (1998).

[93] A. Elaissari, A. Haouam, C. Huguenard, E. Pefferkorn, J. Colloid Interf. Sci. **149**, 68 (1992).

[94] A. Elaissari, E. Pefferkorn, J. Colloid Interf. Sci. **143**, 85 (1991).

[95] J.J. Ramsden, Phys. Rev. Lett. **71**, 295 (1993).

[96] J.J. Ramsden, G.I. Bachmanova, A.I. Archakov, Phys. Rev. E **50**, 5072 (1994).

[97] E.C. Constable, P. Harverson, J.J. Ramsden, Chem. Commun., 1684 (1997).

[98] R. Kurrat, J.E. Prenosil, J.J. Ramsden, J. Colloid Interf. Sci. **185**, 1 (1997).

[99] Q.M. Mao, A. Johnson, I.G. Prince, M.T.W. Hearn, J. Chromatogr. **548**, 147 (1991).

[100] Z. Adamczyk, B. Siwek, M. Zembala, Bull. Pol. Acad.: Chem. **44**, 113 (1996).

[101] Ph. Lavalle, J.-F. Stoltz, B. Senger, J.-C. Voegel, P. Schaaf, Proc. Natl. Acad. Sci. USA **93**, 15136 (1996).

[102] Ph. Lavalle, J.-F. Stoltz, B. Senger, J.-C. Voegel, P. Schaaf, Clin. Hemorheol. Microcircul. **17**, 307 (1997).